Design of an external patient specific guide for drilling a tunnel through the scaphoid

O. Hiemstra

Technische Universiteit Delft

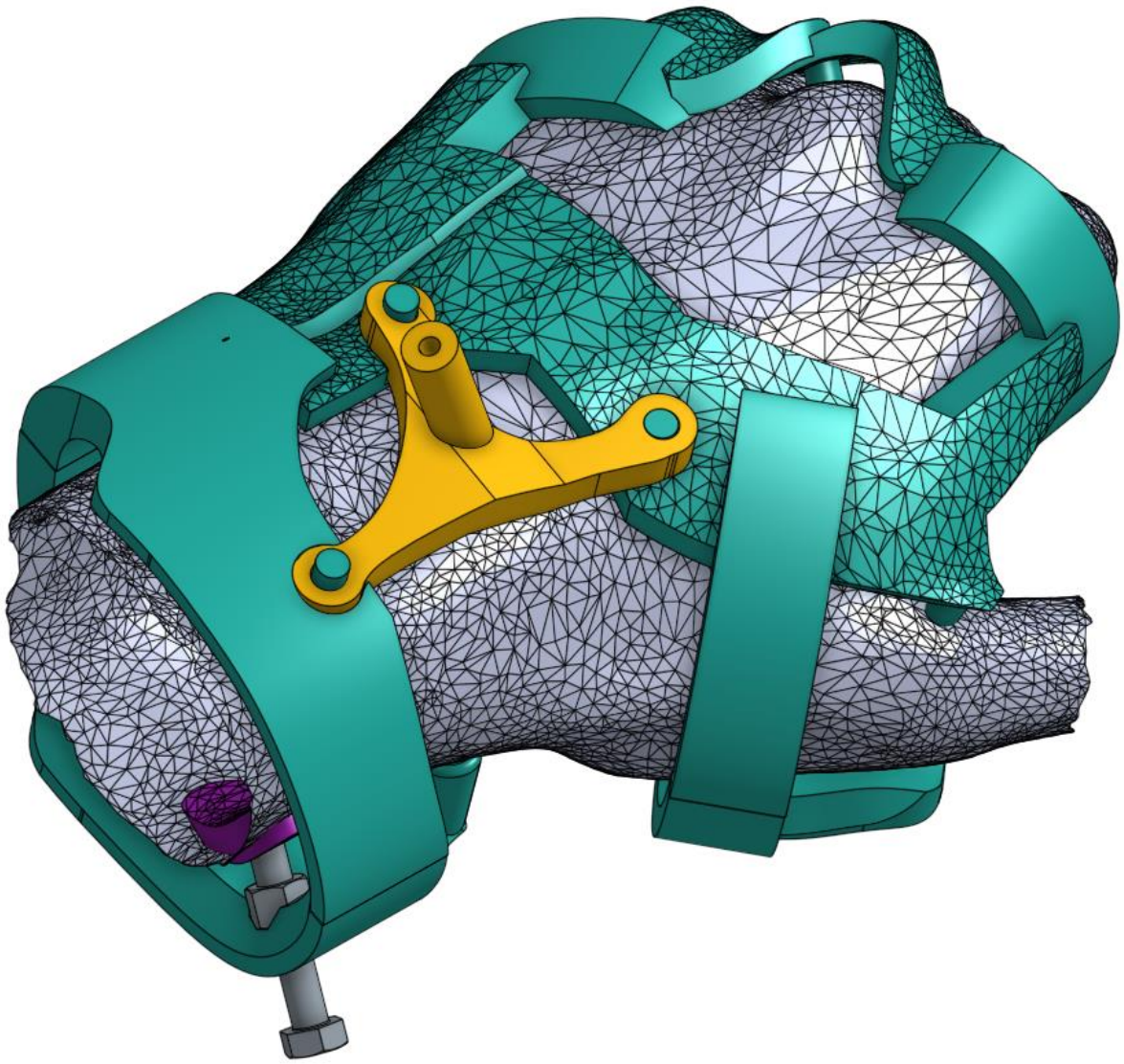

TU Delft Delft University of Technology

Challenge the future

Design of an external patient specific guide for drilling a tunnel through the scaphoid

By

O. Hiemstra

in partial fulfilment of the requirements for the degree of

Master of Science
in Mechanical Engineering

at the Delft University of Technology,
to be defended publicly on Thursday December 17, 2020 at 10:00 AM.

Student number:	4288769	
Supervisors:	Prof. dr. ir. P. Breedveld, Ir. E. de Kater	
Thesis committee:	Prof. dr. ir. P. Breedveld,	TU Delft, Chair
	Prof. dr. ir. J. Harlaar,	TU Delft
	Dr. G.A. Kraan	Reinier de Graaf Gasthuis

This thesis is confidential and cannot be made public until December 17, 2020.

An electronic version of this thesis is available at http://repository.tudelft.nl/.

TU Delft Delft University of Technology

Reinier de Graaf

“Het begin van wijsheid is ontzag voor de Heer,
wie leeft naar zijn wet, getuigt van goed inzicht.
Zijn roem houdt stand, voor altijd.”

– Psalm 111:10, NBV

Preface

Almost one and a half years ago I started an internship at a hospital despite having previously decided on various occasions that I was not really interested in the medical field. Given this unique chance to observe many orthopaedic surgeries being performed however, I quickly became intrigued by the great variety and ingenuity of the surgical instruments being used. Furthermore, various ideas started popping up in my mind for possible improvements or new devices. This was largely thanks to the many extensive conversations I had with dr. Kraan during my entire internship. I would like to express my deepest gratitude to him for taking so much time to help me throughout this project, as well as for his enthusiasm for the work I was doing. Our meetings always renewed my motivation by reminding me of the practical implications of the project.

Having come upon an idea that was in line with other research being done at the Bio-inspired Technology department, I got the opportunity to develop it into a prototype as my graduation project, resulting in this master thesis. I am very grateful to prof. Breedveld for giving me so much freedom to explore and choose the subject for this project, and for challenging every assumption that I made along the way. Being forced to continuously simplify and abstractify my ideas enabled me to find the core of the problem I was trying to solve. I would also like to extend my sincere thanks to Esther de Kater for her kind encouragement, the nuance that she often brought to the conversation, and her practical support in setting up the measurements and writing my thesis.

Looking back, this project and the rest of the years I spent studying at 3mE have given me a broad toolbox of theoretical knowledge, and helped me discover my passion for applying it in finding creative technical solutions for problems in various fields. As this thesis marks the conclusion of my time as a student, I would like to end by thanking my family and friends for their love, support, and guidance not only during this project but throughout this brilliant period in my life.

O. Hiemstra
Delft, December 2020

CONTENTS

I. Introduction 1

A. Patient specific instrumentation 1

B. External fixation 1

C. Modified Brunelli procedure 2
1) Relevant hand anatomy: 2
2) Scapholunate Dissociation: 3
3) Procedure: 3
4) Application of PSI: 3

D. Exact constraint design: 3

E. Problem Definition 4
1) Subsystems: 4
2) Design requirements: 4

F. Goal of this research 5

G. Layout of this report 5

II. Method for determining contact locations 5

A. Requirements and assumptions 5

B. Analysis of anatomy 5
1) Surrounding anatomy: 5
2) Suitable contact locations: 5

C. Simplified mechanical model 6
1) Mechanical system 6
2) Number of constraints needed: 6
3) Constraint locations and directions: 6

D. Mathematical evaluation 6

E. Finding a solution 7
1) Initial guess: 7
2) Reuleaux Method: 7
3) Reaction forces 7
4) Adjusting the position of the hand: 7

III. Prototype design 8

A. Introduction 8

B. 3D Surface scan 8

C. Modelling contact surfaces 8

D. Connecting contact surfaces 9

E. Drill guide 9

F. Implementing nesting force 9

G. 3D Printing Prototypes 9

IV. Measurement Methods 10

A. Accuracy measurements 10
1) Measurement goal: 10
2) Measurement protocol: 10

B. Stiffness measurements 11
1) Measurement goal: 11
2) Measurement setup: 11
3) Measurement protocol: 11

V. Measurement Results 12

A. Accuracy measurements 12
B. Repeatability 13
C. Stiffness measurements 13
D. Qualitative observations 14
1) Defining contact locations: 14
2) Positioning the guide: 14
3) Constraining MC1: 14
4) Discomfort: 14

VI. Discussion 15

A. Measurement results 15
1) Accuracy measurement: 15
2) Stiffness measurement: 15
3) Importance of stiffness: 15
B. Prototype 16
1) Contact assumptions: 16
2) Surface scan vs. CT-scan: 16
3) Hand pose: 16
C. Selection of contact points 16
1) Systematic approach: 16
2) Force analysis: 17
3) Constraint stability: 17
D. Comparison to previous studies 17
E. Further instrumentation 18
F. Viability of external PSI 18

VII. Conclusion 18

Appendix I - Matlab code used to verify a set of contact locations 23

Appendix II - Description of selected set of constraint locations 27

Appendix III - Technical drawings of the designed prototype 29

Appendix IV - Informed consent form and accompanying information letter 31

Appendix V - Matlab scripts used to measure the angles and translations for stiffness testing 35

Appendix VI – Literature study: Minimally Invasive Hand and Wrist Surgery 39

Design of an external patient specific guide for drilling a tunnel through the scaphoid

O. Hiemstra

***Abstract* – In recent years, patient specific instrumentation (PSI) has shown to be a promising application of 3D printing in orthopedic surgery. By aiding the surgeon with accurate placement of instruments such as saws or drills, surgeries can be performed faster, and require less surgeon experience. While most of these devices interface directly with the bone, invasiveness can be greatly decreased by applying the device to the outside of the body. Such an external device also allows for guidance with respect to bones that are too small to place a device on directly, for example the carpal bones in the wrist. In this thesis, an external PSI is designed to aid surgeons in accurately drilling a tunnel through the scaphoid; one of the carpal bones. The main challenge addressed in this thesis is how to rigidly attach a guide to the largely soft and elastic exterior of the hand. This was overcome by ensuring that the guide only contacts the hand at locations where the bone lies directly under the skin. Exact constraint design was applied to determine a minimal set of such contact locations that fully constrain the relevant anatomy. A 3D printed prototype was made for 6 participants and measurements were done to determine the positioning accuracy as well as the stiffness of the connection between the guide and the body. The results show that external PSI is a promising technology for application to wrist surgery, but may not be applicable to other parts of the body due to a limited number of suitable contact locations.**

***Keywords* – Exact constraint design, modified Brunelli procedure, patient specific instrumentation, surgical guide, wrist surgery.**

I. Introduction

A. Patient specific instrumentation

In recent years, patient specific instrumentation (PSI) has been applied in various complex orthopedic procedures in an attempt to improve accuracy [1] and reduce costs by reducing both surgery time and the number of instruments needed [2]. It has been trialed for many procedures that require either sawing or drilling in bone, such as knee arthroplasty [3], hip arthroplasty [4], and distal radius osteotomy [5], among others. The general procedure for such surgeries consists of three stages (Figure 1). First a CT-scan is made of the relevant anatomy. This scan is then used to construct a 3D model in which the surgery can be planned and necessary tool trajectories are determined. The last stage is the surgery where a 3D printed guide aids the surgeon to perform the procedure as planned.

As of now, such guides almost exclusively rely on interfacing directly with the surface of the bone, requiring the bone to be laid bare during the operation. Furthermore, as the bones become smaller, it becomes increasingly difficult to sufficiently stabilize the guide on the bone surface. Both these limitations are pertinent when attempting to apply PSI to hand and wrist surgery. The bones in the hand are among the smallest in the human body, making a stable connection between the bone and the guide challenging. What makes the wrist surgery even more challenging is the complex array of ligaments and tendons, damage to which can lead to severely impairing complications [6].

In order to avoid these problems, the PSI can also be applied on the outside of the body. This technique is much less common. A brief literature search resulted in only nine examples of such an approach[7]–[15]. In all cases the device was designed to match the skin surface in order to be positioned. In addition, one study [14] used radiographic markers that remained on the body between the CT-scan and the operation. These aid in the accurate positioning of the PSI with respect to the relevant anatomy.

By attaching the guide to the outside of the body, the size of the needed incisions can be greatly reduced, while still ensuring an accurate procedure. This is a promising combination for new alternatives for complex wrist surgeries that require drilling or manipulation of the small carpal bones in the wrist.

B. External fixation

While PSI guides that attach to the outside of the body are still a novel concept, external devices have long been employed in orthopedics for the fixation of fractures. These generally rely on pins inserted into the various bone fragments through the skin which are then fastened to a rigid external frame. While this is much less invasive than the use of plates that attach directly to the bone, the penetration sites are prone to infection, especially if not carefully cleaned regularly [16].

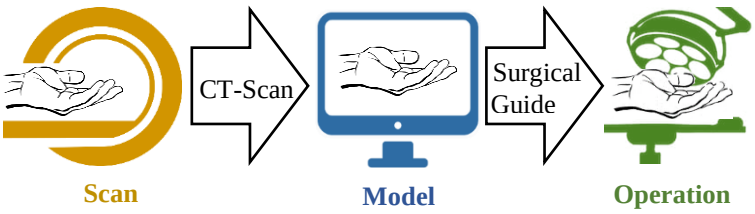

Figure 1 A flowchart showing the general workflow in the use of patient specific instruments.

In spine surgery, a device called a halo vest immobilizer is used to stabilize and fixate the position of the spine [17]. The working principle of this device differs from other external fixators because the device does not directly attach to the bones which it is designed to stabilize. Instead, it is designed to fix the position of the skull with respect to the shoulders of the patient. Subsequently, the damaged vertebrae located in between the skull and shoulders are also fixed because they cannot move independently of the head. This concept of indirectly fixating bones via the anatomy to which they are connected may be a solution to the challenge of constraining the small and hard to reach carpal bones in the wrist.

C. Modified Brunelli procedure

1) Relevant hand anatomy: One procedure where this could be of great benefit is the modified Brunelli procedure. This procedure is one of a few methods for the treatment of advanced stages scapholunate (SL) dissociation. In a literature review, it was found that an effective minimally invasive method has yet to be developed for this surgery, despite the potential benefits of such a method (Appendix VI).

The skeletal structure of the hand and wrist is shown in Figure 2. The forearm consists of two bones, namely the radius on the thumb side, and the ulna on the side of the little finger. The wrist contains 8 small bones known as carpal bones that work together to allow for smooth movement and a large range of motion. These bones are held together by a complex network of interconnecting ligaments. As seen in Figure 3, each ligament connects two carpal bones to each other, the names of which form the name of that ligament. The interplay of these ligaments ensures that the carpal bones stay where they should, while still allowing for complex motion of the wrist. The hand itself is made up of the five metacarpal (MC) bones, to which the fingers (called phalanges) are attached.

In this report, various terms are used to describe different planes and directions with respect to the hand (Figure 4). If your left hand is laid flat on a table in front of you, the planes are as follows: The table represents the coronal plane, the vertical plane that runs parallel to your fingers is the sagittal plane, and a vertical plane that faces you is the transverse plane. The fingertips are located distal, and the forearm proximal. The left and right sides are called ulnar and radial respectively. The top of the hand is called the dorsal side, and the bottom or palm is called the palmar or volar side.

Lastly, the possible rotations of the wrist are also named. Rotating the hand off of the table is called extension, and rotating down, towards the table is called flexion. Rotating to point the fingers to the left or right is called adduction and abduction respectively. Lastly, rotating the thumb upwards is referred to as supination, and rotating it downwards is pronation.

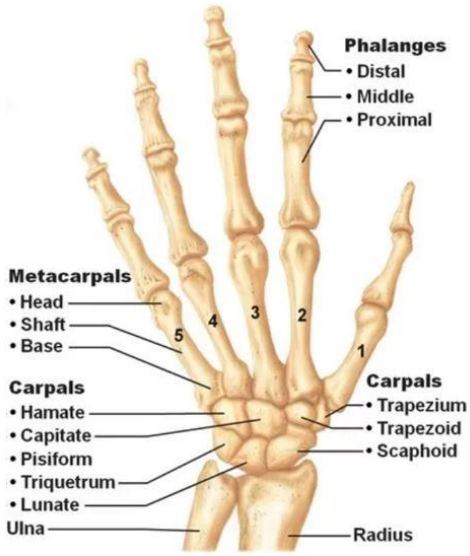

Figure 2. Bones of the hand. Source: adapted from [16]

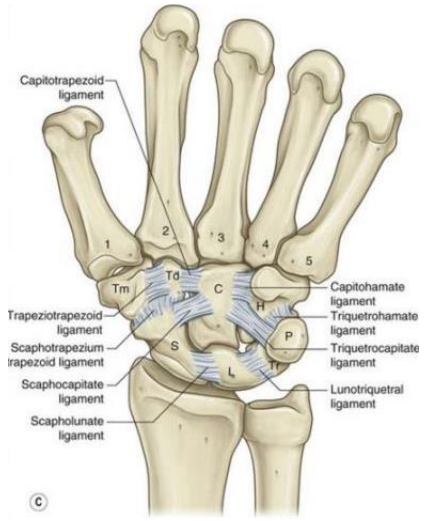

Figure 3. Carpal ligaments on the dorsal side of the hand. Source [17]

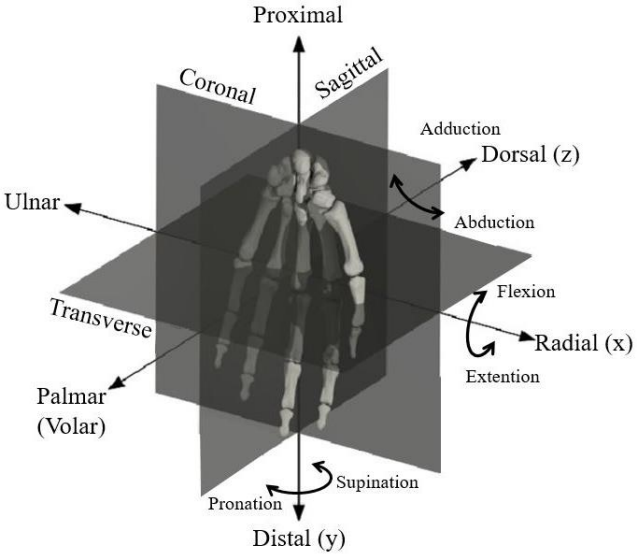

Figure 4. Image of the hand showing anatomical planes and names of directions and rotations. Source: adapted from [18]

2) Scapholunate Dissociation: Damage to a single carpal ligament disrupts this intricate balance of forces, leading to pain, loss of mobility, and in severe cases dislocation of one or more carpal bones. Specifically, a partial or total tear of the SL ligament, which connects the scaphoid to the lunate, is a common example of this. Often resulting from trauma to the wrist sustained from a fall or during sports, damage to this ligament starts a destructive chain reaction in the wrist. At first, the surrounding ligaments may absorb the extra force, but over time a gap can arise between the scaphoid and lunate, which increases during movement or loading. This is known as SL dissociation. This can occur in various degrees, categorized in six stages, as described in Table 1.

The Brunelli procedure is one of a few methods for the treatment of stage 4 scapholunate dissociation. This is categorized by an irreparable rupture of the SL ligament, in addition to a reducible malalignment of the scaphoid. This means two objectives must be achieved, namely the reduction (movement back to the anatomical position) of the scaphoid and the replacement of the broken ligament.

3) Procedure: In order to gain the necessary access to the carpal bones, an 8cm incision is made on the back of the wrist. A second 1.5 cm incision is made on the palm of the hand at the base of the thumb. Theses incisions are positioned so that the scaphoid can be accessed from both sides. The next step is to drill a 3 mm hole through the scaphoid, from the back to the palm of the hand. First, the surgeon drills a guide wire through the scaphoid, placing a finger on the back of the scaphoid to gauge the proper direction. This is the most challenging part of the procedure, as it requires a lot of experience to drill in the correct direction. The trajectory can be checked using fluoroscopy, but due to the small size of the scaphoid, only one or two attempts are possible before causing too much damage to the bone. If the surgeon is satisfied with the placement of the k-wire, a cannulated drill is used to drill the tunnel.

Via the palmar incision and one or two more proximal incisions, an 8 cm strip is cut from the flexor carpi radials (FCR) tendon, starting at the entrance of the previously drilled hole. A wire loop is then used to pull the tendon strip through the tunnel in the scaphoid, and across the lunate, where a suture anchor is placed to which the tendon graft will be attached. The tendon is then looped through a slit in the radiotriquetral ligament, which is later used as a pulley to tension the tendon.

Table 1 Staging of Scapholunate Dissociations. Source:[19]

SLD Stage	1	2	3	4	5	6
Is there a partial rupture with a normal dorsal SL ligament?	Yes	No	No	No	No	No
If ruptured, can the dorsal SL ligament be repaired?	Yes	Yes	No	No	No	No
Is the scaphoid normally aligned (radioscaphoid angle ≤ 45°)?	Yes	Yes	Yes	No	No	No
Is the carpal malalignment easily reducible?	Yes	Yes	Yes	Yes	No	No
Are the cartilages at both RC and MC joints normal?	Yes	Yes	Yes	Yes	Yes	No

Before tensioning and fixating the tendon graft, the other objective, namely the reduction of the scaphoid must be achieved. This is done by rotating the scaphoid to the right anatomical position, and securing it to both the lunate and capitate with k-wires. Once this is complete, the surgeon tensions the tendon as tight as possible, and sutures it to the lunate using the previously placed anchor. The last step of the procedure is to reconstruct the surrounding tissues and close the incision. A cast is placed for a total of 6 weeks, and after 8 weeks the k-wires are removed, the surgery generally takes one to two hours to complete [21].

4) Application of PSI: Implementing external PSI in this procedure has the potential to greatly decrease the size of the incisions needed, and decrease the difficulty of the procedure. External PSI has already been applied to the treatment of scaphoid nonunion by Wan et al [7], Yin et al [11], and Salabi et al [15]. This similar procedure requires a k-wire to be drilled lengthwise into the scaphoid, which is then used to guide the placement of a screw. All three used an external PSI based on the surface of the skin to guide the surgeon in placing the k-wire at the correct angle and location, showing promising preliminary results.

D. Exact constraint design:

The determining factor for the performance of PSI is how precisely the placement of the guide on the body coincides with the digital model. Currently, the placement of PSI still relies heavily on the subjective feeling of the surgeon[1]. This challenge of accurately and precisely connecting two bodies to each other is not unique. In the design of precision mechanisms, kinematic couplings are commonly used as a dependable and accurate way of connecting bodies to each other[22]. These couplings implement the principles of exact constraint (EC) design, which "provide precision, robustness, and certainty of location and design"[22].

The fundamental principle of EC design is to constrain each degree of freedom (DOF) of a system exactly once. The number of DOFs of a system in 3D can be calculated using Greubler's equation, as shown in (1).

$$6(\#\ of\ bodies) - \#\ of\ constrained\ DOFs = \#\ DOFs \quad (1)$$

In many real world applications however, this equation results in either a negative value, or a value that is lower than the actual mobility of the system. This occurs when a single DOF is constrained by multiple constraints, and is referred to as an over-constrained system. A simple example of this is a door, which often has two or three hinges which each remove 5 DOFs. According to (1) one hinge would be sufficient to reduce the number of DOFs to one rotation, but more are added to improve the strength of the connection. The downside of adding over-constraints, is that they result in internal stress in the system when not perfectly aligned.

More importantly, over-constraints can also jeopardize the certainty of the position of the system. For example, a table with 4 legs that is placed on uneven ground can rock back and forth between two distinct positions. These issues can be avoided by ensuring that each DOF is constrained by a single constraint.

Expanding on the previous example, if the amount of legs of the table is reduced to three, its position is always uniquely determined. This intuitive observation is a result of the second table being statically determinant, which means that all the reaction forces (in this case the force at each leg) can be calculated using only the equations of static equilibrium. This is true for all EC systems.

Applying this principle to external PSI can provide a theoretical basis for design choices, potentially improving positioning accuracy and reducing the role of the surgeon in correct placement. In addition this can give broader insight into the stresses imposed on skin, and what kinds of procedures can and cannot be improved with PSI.

E. Problem Definition

1) Subsystems: The design of an external PSI to aid in the performance of a Brunelli procedure consists of two essential subsystems; one that accurately positions and attaches the guide to the hand, and a second that guides the instrumentation in the desired fashion. While these subsystems are often combined in one part, they form two distinct problems that can be approached separately.

As previously mentioned, the first problem of accurate positioning and attachment forms the most significant challenge for PSI, and is therefore the focus of this research. In order to properly plan and execute the procedure the hand must be in the exact same position on the operating table as when the CT-scan was made. The guide must therefore be placed on the hand in a way that ensures it is in the same position as the digital model used to plan the procedure. In addition, it must be attached in such a way that it does not move during the procedure, all while interfacing with the relevant structures through the skin, which is soft and elastic.

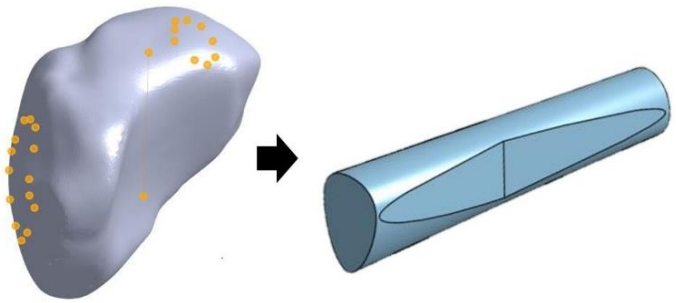

Figure 5. A 3D model of the scaphoid with boundaries for an acceptable drill trajectory (left) Souce: adapted from [21]. And a simplified version of the volume within the boundaries (right).

2) Design requirements: Such a frame must satisfy the following requirements:

- Only interface with the outside surface of the skin
- Position instruments according to a digital model with sufficient accuracy and repeatability.
- Connect the guide to the hand with sufficient stiffness to correct surgeon deviations.

In order to minimize the invasiveness of the procedure, the choice was made to only contact the surface of the skin. This is a step further than regular external fixation techniques which rely on piercing the skin to either contact directly against the bone, or penetrate into the bone.

An orthopedic surgeon specialized in hand and wrist surgery was consulted to determine a range of acceptable error for the drill trajectory through the scaphoid. This was done by marking the boundaries of acceptable placement on a 3D model of a scaphoid [23] (Figure 5).These boundaries were then simplified along three parallel planes, one on the volar side of the scaphoid, one on the palmar side, and one at the waist. In addition, the boundaries were offset inwards by 1.5mm to account for the thickness of the drill. These boundaries were then connected with a loft to form a volume through which the center of the drill must pass (Figure 5). From this volume, the maximum allowable deviation in the sagittal plane was determined as 12.5°, and 11° in the coronal plane. In addition, the allowable translation error at the mid-plane of the scaphoid was determined as 1.9 mm in the frontal direction and 1.3 mm in the lateral direction. While certain combinations within these maximal values can still result in an inadequate trajectory, they give a good indication of the accuracy that must be achieved.

In addition to being positioned accurately, in order to function properly a drill guide must also be able to correct deviating forces that arise during drilling. These can be caused by interactions between the drill and the bone or by the surgeon directing the drill in a slightly different direction than intended. In order to achieve this, the guide must be able to counter these deviating forces or moments while still remaining within the allowable trajectory error. Assuming the guide can be designed to be very stiff, this will instead be limited by the stiffness of the connection between the guide and the hand. Therefore, the guide should be designed to be as stiff as possible. No studies could be found pertaining to the deviating loads that occur during surgical drilling which makes it unviable to set specific target values for the stiffness of the guide.

Once such a frame has been established, the secondary challenge consists of guiding a surgical drill to follow the planned trajectory through the scaphoid, and to reposition the scaphoid to the correct anatomical position, which involves a certain rotation of the scaphoid about a planned axis. This however was left outside the scope of this research.

F. Goal of this research

The goal of this research is to design a PSI that accurately and robustly attaches to the outside of the hand by implementing EC design principles, with the aim of aiding surgeons in performing a Brunelli procedure.

G. Layout of this report

The layout of the remainder of this report is as follows. Section II describes the theoretical framework used to find a set of contact locations to connect the guide to the body. This includes both an analysis of the anatomy, as well as the application of exact constraint design principles and the resulting mathematical calculations. In Section III the resulting set of contact locations is implemented in the design and manufacturing of a 3D printed prototype for 6 test participants. Section IV subsequently describes the methods used to test these prototypes with regards to the positioning accuracy as well as the stiffness of the connecting between the guides and the hand. In Section V the results of these measurements are presented, as well as qualitative observations made during the measurement process. In Section VI these results are discussed, as well as various aspects of the methods and findings of the preceding sections. Lastly, Section VII gives an overview of the conclusions that can be drawn from the work done in this thesis project.

II. Method for determining contact locations

A. Requirements and assumptions

This section describes the method used to determine a minimal set of contact points which can be used to connect the guide to the hand. As previously mentioned, the guide must be fully constrained with respect to the scaphoid and lunate using exactly the amount of constraints necessary.

In addition, contact may only be made with the outside of the skin. In order to approach the problem with EC design principles, this contact between a point on the guide and the skin must be categorized in terms of which DOFs are constrained. Due to the highly elastic nature of skin in planar directions, contact can only constrain motion normal to the surface of the skin. Furthermore, a contact point can only constrain this motion in one direction (it can only push, not pull). This is called a unilateral constraint.

Because unilateral constraints only act in one direction, they must be accompanied by a force normal to the contact surfaces which ensures contact is made. In many everyday examples, such as a chair standing on the floor, gravity supplies this nesting force.

Together, a contact point and its accompanying nesting force constrain one DOF. When multiple contact points are used, the nesting forces can be combined into a single nesting force that ensures all points remain in contact.

B. Analysis of anatomy

1) Surrounding anatomy: Since both the scaphoid and lunate bones are positioned inside the wrist and cannot be directly constrained through the skin, they must be constrained via the surrounding anatomy. Medical literature was consulted to determine which surrounding bones have an influence on their position.

With the forearm, consisting of the radius and ulna, taken to be fixed, the immediately surrounding bones are the six other carpal bones and the metacarpals. Since the six other carpal bones cannot be directly constrained either, they could be excluded from further analysis.

The main factors influencing the position of the scaphoid and lunate with respect to the forearm are flexion-extension and radial-ulnar deviation of the wrist. Both of these are commonly defined in literature by the position of the third metacarpal (MC3)[24].

Independent movement of the MC1 also influences the position of both the scaphoid and lunate [25]. MC2 can only move slightly with respect to the MC3 and thus has marginal independent effect on either the scaphoid or lunate. Lastly, MC4 and MC5 can be moved independently of MC3, but their position has no effect on the position of either the scaphoid or lunate[26].

Based on these findings, it was concluded that in order to fully define the positions of the scaphoid and lunate only the forearm and the first and third metacarpals need to be constrained.

2) Suitable contact locations: The next step was to determine all the possible contact locations to constrain these structures. In order to achieve precise positioning the contact between the guide and the hand must be as stiff as possible, so slight deviations in pressure do not result in large changes in position. Therefore, the contact points were chosen to be located on parts of the hand where the bone lies directly beneath the skin.

The possible locations for the application of a nesting force did not have to satisfy this requirement. This is because the point of application of a force can be placed anywhere along its line of action without affecting the reaction forces in the system [27]. Therefore, indentation of the skin does not change the effects of the force, thus it may be applied at ‘soft’ locations on the body.

For both the contact points and the nesting force, vulnerable structures such as nerves and arteries were avoided to ensure the safety of the device. In consult with an orthopedic hand surgeon, all the possible contact locations that fit these requirements were determined (Figure 8).

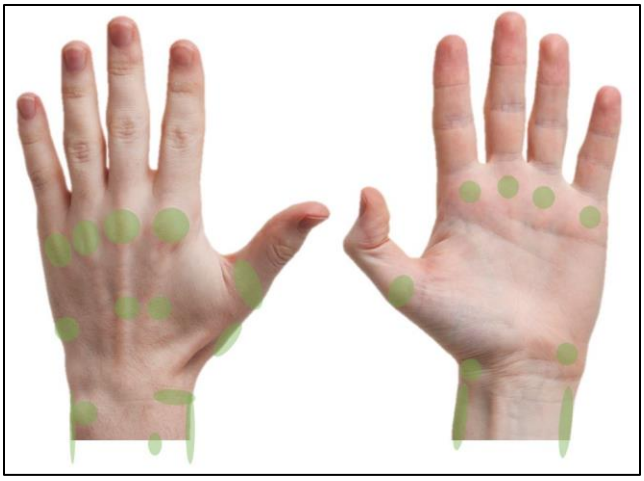

Figure 8. Dorsal and palmar view of the hand with suitable contact locations marked in green.

C. Simplified mechanical model

1) Mechanical system: In order to apply the principles of EC design, a simplified model of the hand was made based on the analysis in the previous section. The purpose of this simplification was to represent the relevant anatomical structures as a simple mechanical system to which contact constraints could be added in order to constrain it. Having previously determined that the MC1, MC3, and the forearm fully define the positions of the scaphoid and lunate, a simplified system was made consisting of only these three bodies (Figure 6). The joints between the bodies were modelled as universal joints, allowing bending in both directions but preventing torsion, as the metacarpals cannot rotate around their long axis.

2) Number of constraints needed: Now that a simplified mechanical model was established, the minimum number of constraints needed could be determined using Greubler's equation (1). The system consists of three bodies, and two universal joints, each constraining 4 DOFs. This results in 10 remaining DOFs, meaning 10 contact points are needed, as well as a nesting force.

3) Constraint locations and directions: Contact constraints could be added to the simplified model as arrows defined at a position and with a certain direction. A simplification was also made with regards to the possible locations of these contact constraints. In order to make the set of possible solutions more manageable, the previously determined areas of suitable contact were added to the model as points or lines as opposed to areas, as seen in Figure 6. As previously mentioned, the direction of each contact force is perpendicular to the surface of the skin at that location. However, because the simplified model did not include a realistic shape of the hand surface, the direction of each constraint had to be defined separately. For points that corresponded to curved structures on the hand, such as the ulnar styloid, the direction could be varied to represent the various possible contact directions as shown in Figure 7.

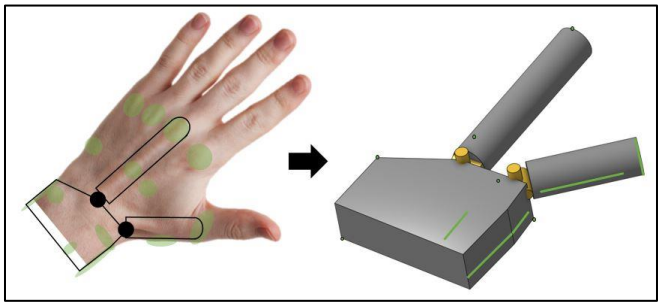

Figure 6. Simplified model of the hand, shown as a projection on an image of the hand (left), and a 3D model (right).

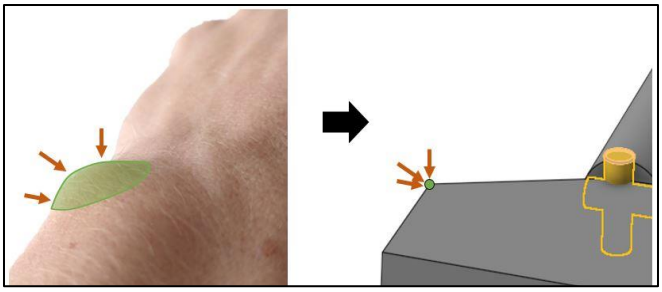

Figure 7. Close-up of the ulnar styloid showing the simplification from contact area to contact point.

These possible directions were simplified into increments of 45° to once again make the set of possible solutions more manageable.

D. Mathematical evaluation

Each set of 11 locations and directions could be evaluated mathematically in order to determine whether or not it fully constrained the system. This was done by solving a system of equations consisting of the six equations of static equilibrium for each body (i):

$$\Sigma \boldsymbol{F_i} = 0 \quad (2)$$

$$\Sigma \boldsymbol{M_i} = 0 \quad (3)$$

For three bodies that gives a total of 18 equations.

Each contact point (n) was defined using two vectors, namely the location ($\boldsymbol{c}_n$) and a unit vector in the direction perpendicular to the model at that location ($\boldsymbol{d}_n$). The nesting force was similarly defined with its location ($\boldsymbol{c}_{nest}$) and direction ($\boldsymbol{d}_{nest}$). The universal joints (m) were defined with a location ($\mathbf{c}_m$) and a unit vector ($\boldsymbol{d}_m$) pointing in the direction of the attached appendage.

The unknowns were the normal force at each contact point (f_n), the reaction forces at each joint ($\boldsymbol{f}_m = [f_{m,x},\ f_{m,y},\ f_{m,z}]$), and the magnitude of the reaction moment at each joint (M_m). For each body two sets ($S_{cp,i}$ and $S_{joint,i}$) were defined to indicate which contact points and which joints act on it respectively. Similarly, a set ($S_{mom,i}$) defined which moments act on said body. The forces and moments at the joints were defined as positive on the body representing the forearm, and negative on the appendages. Expanding (2) and (3) with these variables gives:

$$\Sigma \boldsymbol{F_i} = \sum_{n \epsilon S_{cp,i}} f_n \boldsymbol{d}_n + \sum_{m \epsilon S_{joint,i}} \boldsymbol{f}_m + (f_{nest} \boldsymbol{d}_{nest}) = 0 \quad (4)$$

$$\Sigma \boldsymbol{M_i} = \sum_{m \epsilon S_{mom,i}} M_m + \sum_{n \epsilon S_{cp,i}} \boldsymbol{c}_n \times f_n \boldsymbol{d}_n + \sum_{m \epsilon S_{joint,i}} \boldsymbol{c}_m \times \boldsymbol{f}_m + (\boldsymbol{c}_{nest} \times f_{nest} \boldsymbol{d}_{nest}) = 0 \quad (5)$$

This resulted in a total of 18 unknowns for 18 equations meaning the system is statically determinant and can be solved for a chosen nesting force (f_{nest}).

The set of contact locations was said to fully constrain the system only if all of the resulting constraint forces (f_n) were positive when solved for a positive nesting force. If any resulting contact force was negative, this would mean that equilibrium could only be enforced if one of the contact locations 'pulled' on the body. Since contact points are unilateral, this is not possible, and therefore such a set of locations does not sufficiently constrain the system.

E. Finding a solution

1) Initial guess: An iterative process was used to find a combination of constraint locations and directions that fully constrained the system. First an initial set was selected using the four general rules for EC design[28]:

1. No two constraints should be co-linear.
2. No four constraints are in a single plane.
3. No three constraints are parallel.
4. No three constraints should intersect at a point.

This set was then evaluated mathematically, by implementing (4) and (5) in Matlab (MATLAB R2018b), the code for which is found in Appendix I. If it was found that the set did not fully constrain the system, certain locations were adjusted and the new iteration was checked.

2) Reuleaux Method: A variety of tactics were used to decide how to adjust the constraint set for a new iteration. While no method could give a definitive solution, they all helped to inform the process of trial and error. Firstly, a graphical method was used in 2D based on the concept of instantaneous center of rotation (ICR). This approach was first developed by Franz Reuleaux in 1875 [23]. An ICR is a point around which the system can rotate at a given instance. If a body is fully constrained, there is no ICR since no rotation is permitted. However, if a body is not fully constrained, an ICR can be found about which the body can rotate, with translations being rotations about a point infinitely far away. In 2D, rotation is possible in either the clockwise or counterclockwise direction.

Each contact constraint acting on a body prevents certain rotations, namely clockwise rotations about any point left of the direction of constraint, and counterclockwise rotations about any point right of the constraint direction (Figure 9). Adding more constraints further limits the locations in which either a clockwise or counterclockwise ICR can occur. If the constraint regions overlap sufficiently, no possible locations for either type of ICR remain and it can be concluded that the body is fully constrained.

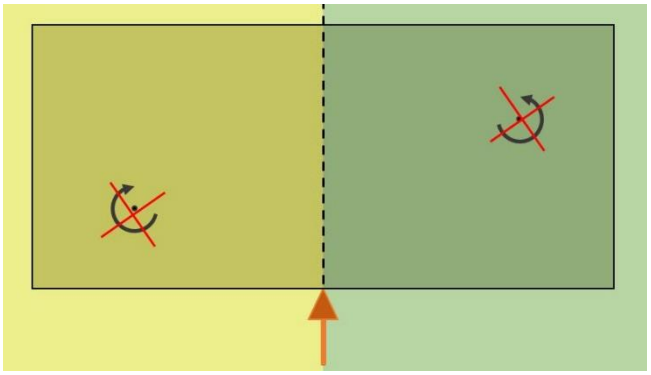

Figure 9. A rectangular body with a single contact constraint (orange). No clockwise rotation can occur around any point in the yellow area, and no counterclockwise rotation can occur around any point in the green area.

While giving valuable insight into the effect of adding or removing certain constraints, this method was limited because of its complexity when also considering the interactions between the different bodies of the system. To fully investigate a certain constraint set, a separate analysis was needed for each body, repeated in each of three orthogonal planes

In addition, the result did was not always accurate when applied in 3D. It was found that despite being fully constrained in 2D in each orthogonal plane, the resulting system could sometimes still rotate about a certain axis when the forces were calculated.

3) Reaction forces

The calculated reaction forces also gave insight into which rotations or translations were not yet constrained. A negative reaction force indicates the hand wanting to pull away from the guide at that location. The contact points could then be adjusted to constrain that specific rotation. If the anatomy allowed it, this constraint could simply be moved to the opposite side of the hand. This was usually not the case however, making it necessary to move the constraint to a position that changed its line of action, which in turn required adjustments to be made to other constraints in the system.

4) Adjusting the position of the hand: For the first attempts, the hand was taken to be in a flat position (as shown in the previous section). In this configuration however, no satisfactory set of contact points could be found. By observing which reaction forces remained negative, it became clear that one specific degree of freedom could not be constrained, namely distal motion. The only place where it was possible to apply a constraint opposing distal motion was at the end of the MC1 body, however, rotation in the joint then still allowed the other bodies to move in the distal direction.

This problem was addressed by changing the position of the hand to have the fingers point downwards at an angle of

Figure 10. Side view of the hand with the fingers at a 45° angle. The red arrow indicates the obtained option to constrain the knuckle in the distal direction.

around 45° (Figure 10). This increased the range of directions in which the knuckle could be constrained, adding the possibility of constraining distal motion at the end of the MC3 body as well. The tradeoff for this was that the contact surface on the palm of the hand became less stiff as the tissue bunches up increasing the amount of soft tissue between the guide and the bone.

With this adjustment it became possible to find a satisfactory set of contact locations. Figure 11 shows the locations of each contact point (orange), and the nesting force (blue). When a positive nesting force was applied, the reaction force at each contact location was calculated to be positive, indicating that contact is enforced at all points, and thus that the system is exactly constrained in all DOFs. A more detailed description of the locations can be found in Appendix II.

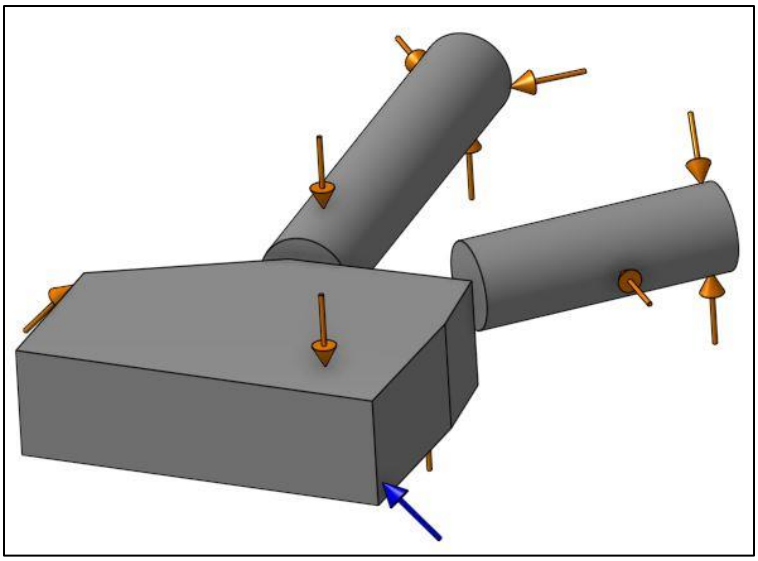

Figure 11. Simplified model of the hand showing a set of contact points (orange) and a nesting force (blue) that fully constrain the system.

III. Prototype design

A. Introduction

In the previous section kinematic principles were used to determine a set of contact points that can fully constrain the hand and wrist. This section describes the design of a 3D-printable prototype that implements these contact points. The designed prototype is aimed solely at testing the effectiveness of using the determined contact points, meaning many practical considerations for the use of the design for surgery are not yet considered. In practice the method is intended to be implemented using a CT-scan. However, due to the practical difficulties of experimenting with CT-scans, the prototyping made using scans of only the exterior of the hand.

B. 3D Surface scan

The design of the prototype began with a surface scan of the hand in the desired position (Figure 12.1). These were made using a ManoX scanner (Manometric, the Netherlands) which consists of a tunnel containing 48 cameras in a cylindrical array. The images from each camera are combined to create a 3D surface of the hand, accurate to 1mm. Prior to scanning, the desired contact locations determined in Section II were marked on the hand. The chosen locations varied slightly per participant, due to differences in anatomy. By feeling the bone structure under the skin, the researcher attempted to match the surface normal at each location to the planned constraint direction as well as possible. In addition, two other points were marked in order to designate a desired drill trajectory, one on the volar side of the wrist, and the other on the palmar side. This desired trajectory was chosen to roughly coincide with a line through the scaphoid, but because it will only be used to compare to a resulting trajectory, the exact location is arbitrary. Lastly, an estimate was made of the expected skin indentation at each point by pressing into the skin with a rod of similar diameter to the contact surfaces.

C. Modelling contact surfaces

Using CAD software, a cylinder was modelled at each selected contact point (Figure 12.2). The cylinders were extended a certain distance under the scanned surface, based on the estimated amount of indentation of the skin. When choosing the diameters of the contact points, there is a tradeoff between comfort and accuracy. As discussed in Section I, the larger the contact surface area is, the greater the uncertainty becomes of where exactly the guide makes contact, resulting in lower accuracy. Ideally, the contact points should therefore be as small as possible. As the surface area decreases however, the pressure at the contact points increases. Excessive pressure on the skin can result in discomfort, bruising, or permanent damage to the skin and underlying structures. The sensitivity of the skin also varies between contact points. For this initial design, the diameters of each cylinder were chosen by printing multiple iterations

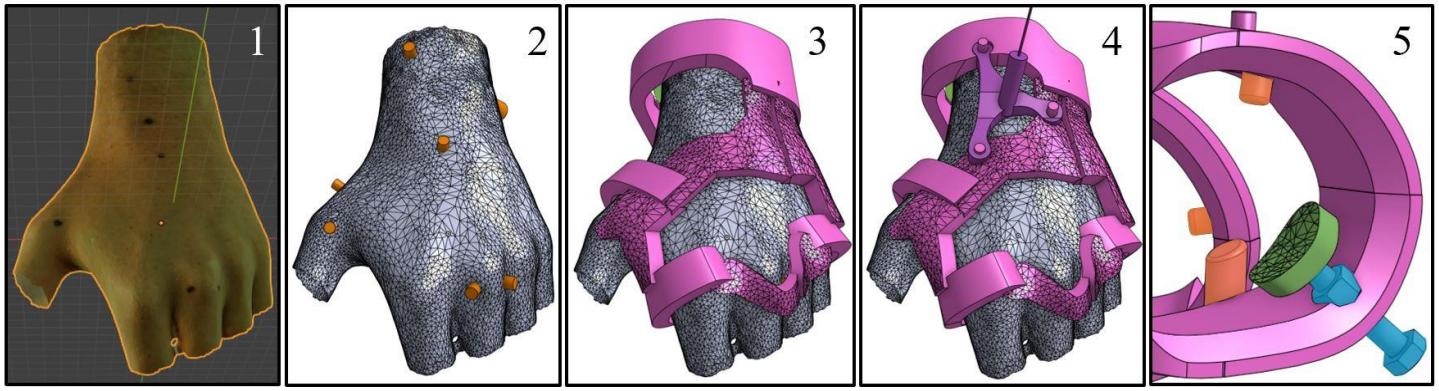

Figure 12. Steps taken to design a prototype guide that was used for testing. Orange: cylinders contacting the skin. Pink: Frame used to connect contact cylinders. Purple: guide part in line with the desired trajectory. Green: Part used to apply nesting force. Blue: bolt and nut used to adjust the nesting force.

of the prototype, and increasing the diameter if the discomfort at a certain contact point was too great.

Initially all contact surfaces were defined to be perpendicular to the skin. In practice however, at two contact locations the angle of the contact surface had to be adjusted in order to be perpendicular to the underlying bone. This was necessary for the cylinders on the palmar side of the ulnar and radial styloids (points 3 and 4 in Appendix II). This issue is further discussed in Section VI-B.

D. Connecting contact surfaces

The resulting cylinders were then connected by various sweeps and extrudes to form a single frame (Figure 12.3). These pieces were designed to ensure a stiff connection between all the contact surfaces, while leaving sufficient line of sight to locations of the hand that were necessary for the measurements which will be described in Section IV. After joining all the contact cylinders and connecting pieces together, the part was then split into an upper and lower half to allow for donning and doffing of the device. Locating pins were added to aide in the joining of the halves.

E. Drill guide

The desired drill trajectory was created by drawing a line through the two previously mentioned points. A rudimentary drill guide was then added based on this trajectory. First, a cylinder of 8mm diameter was extruded, the center of which coincided with the desired trajectory. This cylinder was then attached to the frame using a baseplate and three locating pins. This part serve two functions: one was used to digitally compare trajectories the accuracy measurements, and the other to serve as a point of engagement for the force in the stiffness measurements.

In order to calculate the moment generated by this force, a groove was added to the cylinder a fixed distance from the mid-plane of the hand. This plane was defined parallel to the coronal plane, and half way between the most volar and most palmar point of the wrist, measured at the carpal bones. The groove was then added 57mm volar of this plane.

F. Implementing nesting force

As mentioned in the previous Section II-C, a nesting force is required in addition to the 10 contact points. In order to achieve this, an additional part was extruded at the determined position. This part could then be adjusted by turning a bolt which was connected to the frame with an embedded nut. This allowed for the tightening of the guide to the hand. The surface area of this part could be greater since it does not contribute to the positioning accuracy, but instead applies a nesting force in the determined direction. A technical drawing of the resulting prototype can be found in Appendix III.

G. 3D Printing Prototypes

Using this design process, guides were made for the left hand of six participants. Four participants were male and two were female, with an average age of 23 (σ= 2.9) years. Participants were asked to reapply the two marks used to determine the trajectory to ensure that they would still be visible when they returned for testing nine days later. A photograph was also taken of these points in case the marks were removed. The participants were then instructed to hold the hand forwards with a straight wrist, and the fingers at downward angle of 45° while a scan was made.

Using this scan, the CAD model was then adjusted to match the specific anatomy of each participant, positioning the contact surfaces at the marked locations. The guide was then printed using PLA, with an infill of 10% and a layer thickness of 0.2 mm. The prototype was then painted black, and green spots were added. This was done on the advice of Manometric to improve the quality of the second scans.

A signed informed consent form was obtained from all participants for the making of these scans, as well as the measurements described in the following section. The form and accompanying information letter can be found in Appendix IV. Ethical approval for the measurements was obtained from the Human Research Ethics Committee of the TU Delft.

IV. Measurement Methods

A. Accuracy measurements

1) Measurement goal: After the prototypes had been printed, the participants returned for measurements to be done to determine if the device met the design requirements. One measurement was designed to measure how accurately the guide replicated the desired trajectory, and a second measurement setup was used to measure the stiffness of the connection between the guide and the hand.

The first measurement was taken to determine the accuracy and repeatability of the placement of the guide with respect to the hand. This was done by comparing a simulated drill trajectory based on the position of the guide with the desired trajectory designated by the previously mentioned marks on the hand. The outcomes of this measurement were the angle between the achieved and desired trajectories, and the x and y deviation of the achieved trajectory in the coronal plane.

2) Measurement protocol: First, the printed guide was donned on the participant and secured with medical tape. The nesting force was then gradually increased by turning the bolt until the participant indicated further tightening would cause too much discomfort. Subsequently, a scan was made of the hand and guide (Figure 13.A). This was repeated three times.

These scans were analyzed to determine the desired trajectory, as well as the simulated drill trajectory based on the position of the guide. The desired trajectory (cyan) was determined by drawing a line through the volar and palmar marks on the hand that had previously been used to design the guide (Figure 13.B).

The achieved trajectory (pink) was simulated by first positioning the digital model of the printed guide, including the guiding part, to match the scanned topology as well as possible (Figure 13.C). This step was necessary because if the scan was made with the guiding part attached, it disrupted the line of sight to the volar mark used to define the desired trajectory. Therefore the guiding part had to be matched onto the scan digitally.

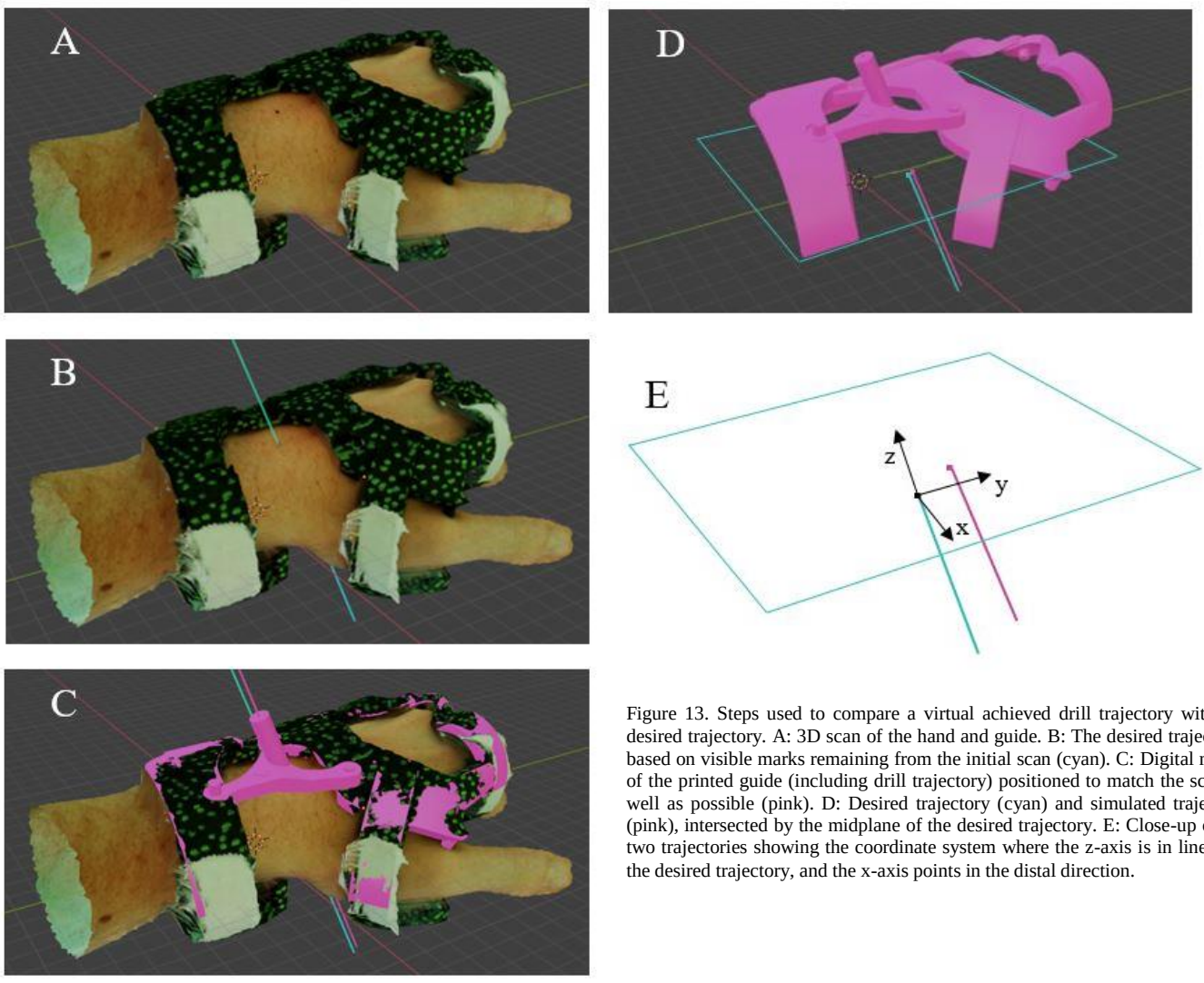

Figure 13. Steps used to compare a virtual achieved drill trajectory with the desired trajectory. A: 3D scan of the hand and guide. B: The desired trajectory, based on visible marks remaining from the initial scan (cyan). C: Digital model of the printed guide (including drill trajectory) positioned to match the scan as well as possible (pink). D: Desired trajectory (cyan) and simulated trajectory (pink), intersected by the midplane of the desired trajectory. E: Close-up of the two trajectories showing the coordinate system where the z-axis is in line with the desired trajectory, and the x-axis points in the distal direction.

A plane was then created orthogonal to the desired trajectory, halfway between where it entered and exited the hand (Figure 13.D). This mid-plane, and the resulting orthogonal planes are similar anatomic planes described in Section I, but varied slightly because the desired trajectory was not perfectly vertical. For simplicity, they will still be referred to according to the previously defined names. The resulting coordinate system (Figure 13.E) was used to measure the positioning error of the achieved trajectory with respect to the desired trajectory. The x and y distance between the origin and the point where the achieved trajectory intersected the coronal plane were measured as d_x and d_y. The angle between the trajectories was measured in both the transverse x-z plane (α), and the sagittal y-z plane (β).

B. Stiffness measurements

1) Measurement goal: As mentioned in Section I-D, while the stiffness of the guide with respect to the hand is important for the performance of the device, no information could be found pertaining to the nature and magnitudes of the deviating forces that can occur during drilling. This limited the degree to which a realistic loading situation could be recreated for measuring the stiffness. Due to this lack of information, as well as practical limitations, the decision was made to simply load the drill guide cylinder in each of the four planar directions.

Using the experimental setup shown in Figure 14, the influence of forces perpendicular to the drill guide on the position of the guide with respect to the hand were determined. This can help give an indication of how much guiding force the guide can give the surgeon while remaining sufficiently accurate. The outcomes of this measurement were two force deflection graphs, one for proximal-distal loading and one for radial-ulnar loading. These graphs were then used to estimate a stiffness k in each direction.

2) Measurement setup: For the measurement, the 3D printed guiding piece (shown in red) was attached to the frame of the guide. The cylinder was attached to a 45N load cell (Futek, 2) with woven fishing line which fell into the groove ensuring the line was connected 57mm away from the mid-plane of the hand. The force sensor was plugged into a CPJ signal conditioner (Scaime, 5) which amplified the signal to a range of -25N to 25N. This signal was fed to a NI-DAQ MX data acquisition device (National Instruments, 6), which was connected to a PC using LabView 2018 (National Instruments, 7).

Using a wide nut and a threaded rod (3), tension on the line could be gradually increased. A webcam (Trust,4) was positioned perpendicular to the line. The frame containing the threaded rod and webcam could be placed over the hand in various positions in order to apply a force in each planar direction.

3) Measurement protocol: After donning the guide and applying the nesting force, the arm of the participant was strapped to the measurement setup using Velcro and the line was attached to the guide. Marks were made on the hand using marker to observe the relative motion. Using a drill, the threaded rod was then turned, gradually increasing the tension in the line. Every 0.5 seconds, a still image was recorded as well as the corresponding force measurement. The tension was increased until the participant indicated more than slight discomfort (in most cases this occurred at a force of around 15N). This amount of force was observed to be much greater than the magnitude forces that generally occur during surgery but as mentioned before there are no sources available that confirm this. The measurement was repeated 3 times in each planar direction for a total of 12 runs.

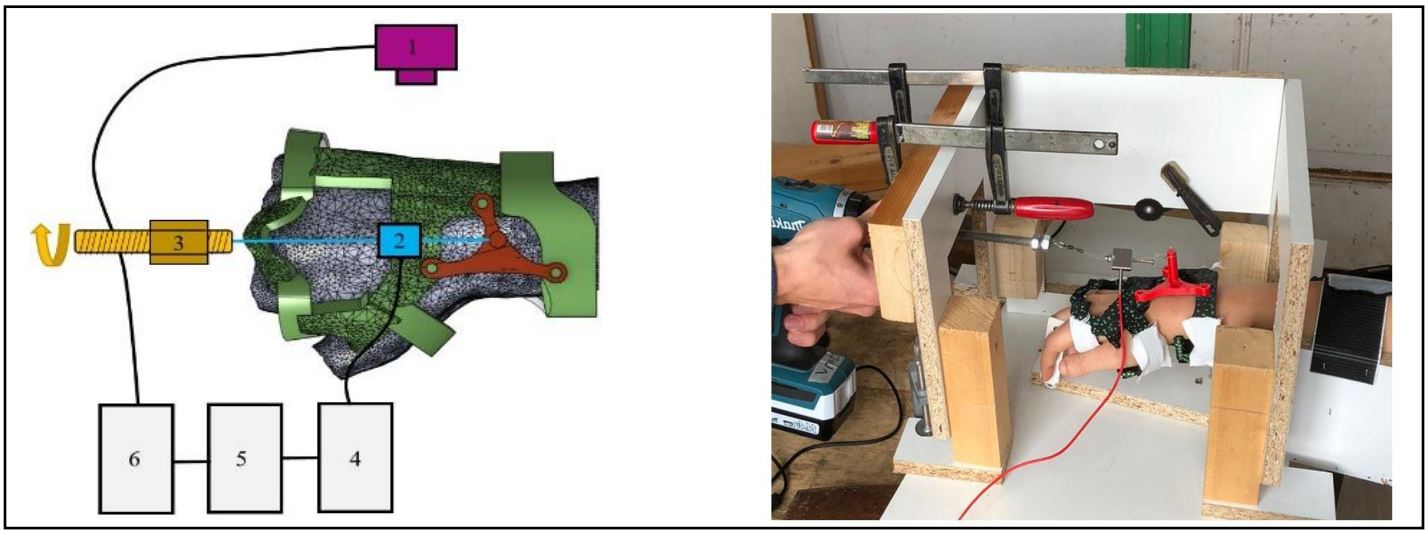

Figure 14. Test setup used to determine force displacement behavior of the guide with respect to the hand. 1: Webcam. 2: Load cell. 3: Nut and threaded rod. 4: Signal conditioner. 5: Data acquisition device. 6: PC running LabView 2018.

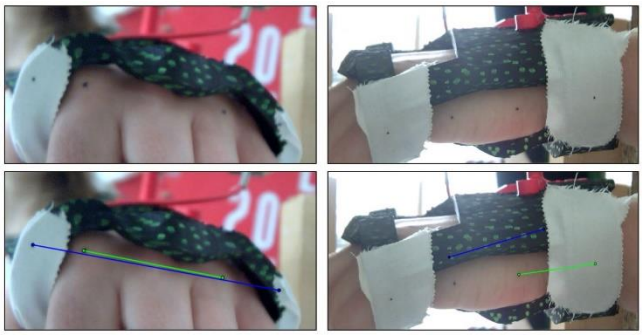

Figure 15. Webcam images showing the measurement lines added using Matlab. Left: lines to calculate change in angle about the frontal axis. Right: line used to measure translation along the frontal axis (green), and a line between two points on the guide used to scale pixels to millimeters.

The data from each run was then analyzed using Matlab (Appendix IV) to determine the change in angle between the guide and the hand. This was done at ten evenly spaced intervals between zero and the maximum measured force. At each interval a straight line was drawn between two determined points on the guide, and two points on the hand (Figure 15). The angle between these two lines was calculated, and the angle measured at zero force was subtracted from this value to give the rotation.

In addition, in the first frame a line was also drawn along the guide rod. Assuming the guide to be stiff, this was then used to calculate the angle between the force applied by the wire and the rod at each frame. Using the known distance between the wire and the mid-plane of the hand, and the angle of the rod, the moment could be calculated.

When applying the force in the anterior and posterior directions, the amount of rotation was marginal, so the translation in the direction of the force was calculated instead of a change in angle. This was done in a similar fashion, by measuring the change in distance between a point on the guide and a point on the hand. In order to convert the pixel distance to millimeters, the distance between two points on the guide, which could be measured afterwards, and were at a similar distance from the camera was used as a reference (Figure 15).

V. Measurement Results

A. Accuracy measurements

As shown in

Table 2, the results from the position measurements show an overall average α and β angle of 7.2° and 2.1° respectively. This falls well within the minimum requirements determined in Section I. The standard deviations of α and β were 3.3° and 2.7° respectively. Participant 1 had the highest α deviation at -12.2°, only just below the maximum allowable error. For α, participant 3 had the highest error at 5.3°. The angle α was negative in every measured trajectory, while β had both positive and negative values.

The average translational error at the mid-plane in the x and y direction were 2.5 mm and -0.6 mm respectively, with standard deviations of 2mm and 1mm. The average d_x thus exceeds the maximum acceptable value by 1.2mm while the average d_y was acceptable. Only participants two and five had d_x values within the acceptable range, while for d_y only participant one exceeded the acceptable error.

All 18 measured trajectories are visualized graphically in Figure 16, with each dot showing where the trajectory passes through the mid-plane of the hand, and the lines showing the trajectory to 8mm below this mid-plane. This length was chosen as it is half the length of the tunnel through the scaphoid, thus giving an indication of where the trajectory would exit bone. From the figure it is clear that the both the angular and translational errors were much greater in the x-direction. In addition, all the trajectories show an error in the positive x direction (corresponding to a negative α).

Figure also shows all 18 measured trajectories, but than in three dimensions instead of only the x-y plane. The volume through which an acceptable drill trajectory must pass is designated by three ellipses, one for the entry in to the scaphoid, one for the waist, and another for the exit. Despite all the angles being within the acceptable range, the larger translational errors result in only three trajectories falling entirely within the volume.

Table 2. Results of test 1 showing averages over the three measurements for each participant and the average across all measurements. Standard deviations of each value are given in parentheses.

Assessments	1	2	3	4	5	6	Average
α [°]	-12.2 (0.6)	-6.0 (2.2)	-10.4 (1.0)	-3.5 (1.1)	-5.9 (1.3)	-5.4(1.7)	-7.2 (3.3)
β [°]	0.1 (0.5)	1.6 (0.7)	5.3 (0.6)	-1.8 (0.4)	-1.8 (0.6)	-1.8 (0.8)	0.3 (2.7)
d_x [mm]	4.4 (0.2)	1.1 (0.8)	3.6 (1.2)	4.1 (0.3)	-0.7 (0.6)	2.2 (1.2)	2.5 (2.0)
d_y [mm]	-1.9 (0.2)	0.2 (1.2)	-0.6 (1.3)	-0.5 (0.3)	-0.4 (0.2)	-0.6 (0.4)	-0.6 (1.0)

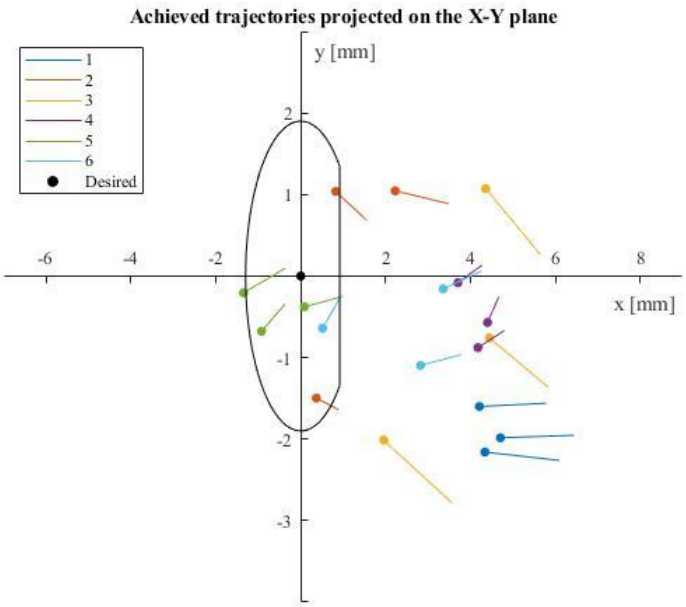

Figure 17. A graph showing the three measured trajectories of each participant. Dots shows the location where each trajectory intersects the midplane of the desired trajectory. Each line shows the trajectory to 8mm below the midplane. The black dot at (0,0) represents the desired trajectory which defines the z-axis. The black elipse shows the area on the mid-plane through which a trajectory must pas to be acceptable, defined in Section I-D.

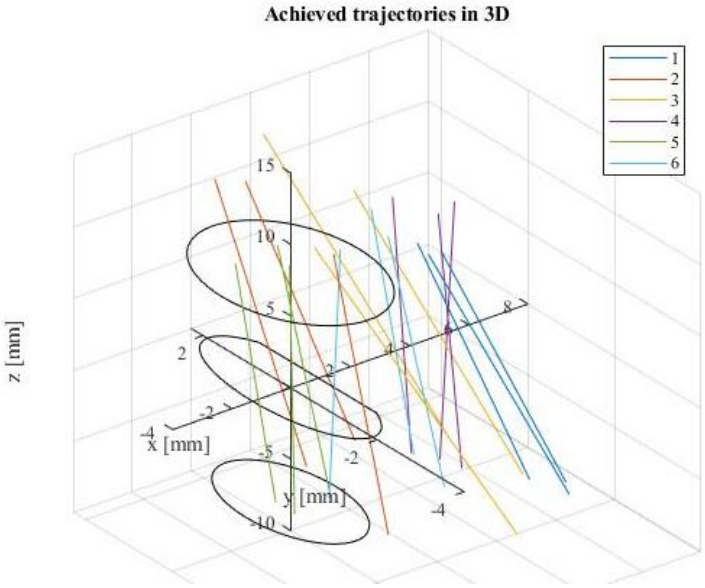

Figure 16. A graph in 3D showing the measured trajectories. The black ellipses display the volume through which the trajectories must pass to be acceptable.

B. Repeatability

Table 2Table 2 also shows the standard deviations per participant, which are much lower than the overall standard deviation. Averaging across all the participants, the standard deviation is 1.32° for α, 0.6° for β, 0.73 mm for d_x, and 0.6mm for d_y. This is also evident in Figure 16 as the trials for each participant are quite clustered, with the exception of two and three, who showed a greater spread, mainly in the y direction. Especially participant three was an outlier, showing both large angular errors, as well as large deviations between measurements.

C. Stiffness measurements

As mentioned in the Section IV-C, the main mode of movement under lateral loading was rotation. Therefore the results are best shown as a moment-rotation graph (Figure 18). Clockwise rotation (when viewed by the participant) is defined as positive, this is referred to as pronation. Supination (counterclockwise rotation) is thus negative. All the data points are shown as well as an average linear fit line for each participant. A linear fit was deemed to be appropriate based on observation of the data points. Since each direction was measured separately, a separate fit was made for each. Taking the inverse of the slope of these lines gives a value for the rotational stiffness (*Nm/°*) of the guide on the hand. These values are listed in Table 3. One measurement of participant 4 in pronation was excluded when calculating the means as it showed stiffness more than 100 times higher than the other two measurements from the same participant.

Under lateral loading translation was the main mode of movement. Therefore the results of the anterior and posterior forces are best shown in a force deflection graph (Figure 19), with movement away from the body (anterior) is defined as positive. Linear fit lines were calculated in the same way as before. In this case, taking the inverse of the slopes gives the translational stiffness in *N/mm*.

The values of the average rotational stiffness are similar in both directions at 0.45 *Nm/°* and 0.41 *Nm/°*. The standard deviations of these values are very high which can also be

Table 3. Results of test 2 showing averages over the three measurements for each participant and the average across all measurements. Standard deviations of each value are given in parentheses.

Assessments	1	2	3	4	5	6	Average
$k_{supination}\left[\frac{Nm}{°} \times 10^{-1}\right]$	5.0 (1.7)	7.1 (3.2)	0.9 (0.2)	1.7 (0.1)	8.2 (1.8)	5.9 (1.7)	4.5 (3.1)
$k_{pronation}\left[\frac{Nm}{°} \times 10^{-1}\right]$	3.9 (2.7)	1.8 (0.3)	0.3 (0.1)	1.8 (0.7)	7.2 (2.1)	8.8 (7.9)	4.1 (4.4)
$k_{anterior}\left[\frac{N}{mm}\right]$	5.0 (1.0)	5.3 (1.1)	4.5 (1.8)	3.4 (0.4)	4.6 (0.5)	7.2 (2.5)	5.0 (1.7)
$k_{posterior}\left[\frac{N}{mm}\right]$	3.9 (0.7)	6.0 (1.4)	5.4 (0.7)	8.0 (1.5)	14.6 (3.3)	11.8 (2.4)	8.3 (4.2)

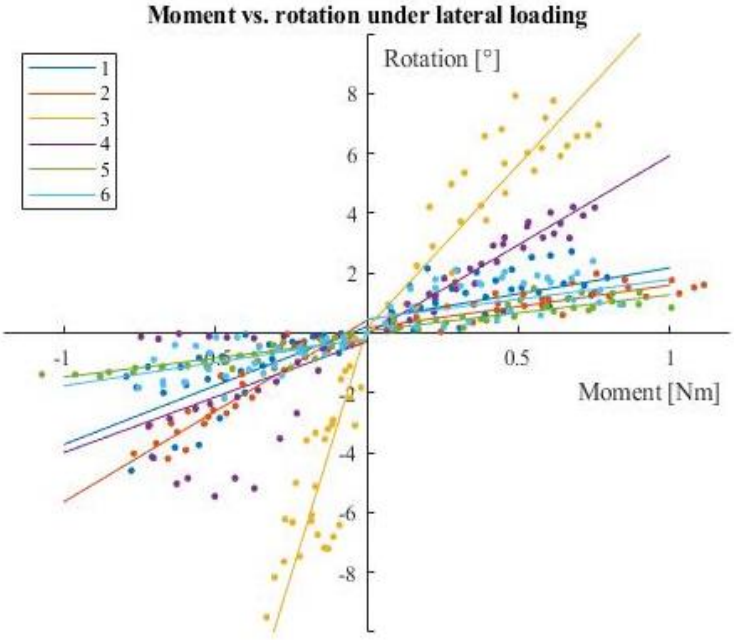

Figure 18. A graph showing the moment vs. rotation behavior of the guide with respect to the hand. Positive moment is defined as clockwise about the frontal axis (pronation for the left hand).

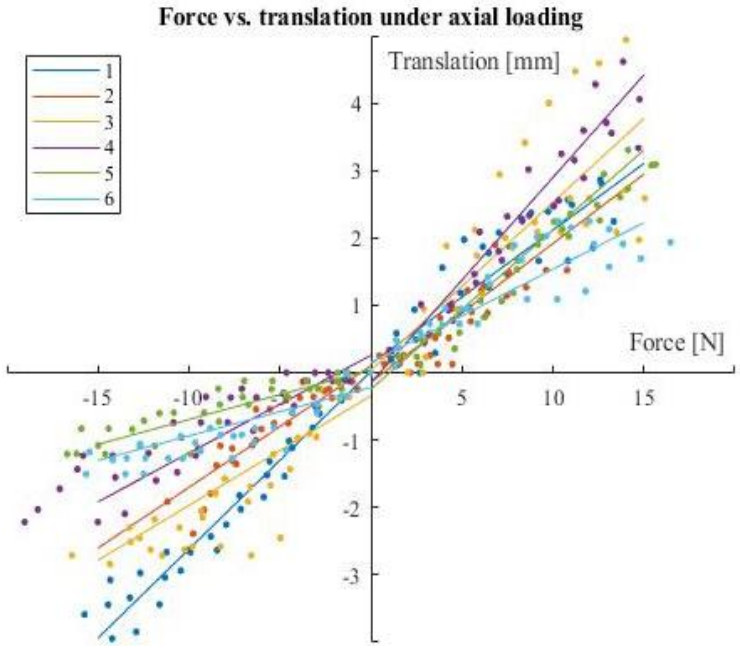

Figure 19. A graph showing the force vs. translation behavior of the guide with respect to the hand. The force is defined as positive in the anterior direction.

observed from the large variation of slopes in the graph. In particular participant three showed a much lower stiffness than the rest. Despite the average stiffness being quite similar in both directions, within each participant the stiffness sometimes varied greatly between pronation and supination.

As can also be seen in the graph, participant three was a clear outlier with regards to the rotational stiffness. In supination the stiffness was a factor of 5 lower than average, and in pronation a factor of almost 14.

For the translational stiffness there was a large difference between the anterior and posterior directions with averages of 5.0*N/mm* and 8.3 *N/mm* respectively. The results were more consistent than under lateral loading with the standard deviations relative to the mean being 34% and 50 % as opposed to 69% and 107%.

D. Qualitative observations

1) Defining contact locations: In addition to these measured results, various observations were made in the process of manufacturing and testing the prototypes. Firstly, personal anatomical variations made it more challenging than expected to mark the desired contact locations on every participant. For example, the prominence of the ulnar styloid varied greatly per participant. With a less prominent styloid, it was more challenging to achieve the planned constraint direction. Another point that had showed similar problem was at the bottom of the radial styloid.

2) Positioning the guide: During testing it sometimes required a few attempts to properly don the guide on the hand, but as the researcher became more experienced this process became more consistent. If the guide was misaligned, the participant reported greater discomfort when closing the guide or applying the nesting force. This was useful feedback, as then the guide could be repositioned in the desired position.

3) Constraining MC1: Three of the six prototypes did not constrain the knuckle of the thumb very well. For participants 2 and 6, the guide was too loose, allowing the thumb to rotate towards the fingers. For participant 5, the opposite was the case, with the guide being very tight, causing greater discomfort than at the other contact points.

4) Discomfort: The level of discomfort during testing remained tolerable for all participants. The guide was only donned for short periods of time however (up to 10 minutes), with participants reporting an increase in discomfort as time went on. Figure 20 shows the marks left on the skin of a participant after testing.

Figure 20. Image of a participants hand after having donned the guide for around 10 minutes.

VI. Discussion

A. Measurement results

1) Accuracy measurement: The results of the simulated trajectories suggest that the prototype design was close to being sufficiently accurate but had some shortcomings. Despite only 3 of the 18 trajectories falling completely within the acceptable volume, the average error was lower than the required values in three of the four assessments. The errors in both rotation and translation were greatest in the lateral (x,y) plane which clearly indicates a systematic error in the prototype.

This could have been caused by a variety of factors. One reason that the errors were greatest in the lateral direction purely has to do with the geometry of the hand and wrist. The forearm is almost cylindrical in shape. Intuitively one can imagine that it is much more difficult to stop a cylinder from turning about its longitudinal axis than its lateral one. The reason for this has to do with the amount moment that the constraints can exert on the body. As the cross section becomes more circular, all of the directions normal to the surface intersect closer to a single point. In the limit case of a perfect cylinder it would even be impossible to prevent it from rotating as none the forces perpendicular to the surface can exert any moment on the body.

Another geometrical factor that makes it more difficult to constrain rotation about the frontal axis is the aspect ratio of the system as a whole. The maximum possible distance between two constraints in the x-direction is around two thirds as big as in the y-direction. The problem with this is that as constraint points get closer to each other, small variations in the constraint location cause increasingly large rotational errors.

Despite giving a positive preliminary indication of the potential of this design, both measurement methods are limited in accuracy and realism by a variety of factors. For the accuracy measurement one of two main sources of inaccuracy were errors in matching the digital model of the guide to the scan of the guide and hand (Figure 13. C). Because the surface resolution of the 3D scan was not great, it was a time consuming task to position the digital model onto it as accurately as possible. Even then, there always remained slight deviations between the two surfaces, which directly translate to deviations in the angle and position of the simulated trajectory.

The second main source of measurement inaccuracy was the choice to base the desired trajectory on marks on the skin. Because the skin is flexible, it is possible that donning the guide caused the marks defining the trajectory to move a little due to the contact points pushing into the skin. In addition, because the marks had to be reapplied to stay visible, there is a chance that their location changed slightly in the 9 days between the scans.

Both of these problems stem from the fact that the act of drilling, for which the device is designed could not actually be performed. This resulted in the need to simulate an achieved drill trajectory digitally in this way.

2) Stiffness measurement: The stiffness of the connection between the prototype guides and the hand was measured in order to gain insight into how loads on the drill guide would affect the trajectory being drilled. While the experimental results give a general picture of the order of magnitude of the stiffnesses in different directions, much more information is still needed to make useful conclusions about the performance of these guides in surgery.

Most importantly, information is needed about forces and moments that the guide must correct during surgery. With this information and the measured stiffnesses, it could be concluded if the trajectory would remain within the required tolerances under theses loads. As previously mentioned, no such literature could be found, which makes it difficult to apply the results to actual surgery at this moment.

Another step that can be taken is to investigate the correlation between the stiffness of the guide on the hand and the magnitude of the nesting force. This can be done by repeating the experiment with a varying and measurable nesting force. The nesting force could be measured by adding a spring of known stiffness to the nesting force mechanism, which could then be tightened to a certain distance.

The main shortcoming of the stiffness measurements was the realism of the load case. Once again this problem arose because actual drilling could not be performed, and this had to be simulated. The main difference in actual drilling would be that as soon as the drill enters the bone, the point of the drill can no longer translate with respect to the hand. This would greatly increase the stiffness, as the drill (and thus the guide) can no longer move freely across the hand. This much more complex loading situation is however very impractical to simulate without being able to drill into the hand.

Therefore, the next step in the validation of the prototype should be to perform a cadaver study allowing the guide to actually be used for drilling. This would enable the use of CT-scans as opposed to surface scans (the benefits of which are discussed in the next section) and allow for much simpler comparison between the desired and achieved trajectories. This would also eliminate the need to first study and then attempt to replicate the loads that occur during drilling, although this can still be interesting for the modelling and design of further devices.

3) Importance of stiffness: In Section I-4, the importance is expressed of achieving a stiff connection between the guide and the hand to aid the surgeon during drilling. In practice however, this may have a less important role in accurate drilling than first thought. Based on personal observation of surgeons using other kinds of PSI drill guides, the largest part of their use is actually aiding the surgeon in positioning the drill in the required trajectory prior to the drill entering the bone. Once the actual drilling starts, the entry location into the bone is decided, and as the drill penetrates a bit deeper, the trajectory is also largely fixed since drills

tend to drill in a straight line. Thus the main function of the drill guide actually occurs before the drilling starts, when the forces acting on the drill are minimal. Stiffness may be of greater importance however if we consider applications of this external PSI beyond drilling which are discussed later in this section.

B. Prototype

1) Contact assumptions: Throughout the design process, the assumption was made that the direction of constraint was perpendicular to the skin at all the selected points. However, despite only selecting points where the bone was close to the surface of the skin, the reality was slightly different. In practice the direction of constraint was actually perpendicular to the underlying bone surface, as opposed to the surface of the skin. For certain points such as the knuckle of the middle finger this made no difference, as the skin there has very little indentation, lies parallel to the underlying bone.

At other points however the amount of soft tissue between the skin and bone varied by a few millimeters. The result of this is that the surface of the skin has a different normal than that of the bone, which in turn results in the constraint acting in a different direction than expected. A clear example of this was the contact point at the bottom of the wrist, at the base of the thumb as shown in Figure 21. Such a difference in angle can have a large impact on the ability of that point to constraint certain motion.

2) Surface scan vs. CT-scan: This was also one of the main shortcomings of using a surface scan as opposed to a CT-scan. Because only a surface scan was available, no information was available about the thickness of the skin at the contact locations, nor about the underlying bone structure. Because this information was missing, the indentation depth of each point had to be estimated, as well as the location that would have the desired constraint direction on the bone surface. This was especially evident in combination with the anatomical variations mentioned in the previous section, which made it difficult to accurately place certain contact points.

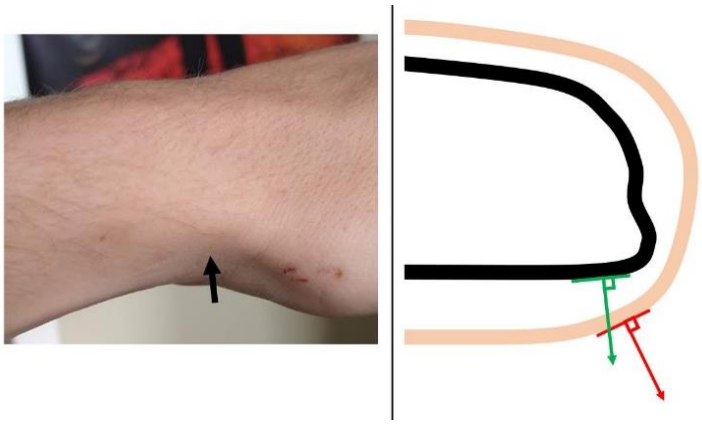

Figure 21. Image of wrist with the bottom of the radial styloid marked by a black arrow (left). Cross section of the wrist at that point showing the surface of the bone (black), and the surface off the skin (pink) as well as the respective normals at the marked location.

Furthermore, without information about the position of the scaphoid and lunate, the assumptions made in Section II-B about the movability of these bones with respect to the surrounding anatomy cannot be validated. For the comparison of the trajectories, the desired trajectory was defined by points on the skin, when in practice, the desired trajectory will be defined by points on the scaphoid.

3) Hand pose: Another factor that caused differences between prototypes' and the planned constraint directions was the pose of the hand. While participants were clearly instructed on the angle in which their fingers and wrist had to be held in the sagittal plane, the instructions were as clear for other aspects of the pose of the hand. The scans showed quite some variation in radial and ulnar deviation, as well as in the position of the thumb. Depending on the constraints, these factors can have a large impact on the performance of the chosen constraint set.

C. Selection of contact points

1) Systematic approach: In Section II, EC design principles were used to determine a suitable set of contact points to fully constrain the hand and wrist. This was done successfully through trial and error, and by adjusting the position of the hand to create additional options for constraint directions. Because of the use of a trial and error approach, many simplifications were made in order to find a solution in a reasonable amount of time. While the found solution did satisfy the mathematical requirements and resulted in a prototype that performed reasonably well, it is quite probable that better solutions could be found by using a more systematic approach.

Instead of using trial and error, an algorithm can be used to search the entire solution space, most likely resulting in a variety of different possible solutions. This can save a lot of time, but more importantly gives the opportunity to choose an optimal solution based on additional design wishes, such as which anatomy to leave free for the surgeon, or minimizing the reaction forces on the contact points (this is further discussed in the next section).

Implementing such an algorithm can also reduce the need for these simplifications, resulting in a solution that better matches reality. The main simplification that could be avoided is the decoupling of the position and direction vectors of each constraint. If the allowable contact areas are taken directly from a 3D scan of the hand, the direction of constraint at any given location is simply a vector normal to the surface at that location. If the ideal constraint locations can be calculated directly from the 3D scan, they can also be optimized per patient. This can improve performance since it was observed during testing that the relevant anatomic structures varied quite a lot per participant.

The algorithm could be further expanded by also taking into account various positions of the bodies with respect to each other. The hand can be held in a range of different positions without interfering in the procedure. This adds even more options to vary the possible constraint directions,

allowing for further optimization of the constraints. Adjusting the angle of the fingers for example proved to be effective in constraining the hand in the frontal direction. Applying this concept to the thumb as well has the potential to also improve the constraints in the lateral direction, which were shown to be lacking in the current prototype.

2) Force analysis: One of the advantages of using an EC design is that the reaction forces at each contact point can be easily calculated. In this research this property was only used to check if all of the reaction forces were positive which confirmed that the system was fully constrained. However, a more detailed analysis of the reaction forces can allow for safer and more accurate design in the future.

Ideally, the constraint set could be optimized to ensure that each contact point is loaded equally. This can greatly reduce the peak stresses on the skin, allowing the nesting force to be increased without damaging the body. This in turn should result in a stiffer connection between the guide and the body.

The magnitude of the peak stresses on the hand can also be used to determine for how long the guide can be safely donned. As mentioned in Section III-C, the size of the contact surfaces was limited by the discomfort due the pressure on the skin. For the prototypes this was not a main concern since the guide were only donned for short periods of time. To be used in surgery however, it must be safe for the guide to be donned for longer periods of time without causing damage to the skin or underlying structures. As seen in Figure 20, wearing the prototype for a duration much shorter than an average surgery already left quite severe marks.

No studies were found however that detail the relation between pressure and duration for which skin can be safely loaded. However, studies focused on the formation of bedsores do give an indication of safe pressure for a given timespan [29] (Figure 21). This shows that for a surgery of around two hours, a maximum pressure of 150 mmHg can be safely applied to the soft tissue.

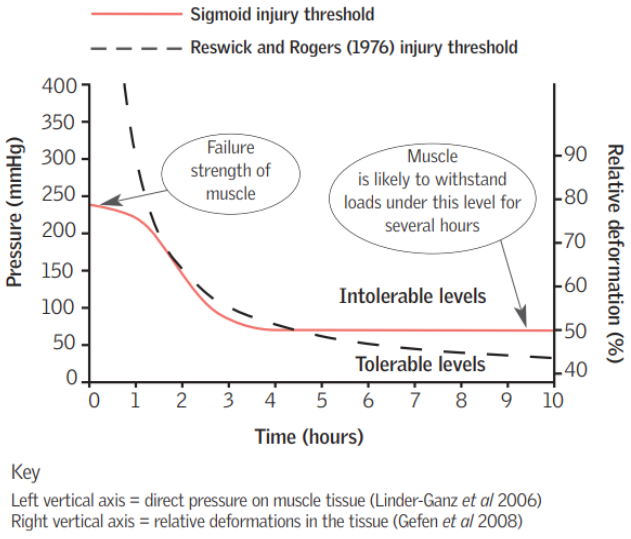

Figure 22. The Reswick and Rogers (1976) pressure-time curve. Source [27]

3) Constraint stability: Another important insight that can be gleaned from the mathematical model is the effects of small variations in the constraints on the performance of the system. A set of constraint locations can be considered stable if small variations in a constraint location or direction, do not prevent the system from being fully constrained. A brief stability analysis was done on the set of constraints used in the prototype by repeating the calculation while slightly varying the direction of each constraint in all directions. It was found that one constraint was not stable. If the constraint at the bottom of the radial styloid (Figure 21) was angled slightly towards the wrist as shown by the red arrow, the system was no longer fully constrained. This, combined with the difficulties discussed in Section VI-A2, is likely to have had a large influence on the large errors in the lateral direction.

D. Comparison to previous studies

In Section I-B it was mentioned that three studies had been found that applied an external PSI to the hand in order to place a screw through the scaphoid, as opposed to drilling a tunnel. While this application is slightly different, these studies can still give an indication of how good the achieved accuracy is compared to similar devices.

The work of Salabi [15] is most straightforward to compare as the same metrics were used to report the accuracy, namely the displacement at the mid-plane of the scaphoid (d_x and d_y) and the angles in the transverse and sagittal planes (α and β). In addition, these measurements were also taken from screw placed using the conventional technique of fluoroscopic guidance, this gives a control group to the data. Table 4 shows that the errors achieved in this thesis are slightly higher than their PSI device, but lower than those of traditional methods. Notably, the guide of Salabi showed greater deviations in α than in β, contrary to the results of this prototype.

Wan et. al [7] reported their results as a single angle of deviation, and the distance deviation at the point of entry into the scaphoid. For better comparison the average overall angle was calculated for the trajectories measured in this Section IV-B giving an average angle of 7.7°. This is higher than the value reported by Wan (2.7°). Yin et. al [11] did not report any metrics of the performance.

Table 4. Comparison of the average trajectory errors compared to those in the work of Salabi et al. [15]. Standard deviation is shown in parenthesis. PSI: Patient specific instrumentation, CF: Conventional fluoroscopy.

Assesments	Average	Salabi (PSI)	Salabi (CF)
α [°]	-7.2(3.3)	1.6(0.7)	13.8(4.6)
β [°]	0.3(2.7)	3.3(2.4)	9.2(2.7)
dx [mm]	2.7(2.0)	0.3(0.2)	1.2(0.5)
dy [mm]	1.0(1.0)	0.3(0.2)	1.3(0.9)

As previously mentioned, all three of these studies used a guide based on the matching the entire surface of the wrist as opposed to the distinct points used in this thesis. However, because of the shortcomings of this prototype, it is too soon to conclude which method works better in terms of positioning accuracy. A controlled study comparing these two methods should be performed in order to better understand the advantages and disadvantages of each.

E. Further instrumentation

This research focused on the drilling of a tunnel through the scaphoid, which was guided using a simple cylindrical shaft. Many other parts of the surgery may also benefit from some form of guidance however. Once sufficiently accurate and stiff connection is achieved between the guide and the bod, other parts can be added onto the device that guide other instruments as well. For example, after drilling, the scaphoid must also be restored to its correct anatomical position. This could be guided by inserting a k-wire in the scaphoid which can then be used as a joystick which can subsequently be guided to the desired position. The required motion could be guided by a specifically shaped slot in the guide as shown in Figure 22. Other steps such as placing the sutures endoscopically and placing the k-wires for fixation may also benefit from some form of guidance and should be investigated further.

F. Viability of external PSI

Looking beyond the modified Brunelli procedure, the application of EC design principles also gives insight into the possibilities and limitations of PSI that attach to the outside of the skin. In this research the challenge of rigidly attaching the guide to the largely soft exterior of the body was approached by limiting contact to locations where the bones lie just under the skin. For the hand and wrist, this works, as sufficient locations could be found to fully constrain the relevant anatomy.

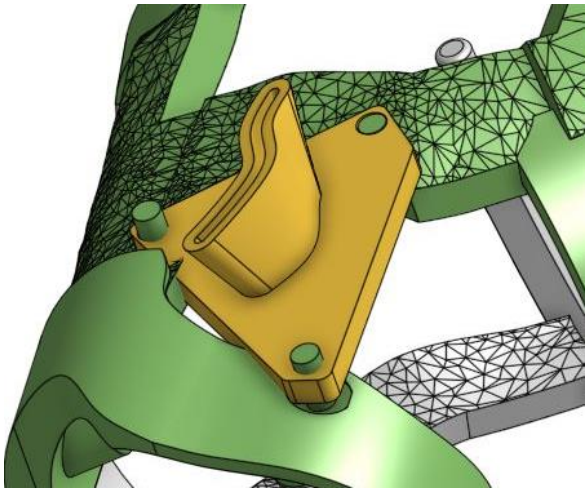

Figure 23. An impression of a guide piece designed to aid in the repositioning of the scaphoid, using a k-wire as a joystick.

For other parts of the body however this is probably not the case. For any given anatomy, the minimum amount of constraints can be calculated and is at least 6 as at least one body needs to be constrained for guidance in any surgery. Thus, the anatomy must have at least 6 ‘bony’ locations in order for this approach to work. Furthermore, these locations must also allow for the constraints to be placed in a way that they all constrain a different DOF.

A possible solution to this limitation is to implement other types of constraints beyond simple contact that remove more than one DOF. A promising option is to pin the guide to the bone through the skin with a k-wire. So called percutaneous pinning is commonly used in orthopedic surgery and causes little damage to the skin or the bone [30]. This is also the method employed by external fixators as mentioned in Section I-A. A constraint like this can constrain two extra DOFs, namely the two translations parallel to the contact surface. This makes the surgery slightly more invasive, but can greatly increase the variety of constraint sets available.

VII. Conclusion

In this research, the first steps were made to design a patient specific surgical guide that could be attached to the outside of the hand with the purpose of aiding a surgeon in performing a modified Brunelli procedure. The main challenge of connecting such an external guide to the body with sufficient accuracy was approached by applying the principles of exact constraints, from the field of precision mechanism design.

Applying this concept successfully resulted in a theoretical basis for determining the minimal amount of constraints needed, and subsequently choosing where the guide should contact the hand or wrist. Due to the statically determinant nature of an EC design, the reaction forces at each contact location could also be calculated. This provides a basis for many further design choices and optimizations in the future.

Furthermore, the steps taken in this research to first createa simplified model of the anatomy, and then perform kinematic analysis can be applied to other surgeries and parts of the body. Due to the limitation of relying on the bone to be close to the surface of the skin, this method of external attachment is useful for body parts with many bony landmarks, such as the hand/wrist or foot/ankles, but may not applicable to other parts of the body.

The experimental validation of the calculated points using 3D printed prototypes showed promising results, although the prototypes did not fully achieve the accuracy necessary to perform the procedure. Taking into account the various limitations in the experimental process, such as the use of a surface scan instead of a CT-scan, and the simplifications made in determining the contact locations, it can be concluded that the necessary accuracy can be achieved in the future.

In addition to drilling, other instrumentation can be added to the established frame to aid surgeons in other steps of the surgery, such as bone reduction and suturing. Looking further, the basic step of establishing a frame that is fully constrained with respect to the internal anatomy of the wrist gives rise to a myriad of possibilities for instrumentation in surgical procedures. In the future this can result in procedures becoming faster, more accurate, and much less reliant on surgeon experience. This in turn can reduce costs, and make complex surgeries more accessible to people without access to highly specialized surgeons.

ACKNOWLEDGEMENTS

The author would like to thank Manometric for granting access to their ManoX scanner and taking the time to process the large amount of scans. Furthermore the author would like to thank the Reinier de Graaf Gasthuis and especially dr. Gerald Kraan for allowing him to observe a modified Brunelli procedure being performed, as well as his invaluable medical expertise. Lastly the author would like to thank Jos van Driel and the 3me Meetshop for supplying the knowledge and equipment needed to perform the stiffness measurements.

REFERENCES

[1] K. C. Wong, "3D-printed patient-specific applications in orthopedics," *Orthopedic Research and Reviews*, vol. 8. Dove Medical Press Ltd., pp. 57–66, 2016.

[2] F. Conteduca, R. Iorio, D. Mazza, and A. Ferretti, "Patient-specific instruments in total knee arthroplasty," *Int. Orthop.*, vol. 38, no. 2, pp. 259–265, Feb. 2014.

[3] V. Y. Ng, J. H. DeClaire, K. R. Berend, B. C. Gulick, and A. V. Lombardi, "Improved accuracy of alignment with patient-specific positioning guides compared with manual instrumentation in TKA," in *Clinical Orthopaedics and Related Research*, 2012, vol. 470, no. 1, pp. 99–107.

[4] T. Hananouchi, M. Saito, T. Koyama, N. Sugano, and H. Yoshikawa, "Tailor-made Surgical Guide Reduces Incidence of Outliers of Cup Placement," *Clin. Orthop. Relat. Res.*, vol. 468, no. 4, pp. 1088–1095, 2010.

[5] M. Kunz, B. Ma, J. F. Rudan, R. E. Ellis, and D. R. Pichora, "Image-guided distal radius osteotomy using patient-specific instrument guides," *Journal of Hand Surgery*, vol. 38, no. 8. W.B. Saunders, pp. 1618–1624, 01-Aug-2013.

[6] D. J. Graham, H. D. S. Clitherow, H. P. Singh, E. C. Clarke, B. J. Smith, and M. A. Tonkin, "The Effect of Extensor Tendon Adhesions on Finger Motion," *J. Hand Surg. Am.*, vol. 44, no. 10, pp. 903.e1-903.e5, Oct. 2019.

[7] S. xiang Wan, F. bin Meng, J. Zhang, Z. Chen, L. biao Yu, and J. jing Wen, "Experimental Study and Preliminary Clinical Application of Mini-invasive Percutaneous Internal Screw Fixation for Scaphoid Fracture under the Guidance of a 3D-printed Guide Plate," *Curr. Med. Sci.*, vol. 39, no. 6, pp. 990–996, 2019.

[8] M. Deng, H. Cai, W. Fang, and X. Long, "Three-dimensionally printed personalized guide plate for percutaneous radiofrequency thermal coagulation in idiopathic trigeminal neuralgia," *Int. J. Oral Maxillofac. Surg.*, vol. 47, no. 3, pp. 392–394, Mar. 2018.

[9] L. G. Zhang, M. H. Deng, X. Long, and Z. Z. Wang, "3D printing navigation template-guided percutaneous radiofrequency thermocoagulation for V2 trigeminal neuralgia treatment," *Hua Xi Kou Qiang Yi Xue Za Zhi*, vol. 36, no. 6, pp. 662–666, Dec. 2018.

[10] L. Zhang *et al.*, "Three-dimensional printing of navigational template in localization of pulmonary nodule: A pilot study," *J. Thorac. Cardiovasc. Surg.*, vol. 154, no. 6, pp. 2113-2119.e7, Dec. 2017.

[11] H. wei Yin, J. Xu, and W. dong Xu, "3-Dimensional Printing–Assisted Percutaneous Fixation for Acute Scaphoid Fracture: 1-Shot Procedure," *Journal of Hand Surgery*, vol. 42, no. 4. W.B. Saunders, pp. 301.e1-301.e5, 01-Apr-2017.

[12] R. Wang, Y. Han, and L. Lu, "Computer-assisted design template guided percutaneous radiofrequency thermocoagulation through foramen rotundum for treatment of isolated V2 Trigeminal Neuralgia: A retrospective case-control study," *Pain Res. Manag.*, vol. 2019, 2019.

[13] M. Zhang *et al.*, "Evaluation of a Three-dimensional printed guide and a polyoxymethylene thermoplastic regulator for percutaneous pedicle screw fixation in patients with thoracolumbar fracture," *Med. Sci. Monit.*, vol. 26, pp. e920578-1, Jan. 2020.

[14] J. Li, J. S. Lin, Y. Yang, J. C. Xu, and Q. Fei, "3-Dimensional printing guide template assisted percutaneous vertebroplasty: Technical note," *J. Clin. Neurosci.*, vol. 52, pp. 159–164, Jun. 2018.

[15] V. Salabi, G. Rigoulot, A. Sautet, and A. Cambon-Binder, "Three-dimensional-printed patient-specific Kirschner-wire guide for percutaneous fixation of undisplaced scaphoid fractures: a cadaveric study," *J. Hand Surg. Eur. Vol.*, vol. 44, no. 7, pp. 692–696, Sep. 2019.

[16] J. E. Bible and H. R. Mir, "External Fixation," *J. Am. Acad. Orthop. Surg.*, vol. 23, no. 11, pp. 683–690, Nov. 2015.

[17] P. Koutsogiannis and T. J. Dowling, *Halo Brace*. 2020.

[18] "Hand Fractures | Common Hand Injury | Dr. Gordon Groh." [Online]. Available: https://www.drgordongroh.com/orthopaedic-injuries-treatment/hand-wrist/hand-fractures/. [Accessed: 12-Nov-2020].

[19] C. ALLBURY *et al.*, *Advanced Anatomy*, 2nd ed. 2018.

[20] I. M. Bullock, J. Borras, and A. M. Dollar, "Assessing assumptions in kinematic hand models: A review," in *Proceedings of the IEEE RAS and EMBS International Conference on Biomedical Robotics and Biomechatronics*, 2012, pp. 139–146.

[21] M. Garcia-Elias, A. L. Lluch, and J. K. Stanley, "Three-ligament tenodesis for the treatment of scapholunate dissociation: Indications and surgical technique," *J. Hand Surg. Am.*, vol. 31, no. 1, pp. 125–134, Jan. 2006.

[22] A. Slocum, "Kinematic couplings: A review of

design principles and applications," *Int. J. Mach. Tools Manuf.*, vol. 50, no. 4, pp. 310–327, Apr. 2010.

[23] T. Parsons, "Bones of the Hand, 3D model," *Sketchfab*, 2017. [Online]. Available: https://sketchfab.com/3d-models/bones-of-the-hand-08346960edc7408d9d4567c7e1966bb9. [Accessed: 12-Nov-2020].

[24] F. W. Werner, W. H. Short, M. D. Fortino, and A. K. Palmer, "The relative contribution of selected carpal bones to global wrist motion during simulated planar and out-of-plane wrist motion," *J. Hand Surg. Am.*, vol. 22, no. 4, pp. 708–713, Jul. 1997.

[25] Sunagawa, Koike, Kijima, Nakashima, and Ochi, "Role of the Scaphoid Motion during Thumb Opposition."

[26] M. El-Shennawy, K. Nakamura, R. M. Patterson, and S. F. Viegas, "Three-dimensional kinematic analysis of the second through fifth carpometacarpal joints," *J. Hand Surg. Am.*, vol. 26, no. 6, pp. 1030–1035, Nov. 2001.

[27] K. L. Kumar, *Engineering Mechanics*, 3e ed. Tata McGraw-Hill Education, 2003.

[28] A. Hammond, "Establishing A Quantitative Foundation for Exactly Constrained Design," *All Theses Diss.*, 2003.

[29] A. Gefen, "Reswick and Rogers pressure-time curve for pressure ulcer risk. Part 2.," *Nurs. Stand.*, vol. 23, no. 46, pp. 40–44, Jul. 2009.

[30] "Percutaneous Pinning - an overview | ScienceDirect Topics." [Online]. Available: https://www.sciencedirect.com/topics/medicine-and-dentistry/percutaneous-pinning. [Accessed: 12-Nov-2020].

APPENDIX I - MATLAB CODE USED TO VERIFY A SET OF CONTACT LOCATIONS

```
%TestConstraints.m
%Olivier Hiemstra
%11/11/2020

syms f1 f2 f3 f4 f5 f6 f7 f8 f9 f10 f11 mj1 mj2 fj1x fj1y fj1z fj2x fj2y fj2z
clear all
%% Constraints Model
% Body 1
c1=[29.37,4.9,11.027];
d1=[0,0,-1];
c2=[36.313,.787,1.9];
d2=[-1,0.5,1];
c3=[31.939,21.673,0];
d3=[0,0,1];
c4=[0,14.078,10.92];
d4=[1,0,1];

% Body 2
c5=[46.939,34.787,9];
d5=[-1,1,0];
c6=[51.334,45.453,4.472];
d6=[0,0,1];
c7=[50.409,49.234,11.344];
d7=[1,-1,-1];

%Body 3
c8=[17.461,33.439,11.978];
d8=[0,0,-1];
c9=[16.913,68.889,3.289];
d9=[0,0,1];
c10=[12.196,70.598,7.6];
d10=[1,-1,0];
c11=[20.517,70.965,6.916];
d11=[-1,-1,0];
%Joints
cj1=[35.705,20,10.922];
cj2=[17.407,20,10.922];


%% Build model
D=[d1;d2;d3;d4;d5;d6;d7;d8;d9;d10;d11];
C=[c1;c2;c3;c4;c5;c6;c7;c8;c9;c10;c11];
CJ=[cj1;cj1;cj1;cj2;cj2;cj2];


for i=1:length(D)
    D(i,:)=D(i,:)/norm(D(i,:));
end

%% Plot constraints
%plots a rudimentary image of the model to make it easier to draw conclusions (can be
improved)
%xy plane
close all
scale=50;
```

```
pStart=[C(:,1)-scale*D(:,1),C(:,2)-scale*D(:,2)];

for i=1:size(C,1)
    hold on
    plot([C(i,1),pStart(i,1)], [C(i,2),pStart(i,2)])
    plot(C(i,1),C(i,2),'d')
end
annotation('rectangle',[0.333142857142857,0.116666666666667,0.245428571428571,0.204761
904761905]);
annotation('rectangle',[0.509928571428571,0.335714285714286,0.057928571428571,0.397619
047619049]);
annotation('line',[0.776785714285714,0.603571428571429],[0.516666666666667,0.369047619
047619]);
annotation('line',[0.792857142857143 0.616071428571429],[0.464285714285714
0.319047619047619]);
annotation('line',[0.617857142857143 0.601785714285714],[0.315666666666667
0.369047619047619]);
annotation('line',[0.791071428571429 0.773214285714286],[0.460904761904762
0.514285714285714]);

% yz plane
figure
scale=50;
pStart=[C(:,2)-scale*D(:,2),C(:,3)-scale*D(:,3)];

for i=1:size(C,1)
    hold on
    plot([C(i,2),pStart(i,1)], [C(i,3),pStart(i,2)])
    plot(C(i,2),C(i,3),'d')
end
annotation('rectangle',...
    [0.117857142857143 0.476190476190477 0.196428571428571 0.15]);
annotation('rectangle',...
    [0.333928571428571 0.576190476190476 0.367857142857143 0.0490000000000017]);
annotation('line',[0.328571428571429 0.525],...
    [0.549 0.521428571428572]);
annotation('line',[0.328571428571429 0.525],...
    [0.549 0.521428571428572]);
annotation('line',[0.328571428571429 0.525],...
    [0.549 0.521428571428572]);
annotation('line',[0.328571428571429 0.525],...
    [0.549 0.521428571428572]);
%% Attribute to bodies
C1=[C(1,:);C(2,:);C(3,:);C(4,:)];
C2=[C(5,:);C(6,:);C(7,:)];
C3=[C(8,:);C(9,:);C(10,:);C(11,:)];

D1=[D(1,:);D(2,:);D(3,:);D(4,:)];
D2=[D(5,:);D(6,:);D(7,:)];
D3=[D(8,:);D(9,:);D(10,:);D(11,:)];
%% Joints

dj1x=[1,0,0];
dj1y=[0,1,0];
dj1z=[0,0,1];

dj2x=[1,0,0];
dj2y=[0,1,0];
```

```
dj2z=[0,0,1];


DJ=[dj1x;dj1y;dj1z;dj2x;dj2y;dj2z];

MJ1=[0.709,0.713,0];
MJ2=[0,1,0];
MJ1=MJ1/norm(MJ1);
%% Forces
syms f1 f2 f3 f4 f5 f6 f7 f8 f9 f10 f11 fj1x fj1y fj1z fj2x fj2y fj2z mj1 mj2
F1=[D1;zeros(11-length(D1),3);DJ;zeros(2,3)];
F2=[zeros(length(D1),3);D2;zeros(length(D3),3);-DJ(1:3,:);zeros(5,3)];
F3=[zeros(11-length(D3),3);D3;zeros(3,3);-DJ(4:6,:);zeros(2,3)];
F=[F1,F2,F3].';
%% Moments
M1=[cross(C1,D1).',zeros(3,11-length(D1)),cross(CJ,DJ).',MJ1.',MJ2.'];
M2=[zeros(3,length(D1)),cross(C2,D2).',zeros(3,length(D3)),cross(CJ(1:3,:),DJ(1:3,:),2
),zeros(3,3),-MJ1.',zeros(3,1)];
M3=[zeros(3,11-
length(D3)),cross(C3,D3).',zeros(3,3),cross(CJ(4:6,:),DJ(4:6,:),2),zeros(3,1),-MJ2.'];

%% Combine
M=[M1;M2;M3];
A=[F;M];
%% Solve
f=[f1;f2;f3;f4;f5;f6;f7;f8;f9;f10;f11;fj1x;fj1y;fj1z;fj2x;fj2y;fj2z;mj1;mj2];
eqs=A*f;
s=vpasolve([eqs==0;f2==15],f);%designate which constraint is the nesting force by
applying a value
fSol=[s.f1,s.f2,s.f3,s.f4,s.f5,s.f6,s.f7,s.f8,s.f9,s.f10,s.f11,s.fj1x,s.fj1y,s.fj1z,s.
fj2x,s.fj2y,s.fj2z,s.mj1,s.mj2]';
sol=vpa([s.f1,s.f2,s.f3,s.f4,s.f5,s.f6,s.f7,s.f8,s.f9,s.f10,s.f11])';%reaction forces
at the contact points
neg=[];
for i =1:length(sol) %if a reaction force is negative, it is added to neg. If neg
remains empty, all reaction forces are positive!
    if sol(i)<0;
        neg=[neg;i];
    end
end
neg %display which forces are negative
```

APPENDIX II - DESCRIPTION OF SELECTED SET OF CONSTRAINT LOCATIONS

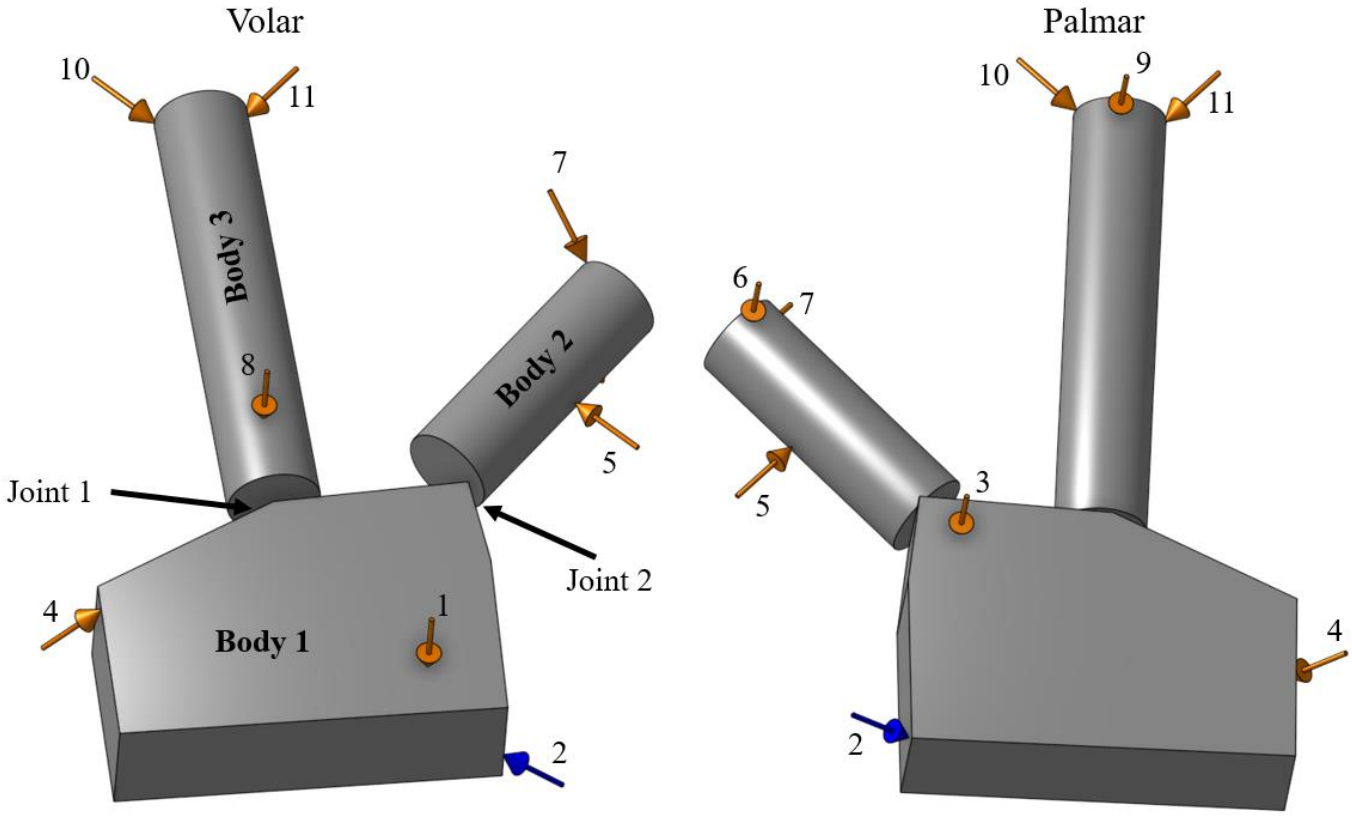

Anatomical descriptions of each point:

1. Volar surface of the radius
2. Radial surface of the radius
3. Volar surface of the radial styloid
4. Ulnar surface of the ulnar styloid
5. Radial surface of the first metacarpal
6. Volar surface of the head of the first metacarpal
7. Ulnar surface of the head of the first metacarpal
8. Dorsal surface of the base of the third metacarpal
9. Volar surface of the head of the third metacarpal
10. Ulnar/distal surface of the head of the third metacarpal
11. Radial/distal surface of the head of the third metacarpal

The location and direction coordinates of each constraint can be found in the Matlab code in Appendix I.

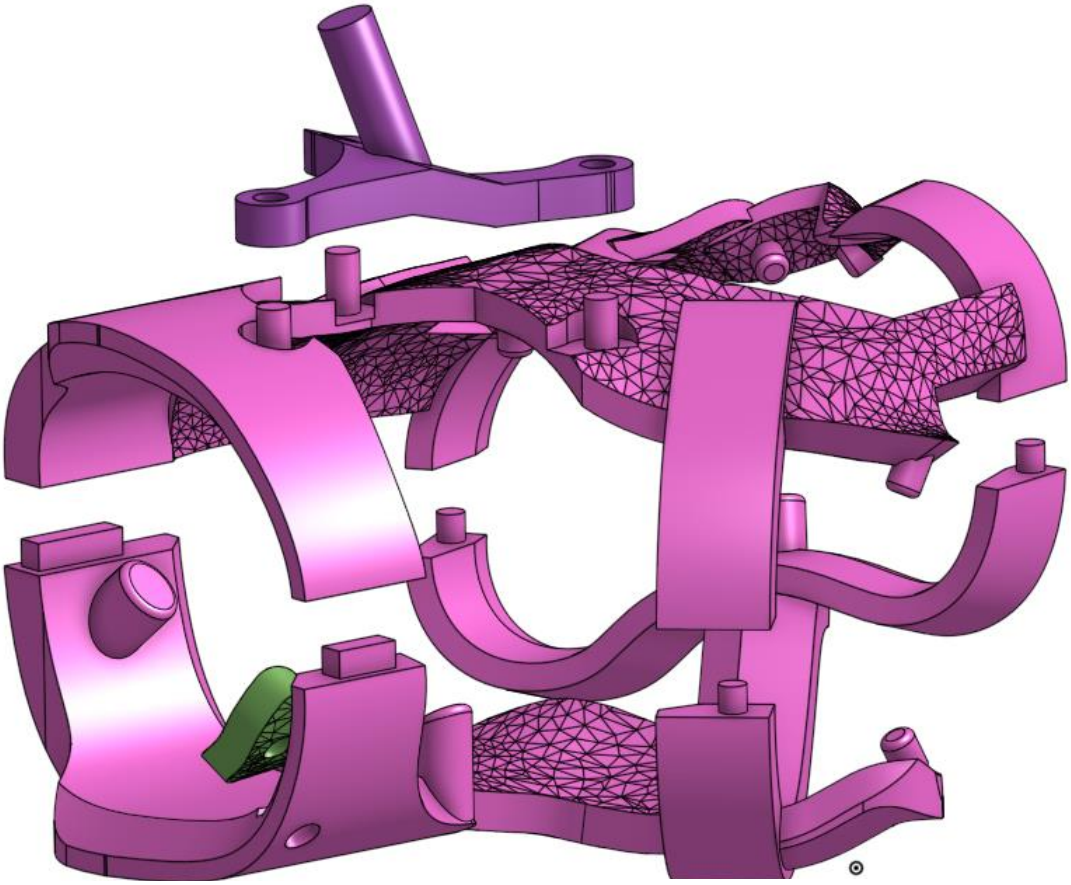

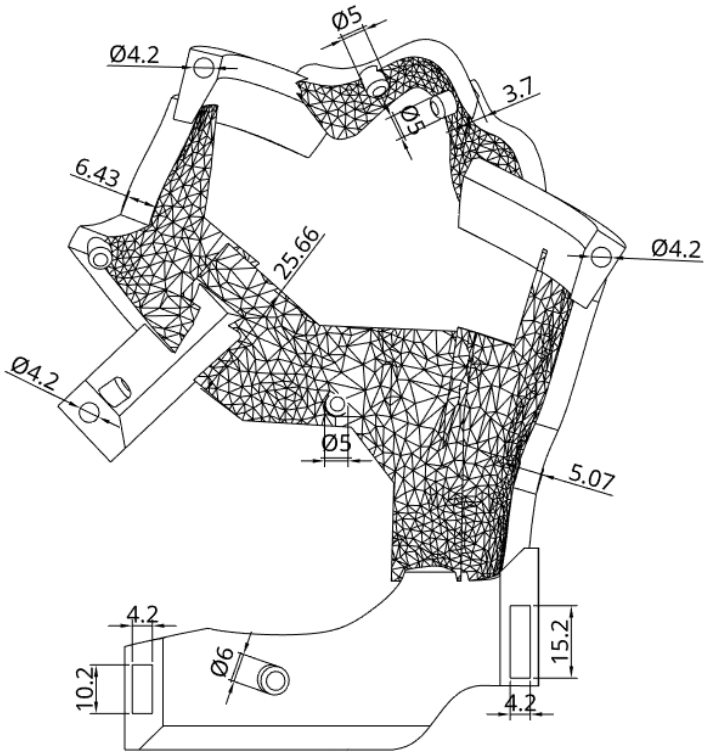

Top half

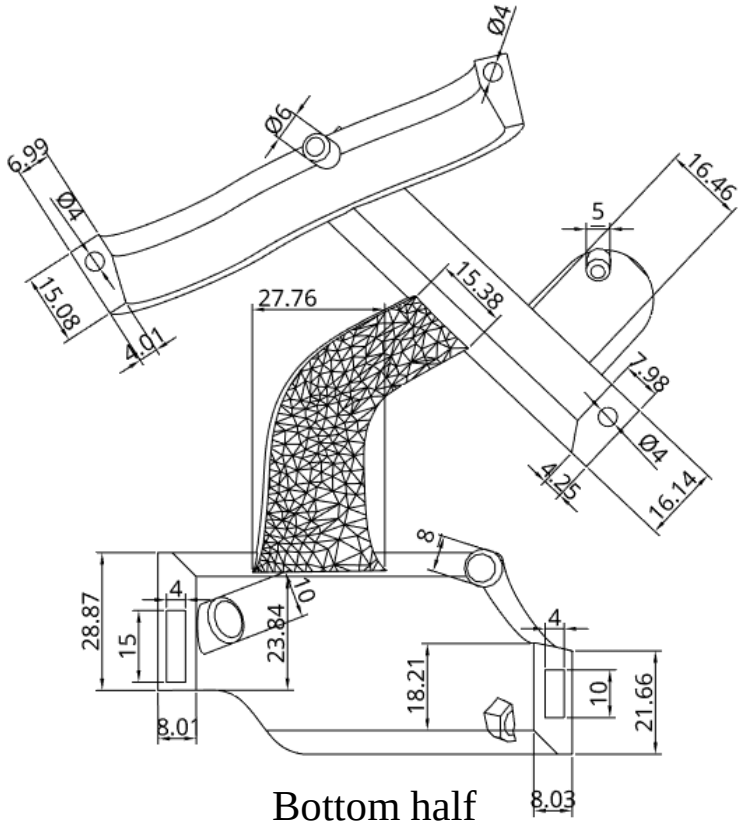

Bottom half

Consent Form for Testing a 3D printed external guide for hand a wrist surgery

Please tick the appropriate boxes	**Yes**	**No**
Taking part in the study		
I have read and understood the study information dated 01/09/2020, or it has been read to me. I have been able to ask questions about the study and my questions have been answered to my satisfaction.	○	○
I consent voluntarily to be a participant in this study and understand that I can refuse to answer questions and I can withdraw from the study at any time, without having to give a reason.	○	○
I understand that taking part in the study involves a 3D scan being made of my hand, and donning a 3D printed device on which force measurements will be taken.	○	○
Risks associated with participating in the study		
I understand that taking part in the study involves the following risks: mild discomfort from pressure at the contact points of the guide.	○	○
Use of the information in the study		
I understand that information I provide will be used for the completion of a master thesis, and possibly in a publication.	○	○
I understand that personal information collected about me that can identify me, such as [e.g. my name and email address], will not be shared beyond the study team.	○	○
Future use and reuse of the information by others		
I give permission for the 3D hand scans that I provide to be archived in 4TU.Centre for Research Data so it can be used for reproduction of the research and future research.	○	○

Signatures

_____ _____ _____

Name of participant [printed] Signature Date

I have accurately read out the information sheet to the potential participant and, to the best of my ability, ensured that the participant understands to what they are freely consenting.

_____ _____ _____

Researcher name [printed] Signature Date

Study contact details for further information: Olivier Hiemstra, olivierhiemstra@gmail.com

PARTICIPANT INFORMATION LETTER

Testing a 3D printed external guide for hand a wrist surgery

1/9/2020

Dear Sir / Madam,

You have been asked to participate in a research study titled “Testing a 3D printed external guide for hand a wrist surgery”. This study is being done by Olivier Hiemstra from the TU Delft. In this letter you will find information about the research. If you have any questions, please contact the persons listed at the bottom of this letter.

Background of the research

In recent years, patient specific instrumentation (PSI) has been applied in many complex orthopedic procedures to improve accuracy and precision. Using a CT-scan, the procedure is first planned out digitally, after which instrumentation can be designed and 3D-printed to achieve the planned operation.

As of now, such guides almost exclusively rely on interfacing directly with the surface of the bone, requiring the bone to be laid bare during the operation. The bones in the hand are among the smallest in the human body, and are surrounded by a complex array of ligaments and tendons which greatly increases the risk of complications when accessing the bone.

In order to avoid these problems, the PSI can also be applied on the outside of the body, interfacing with the skin instead of bone. By attaching the guide to the outside of the body, the size of the needed incisions can be greatly reduced, while still ensuring an accurate procedure. This is a promising combination for new alternatives for complex wrist surgeries.

Purpose of the research

The purpose of this research study is to test a new type of external guide for hand and wrist surgery. More specifically the goal is to determine if the design allows for accurate and repeatable attachment of the guide to the hand, based on a scan of the outside of the hand. The data will be used for completion of a master thesis, and possibly a publication.

Benefits and risks of participating

Mild discomfort may occur due to pressure on the contact points between the guide and the hand/wrist. Precautions have been taken to adhere to all regulations concerning the spread of Covid-19. The researcher will keep a distance of 1.5m and wear a facemask and gloves. In addition, a transparent screen will be present between yourself and the researcher for the necessary steps of donning the guide. All devices and testing equipment will be disinfected before and after each use.

What does participation in the research involve?

Participation in this research involves two appointments.

At the first appointment, a scan will be made of your hand. This involves holding the hand in a defined stance for a few seconds while an array of cameras scan the hand. This scan is the used to design and 3D print the device.

At the second appointment the printed guide will be donned on your hand by the researcher. Subsequently a new scan will be made of your hand with the guide attached. This will be repeated three times.

Next your forearm will be strapped to a measurement setup and you will be asked to hold your hand as still as possible as the guide is pulled in four different directions by a wire as force measurements are taken. This will also be repeated three times.

Procedures for withdrawal from the study

Your participation in this study is entirely voluntary and you can withdraw at any time. If you give your consent to this research, you have the freedom at all times (also during the experiment) to come back on this decision. You can request access to and rectification or erasure of personal data. You do not have to give an explanation for your decision. You can do this by contacting Olivier Hiemstra via email (olivierhiemstra@gmail.com).

Confidentiality of data

This investigation requires that the following personal data are collected and used: age and gender. To safeguard and maintain confidentiality of your personal information, necessary security steps will be taken. Your data will be stored in a secure storage environment at TU Delft. Data will only be accessible to the Olivier Hiemstra and the supervisor Esther de Kater. All data will be processed confidentially.

The personal data will be retained for a maximum of one year, and will be erased earlier if the research is completed before then.

The 3D scans are not considered to be personal data. These will be archived in 4TU.Centre for Research Data, to be available for reproduction of research findings and possible further research, with no connection to your personal data.

The results of this study will be published in possible future scientific publications. Your participant number, name, or contact information will never be shared on publications (master thesis report, scientific publications, reports …) about the research.

Contact Information

If you have any complaints regarding confidentiality of your data, you can contact the TU Delft Data Protection Officer (Erik van Leeuwen) via privacy-tud@tudelft.nl.

On behalf of the researcher(s), thank you in advance for your possible cooperation.

Researcher(s) name and email address(es)

Olivier Hiemstra olivierhiemstra@gmail.com

Esther de Kater E.P.deKater@tudelft.nl

```
%MeasureAngles.m
%Olivier Hiemstra
%11/11/2020

%% clear
close all
clear all

%% paramters
nPoints=10; %desired number of measured points(N)

%% participant info
prompt={'Direction','Participant number','Trial number','Deleted entries'};
title='Input';
dims=[1 35];
input=inputdlg(prompt,title,dims);
dir=cell2mat(input(1,:));
partNum=cell2mat(input(2,:));
trialNum=cell2mat(input(3,:));
numDel=str2num(cell2mat(input(4,:))); %compensate for deleting the first few images if
they were out of focus. So the index is still accurate
%% import data
importData  %script to import recorded force/time data
F=data(3:end,3);
V=data(3:end,2);
t=data(3:end,1);
ind=1:length(F);
%% select data points to use
fInt=(max(F)-min(F))/nPoints; %calculate desired force intervals
Freq=min(F):fInt:max(F);
[~, indUnique] = unique(F);
indSel=interp1(F(indUnique),ind(indUnique),Freq,'nearest'); %select index of nearest
measured force
FSel=F(indSel);
%% Analyse images
F_ang=[];
ang=[];
for i=1:length(indSel)
    img=imread(string(filename(1:end-4)) + int2str(indSel(i)-1+numDel)); %open image
corresponding to selected force
    imshow(img);
    set(gcf, 'units','normalized','outerposition',[0 0 1 1]);
    keypress=0;
    while keypress == 0
        linHand=drawline('Color','g'); %draw line between two defined points on the
guide
        linGuide=drawline('Color','b'); %draw line between two defined points on the
hand

        if i==1
            linMoment=drawline('Color','c'); %for the first image draw line parallel
to the guiding rod
            linPos=linGuide.Position;
            linMoment=linMoment.Position;
                % calculate angle between guide and guiding rod
            v_1 = [linMoment(2,:),0] - [linMoment(1,:),0];
            v_2 = [linPos(2,:),0] - [linPos(1,:),0];
```

```
            ThetaMom = atan2(norm(cross(v_1, v_2)), dot(v_1, v_2));
        end
        uiwait(msgbox('Click enter when finished','!!! INFORMATION !!!','help'));
        keypress = waitforbuttonpress;
    end

    linHand=linHand.Position;
    linGuide=linGuide.Position;
    % calculate angle between hand and guide
    v_1 = [linHand(2,:),0] - [linHand(1,:),0];
    v_2 = [linGuide(2,:),0] - [linGuide(1,:),0];
    Theta = atan2(norm(cross(v_1, v_2)), dot(v_1, v_2));
    Theta = Theta*180/pi;

    %calculate moment
    momentAng= atan((linGuide(1,2)-linGuide(2,2))./(linGuide(2,1)-linGuide(1,1)))-
ThetaMom;
    moment=.057*FSel(i)*-sin(momentAng);
    ang=[ang;momentAng*180/pi];
    F_ang=[F_ang;FSel(i),moment,Theta];
end

%% Calculate change in angle and force
F_ang(:,3)=abs(F_ang(:,3)-F_ang(1,3));
F_ang(:,2)=abs(F_ang(:,2)-F_ang(1,2));
F_ang(:,1)=abs(F_ang(:,1)-F_ang(1,1));
%% Plot
plot(F_ang(:,2),F_ang(:,3))

save(strcat(dir,'_',partNum,'_',trialNum,'.mat'),'F_ang')
```

```
%MeasureDistances.m
%Olivier Hiemstra
%11/11/2020

% see MeasureAngles.m for explanation
%% clear
close all
clear all

%% paramters
nPoints=10; %desired number of measured points(N)
dKnown=.038; %known measured distance between two points on the guide
%% participant info
prompt={'Direction','Participant number','Trial number','Deleted entries'};
title='Input';
dims=[1 35];
input=inputdlg(prompt,title,dims);
dir=cell2mat(input(1,:));
partNum=cell2mat(input(2,:));
trialNum=cell2mat(input(3,:));
numDel=str2num(cell2mat(input(4,:)));
%% import data
importData
F=data(3:end,3);
V=data(3:end,2);
t=data(3:end,1);
```

```
ind=1:length(F);
%% select data points to use
fInt=(max(F)-min(F))/nPoints;
Freq=min(F):fInt:max(F);
[~, indUnique] = unique(F);
indSel=interp1(F(indUnique),ind(indUnique),Freq,'nearest');
FSel=F(indSel);
%% Analyse images
F_dist=[];
for i=1:length(indSel)
    img=imread(string(filename(1:end-4)) + int2str(indSel(i)-1+numDel));
    imshow(img);
    set(gcf, 'units','normalized','outerposition',[0 0 1 1]);
    keypress=0;
    while keypress == 0
        linHand=drawline('Color','g');

        if i==1                 % on the first image, draw a line between the two
points of a know measured distance
            linDist=drawline('Color','b');
            linDist=linDist.Position;
        end
        uiwait(msgbox('Click enter when finished','!!! INFORMATION !!!','help'));
        keypress = waitforbuttonpress;
    end

    linHand=linHand.Position;
    % calculate disp
   dx=linHand(2,1)-linHand(1,1);
   dy=linHand(1,2)-linHand(2,2);

   dist=sqrt((linDist(2,1)-linDist(1,1))^2+(linDist(1,2)-linDist(2,2))^2);

   distx=dKnown*(dx/dist)


   F_dist=[F_dist;FSel(i),distx];
end

%% Calculate change in angle and force
F_dist(:,2)=abs(F_dist(:,2)-F_dist(1,2));
F_dist(:,1)=abs(F_dist(:,1)-F_dist(1,1));
%% Plot
plot(F_dist(:,1),F_dist(:,2))

save(strcat(dir,'_dist_',partNum,'_',trialNum,'.mat'),'F_dist')
```

Minimally Invasive Hand and Wrist Surgery: Extent and Effectiveness

Olivier Hiemstra
4288769

Technical University Delft and Reinier de Graaf Gasthuis
Prof. P. Breedveld
dr. G.A. Kraan

February 2020

CONTENTS

Contents 2
I. Introduction 4
A. Background 4
B. Problem definition 4
C. Goal of this research 4
D. Layout of this report 4
II. Anatomy and pathologies of the hand and wrist 5
A. Bones and Joints 5
B. Muscles and Tendons 5
C. Ligaments 5
D. Nerves 6
E. Blood supply 6
III. Identification of common hand-wrist procedures 7
A. Collecting data 7
B. Selection 10 most common procedures 7
C. Description of identified procedures 7
IV. Literature search of minimally invasive hand-wrist procedures 9
A. Search terms 9
B. Inclusion/exclusion criteria 9
C. Data extraction 9
V. Extent and effectiveness of found procedures 10
A. Citation retrieval 10
B. Amount and level of evidence 10
C. Used techniques and results 10
Tendovaginitis stenosans release 10
Carpal Tunnel Release 11
Trapeziectomy 12
Dupuytren's Fasciectomy 12
Distal radius fracture 12
Cyst/foreign body removal 13
TFCC repair 13
Metacarpal fracture 14
Scapholunate ligament reconstruction 14
Scaphoid nonunion fixation with bone graft 14
VI. Discussion 15
A. Trends per pathology 15
B. General trends 16
C. Limitations of this research 16
VII. Conclusions 16

VIII. Acknowledgments 16
Bibliography 17
Appendix I – Amounts of procedures in 2018, Haga Zieknhuis and Reinier de Graaf Gasthuis 20
Appendix II – Search terms 22
Appendix III – Search flow diagrams of all searches 25

I. Introduction

A. *Background*

Minimally invasive surgical techniques are defined as methods of performing surgery that minimize damage to the surrounding tissue. The benefits of such procedures are decreasing morbidity, reducing the chances of infection, and shortening rehabilitation time. Current advances in materials and technology are opening doors to more and more possibilities to replace open surgeries with minimally invasive techniques.

Hand and wrist surgery is an interesting field for minimally invasive surgery due to the complex anatomy and lack of soft tissue surrounding important structure. Therefore open surgery is often accompanied by damage to surrounding structures. This makes the possible gains from minimally invasive surgery high, while simultaneously making it extremely challenging to perform minimally invasive surgeries as there is very little room for movement and manipulation of instruments inside the hand.

B. *Problem definition*

While many minimally invasive techniques have been suggested many hand and wrist surgeries are still performed using open techniques. There is currently no literature providing an overview of research into minimally invasive techniques throughout the field of hand and wrist surgery.

C. *Goal of this research*

To examine the current research being done into minimally invasive techniques for the 10 most common hand or wrist pathologies that require surgery.

D. *Layout of this report*

First a brief overview is given of the anatomy of the hand and wrist. Relevant structures are described as well as the common pathologies that occur in these structures. To limit the scope of the review a selection is then made of the 10 most common procedures in hand and wrist surgery. These are determined on the basis of data from two hospitals in the Netherlands. Subsequently the method is described by which minimally invasive alternatives are searched for in literature for each of the selected procedures. The data from the discovered literature is presented, first as a whole, and then per procedure. Lastly the resulting conclusions, trends, and gaps in the literature are discussed.

II. Anatomy and Pathologies of the Hand and Wrist

A. *Bones and Joints*

This section gives a brief overview of the anatomy of the hand and wrist based on Gray's Basic Anatomy[1] which should be consulted for more detailed descriptions. The bones of the hand and wrist are divided into three groups; the eight carpal bones, the five metacarpals and the phalanges of which there are three in each digit except the thumb which only has two. The carpal bones are arranged in two rows; the proximal row and the distal row. The proximal row articulates with the distal ends of the ulna and radius forming the wrist joint. The distal row articulates with the metacarpals but with very limited motion. Only the metacarpal bone of the thumb functions independently to provide opposition of the thumb. Although movement between the carpal bones is limited it does play an essential role in movement and function of the hand.

The metacarpals are connected to the phalanges by the metacarpophalangeal joints which allow flexion, extension, adduction, abduction and limited rotation. The phalanges are connected to each other by interphalangeal joints which function as hinges, allowing only flexion and extension.

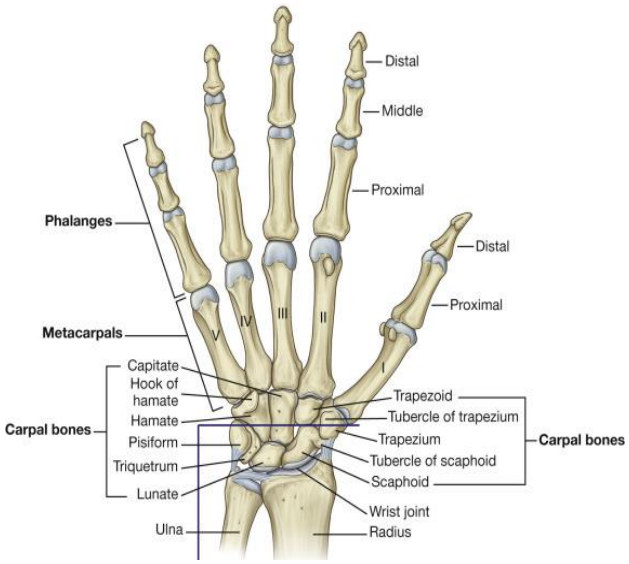

Figure 1. The skeletal structure of the human hand. [1] (fig 7.80)

The most obvious pathologies occurring in the bones are fractures. Fractures can occur in all three groups of bones but are relatively rare in carpal bones other than the scaphoid. Dislocations are another common pathology in which bones are forced from their normal position often immobilizing the joint and causing damage to the surrounding tissue. Dislocations can also occur in all three groups of bones.

In addition to traumatic injuries, there are also degenerative conditions that affect the bones and joints. The most common of these is osteoarthritis in which the joint cartilage which serves as cushioning between bones wears down resulting in painful and damaging bone-on-bone contact. This can occur in many of the joints in the hand and wrist with arthritis between the carpal bones and between the carpal and metacarpal bones being especially debilitating.

B. *Muscles and Tendons*

Movements of the hand and wrist are operated by a combination of the intrinsic and extrinsic muscles. The extrinsic muscles which originate in the forearm function in forceful gripping while the intrinsic muscles located within the hand allow for precision movements of the digits. The forces of the extrinsic muscles are applied to the hand via a system of tendons and tendon sheaths that guide the tendon. The extensor tendons run along the back of the wrist while flexor tendons run along the palmar side.

Traumatic injuries can lead to tendons being ruptured or severed resulting in loss of hand motion. More commonly tendons and their surrounding sheath can become inflamed. This results in tenderness and pain with motion and can lead to 'triggering' where the tendon can no longer move freely and may require extra force to extend or flex fully.

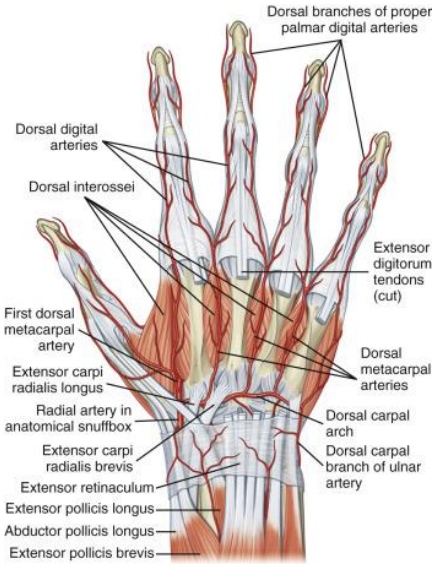

Figure 2 A dorsal view of the hand showing the intrinsic muscles and the extensor tendons. [1] (fig. 7.98)

C. *Ligaments*

Ligaments are bands of fibrous connective tissue that connect bones to other bones. They ensure the stability of the skeletal structures and limit the degrees of freedom of joints. The carpal bones are connected to each other by a complex network of ligaments which play a vital role in the biomechanics of the wrist. Ligaments between the metacarpal bones ensure the stability of the palm of the hand, and the ligaments around the interphalangeal joints limit the motion to extension and flexion. In addition ligaments act as pulleys, redirecting and constraining tendons in the fingers to ensure proper motion and strength.

Due to their varying functions, damage to ligaments can cause a variety of problems. Often occurring together with dislocations, damage to the ligaments around the joints of the fingers can lead to instability of the joint. Damage to the ligaments that connect the carpal bones results in instability

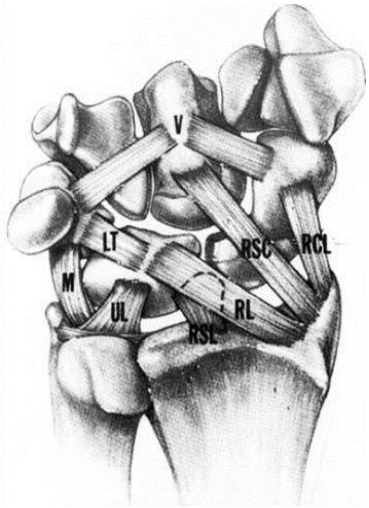

Figure 4 The bones of the wrist with the extrinsic carpal ligaments that stabilize them with respect to the ulna and radius. M: , LT: lunotriquetral, UL: ulnolunate, RSL: radioscapholunate, RL: radiolunate, RSC: radioscaphocapitate, RCL: radial collateral. [A]

of the wrist and disrupts the complex wrist biomechanics leading to pain and severe loss of motion. Damage to a pulley ligament can lead to bowstringing, a phenomenon where the tendon no longer runs closely along the hand resulting in loss of strength.

D. *Nerves*

The hand is supplied by three nerves, namely the ulnar, median and radial nerve. The ulnar nerve innervates most of the intrinsic muscles of the hand and supplies the skin of the little finger and half of the ring finger on the palmar side and the little finger and ring finger on the dorsal side. The median nerve innervates the remaining intrinsic muscles (those responsible for opposition of the thumb) and supplies the skin on the palmar side of the remaining digits and the tips of those digits on the dorsal side. The radial nerve supplies the remaining skin on the dorsal side of the hand, namely the thumb and the index and middle finger, excluding the tips.

Nerve damage can occur due to trauma but is much more commonly caused by compression of the nerve in the body. To reach the hand the nerves pass through a variety of tunnels which can become narrow or inflamed for a variety of

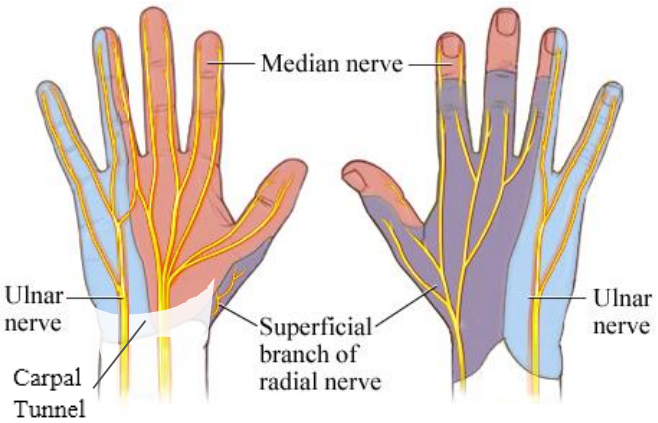

Figure 5 Palmar and dorsal views of the hand showing the different regions innervated by the radial, median and ulnar nerves. [B]

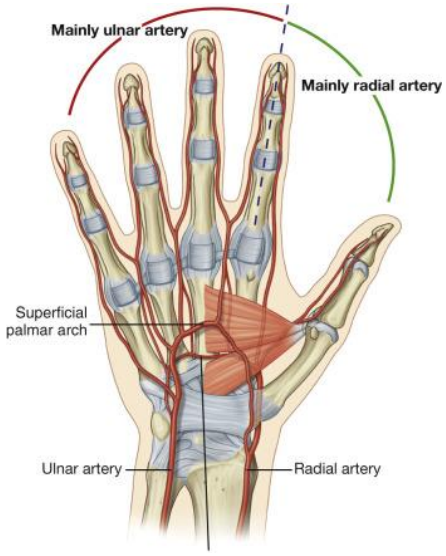

Figure 3 The arterial structures of the hand. [1] (fig. 7.95)

reasons resulting in pressure on the nerve. This is called compression neuropathy which leads to pain, numbness and tingling and if left untreated can result in permanent damage to the nerve.

E. *Blood supply*

The hand is supplied with blood by the radial and ulnar arteries. The ulnar artery supplies the majority of the hand with the radial artery only supplying the thumb and half of the first digit. After passing into the wrist both arteries branch out to supply the muscles, digits and joints, and are also connected to each other by what are known as the superficial and deep vascular arches.

III. Identification of Common Hand-Wrist Procedures

A. *Collecting data*

In order to determine which surgical procedures are most common in hand and wrist surgery data was acquired from two hospitals in the Netherlands. Both the Reinier de Graaf Gasthuis and HagaZiekenhuis employ one orthopedic surgeon specialized in hand and wrist surgery. A list was requested at both hospitals of all surgeries in the year 2018 for which those surgeons were listed as either first or second operator.

B. *Selection 10 most common procedures*

Some types of surgeries were performed with a slightly different method or logged with different names by each surgeon. In those cases the amounts were combined. While most surgeries are logged as a single procedure some consist of two procedures combined. In those cases the main procedure was kept while the secondary procedure was removed from the list. These considerations were made in consultation with the surgeon and can be found in appendix I**.** From the resulting list the top 10 procedures were selected for further investigation in this research. These are shown in Figure 6.

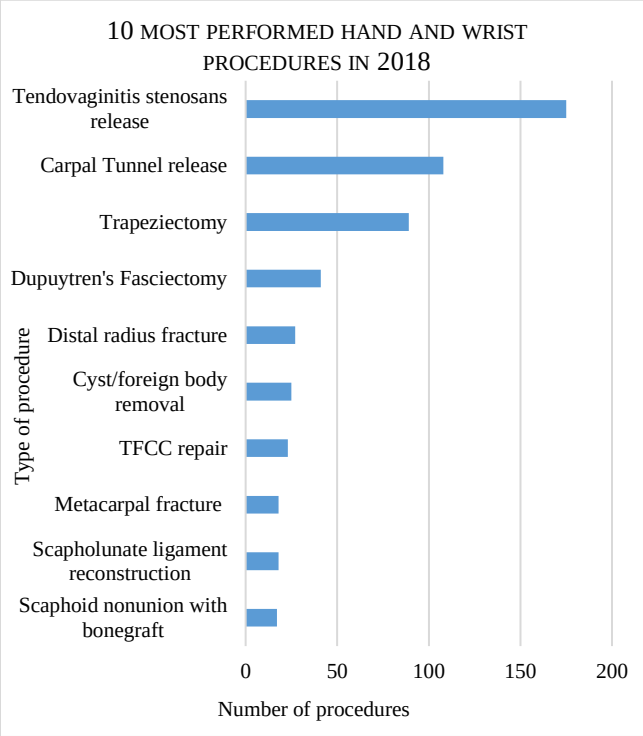

Figure 6 A bar graph of the 10 most commonly performed hand and wrist procedures, showing the amount of times each procedure was performed in 2018 at the Reinier de Graaf Gasthuis and HagaZiekenhuis.

C. *Description of identified procedures*

Tendovaginitis Stenosans Release

In this section a brief description is given of the identified procedures and the relevant pathologies. The descriptions are based on Green's Operative Hand Surgery[2] which should be consulted for more detail. Tendovaginitis stenosans occurs when the flexor tendon sheath becomes inflamed, restricting smooth motion of the tendon. Two common types are called trigger finger and De Quervain syndrome. Trigger finger occurs at the A1 pulley situated at the base of the finger on the palmar side. As a result of the inflammation the tendon becomes thicker, preventing it from moving freely through the pulley or tunnel resulting in further inflammation. In severe cases the tendon can no longer move through the pulley at all, locking the finger in a flexed position. In the case of De Quervain's syndrome, the inflammation occurs on the side of the base of the thumb where the two extensor tendons of the thumb pass through a tunnel known as the 1st dorsal compartment.

The surgical treatment for these conditions consists of releasing the A1 pulley or 1st dorsal compartment with an incision thus freeing the tendon and allowing the inflammation to subside while the pulley or compartment slowly heals.

Carpal tunnel release

Carpal Tunnel Syndrome (CTS) is the most common compression neuropathy. It occurs when the median nerve becomes compressed in the carpal tunnel. In order to release the pressure on the nerve the tunnel must be opened by dissecting the transverse carpal ligament which forms the palmar barrier of the carpal tunnel. The dissected ligament is not reattached but left to heal naturally in its new released position with less pressure on the median nerve.

Trapeziectomy

One of the joints in the hand commonly affected by osteoarthritis is the carpometacarpal (CMC) joint at the base of the thumb. The arthritis primarily occurs between the metacarpal bone of the thumb and the trapezium but can also spread to the intercarpal joints between the trapezium, trapezoid and scaphoid. In a trapeziectomy, the trapezium is removed in order to prevent the painful bone-on-bone contact. Various techniques can be used to subsequently prevent the thumb from shortening by migrating into the open space left behind. For example a strong suture can be used to connect the first and second metacarpals holding the first metacarpal in place. Other methods include passing the FCR tendon through the first metacarpal or interposition of capsule.

Dupuytren's Fasciectomy

Dupuytren's disease is a condition that affects the connective tissues in the hand resulting in what is known as Dupuytren contracture. This is when the bands of connective tissue known as fascia along the palm and digits become fibrous and contract, limiting extension of the fingers. In a fasciectomy the affected fasciae are surgically removed. A variety of incision lengths and shapes can be used depending on the location of the affected fascia and surgeon preference.

Open reduction and fixation distal radius fracture

Distal radius fractures are among the most common fractures commonly resulting from a fall on an outstretched hand. In some cases the fracture can be reduced sufficiently and the wrist can be splinted without the need for surgery. When this is not the case various types of surgery can be done to reduce and fixate the fracture. Commonly an incision is made large enough to visualize the fracture so the bone fragments can be reduced and a plate with screws is used to fixate the fracture in the desired position. This is called open reduction and internal fixation (ORIF).

Removal of a cyst or foreign body

The removal of foreign bodies can refer to the removal of a shard of metal or glass that has entered the body in an accident. More commonly however this procedure refers to the removal of a cyst or tumor that has developed in the hand. The most common cyst occurring in the hand is a ganglion. A ganglion is a mucin-filled cyst that is usually attached to joint capsule, a tendon, or a tendon sheath. While they pose no threat for the patient they are often removed because of the cosmetic appearance and concern that it may be something malignant. They can be effectively removed using an open procedure but the chance of recurrence is very high if it is not completely removed.

TFCC repair

The Triangular Fibrocartilage Complex (TFCC) is a cartilage structure located on the small finger side of the wrist. It acts as a cushion between the ulna and the carpal bones and stabilizes the carpal bones, ulna and radius in grasping and rotation. Degeneration or trauma such as falls or sudden twists of the forearm can lead to a tear in the TFCC resulting in pain and destabilizing the distal radioulnar joint (DRUJ). These tears are categorized by the Palmer's classification depending on the location of the tear and whether they are traumatic (class 1) or degenerative (class 2). In class 1B and 1D the tear occurs at the attachment of the TFCC the ulna and radius respectively. These cases can more easily be repaired surgically because the bone gives a solid surface to which the TFCC can be reattached.

This is most commonly done using the so called outside-in technique. First a 1.5 cm incision is made on the side of the wrist. Then a needle carrying a suture is passed through either the ulnar capsule, and through the torn TFCC. A second needle is then inserted adjacent to the first one. A wire loop through the second needle is then used to retrieve the suture which can then be tied.

K-wire fixation of metacarpal fractures

Another common fracture in the hand is the metacarpal fracture. In many cases metacarpal fractures can be treated conservatively with a cast but if necessary there are a variety of surgical techniques to reduce and fixate the fracture. Most commonly pointed stainless steel wires called Kirschner (K)-wires are drilled through the bone fragments to attach them to each other. This is done percutaneously meaning the wires

Figure 7 Intramedullary (top) and transverse (bottom) pinning of metacarpal fractures. [3] (fig.6)

also go through the skin. Depending on the location and direction of the fracture k-wires can be inserted transversely across the bone or along the bone which is called intramedullary pinning. [3]

Treatment perilunate dissociation

When the ligaments between carpal bones become damaged instability can arise in the wrist. The most common type of carpal instability is scapholunate (SL) dissociation resulting from damage to the scapholunate ligament. Early diagnosis is often missed because there are no clear radiological indications. Due to abnormal wrist kinematics the surrounding ligaments are gradually affected as well eventually resulting in a complex ligament injury and misalignment of the carpal bones called perilunate dissociation. In these advanced cases the SL ligament can no longer be repaired. Instead a flexor tendon is used to replace it. This is done by passing the tendon through a hole drilled in the one carpal bone (the scaphoid) which is first reduced to the right position and then attached to another (the lunate), securing them together in proper alignment.

Scaphoid nonunion with bone graft

Scaphoid fractures are the most common carpal bone fractures. Due to the geometry of the bone and retrograde flow of blood scaphoid fractures are difficult to manage and susceptible to failing to heal resulting in what is called nonunion. If left untreated scaphoid nonunion leads to collapse of the carpal bones and osteoarthritis. The goal of treatment is to restore the scaphoid to the correct shape and allow it to heal into one bone again. In order to do this the bone surfaces must first be debrided, where after a screw or k-wire is used to secure the two pieces in place. The gap between the two pieces is then filled with bone grafted from either the distal radius or the iliac crest of the pelvis, this is done to aid the bone in healing across the gap.

IV. Literature Search of Minimally Invasive Hand-Wrist Procedures

A. *Search terms*

A literature search was conducted in order to find minimally invasive alternatives or improvements for the selected surgeries. A search strategy was developed to identify relevant studies for the minimally invasive treatment of each pathology corresponding to the surgeries. The specific search terms used can be found in appendix II. The searches were performed in PubMed and Scopus. The results were restricted to the last 5 years (jan. 2015- dec. 2019).

B. *Inclusion/exclusion criteria*

Results from both databases were combined and reviewed in a literature review program. Eligibility criteria were outlined based on the goals of the review. Studies were included if they involved a minimally invasive surgical treatment of the pathology in question, and had a systematic methodology described in the abstract, cadaver studies were included. Studies were excluded if they described non-surgical treatments such as splinting or injections. Studies concerning the costs of surgeries were also excluded.

C. *Data extraction*

From the resulting studies the following data was extracted: the level of evidence (LOE), the surgical technique being tested, and the concluded effectiveness compared to open surgery. The level of evidence was split into two categories. Studies were considered high level if they compared different treatment methods and if the different treatment groups were randomized. Systematic reviews of studies that satisfied these criteria were also considered high level. All other studies including comparative studies that were not randomized, case series, and cadaver studies were considered low level.

The comparative effectiveness was only determined for high LOE studies. Studies were scored '+' if the technique gave better results than the control group, '=' if the results were similar, and '-' if the results were worse. For low LOE studies it was only noted if the technique was concluded to be safe and effective.

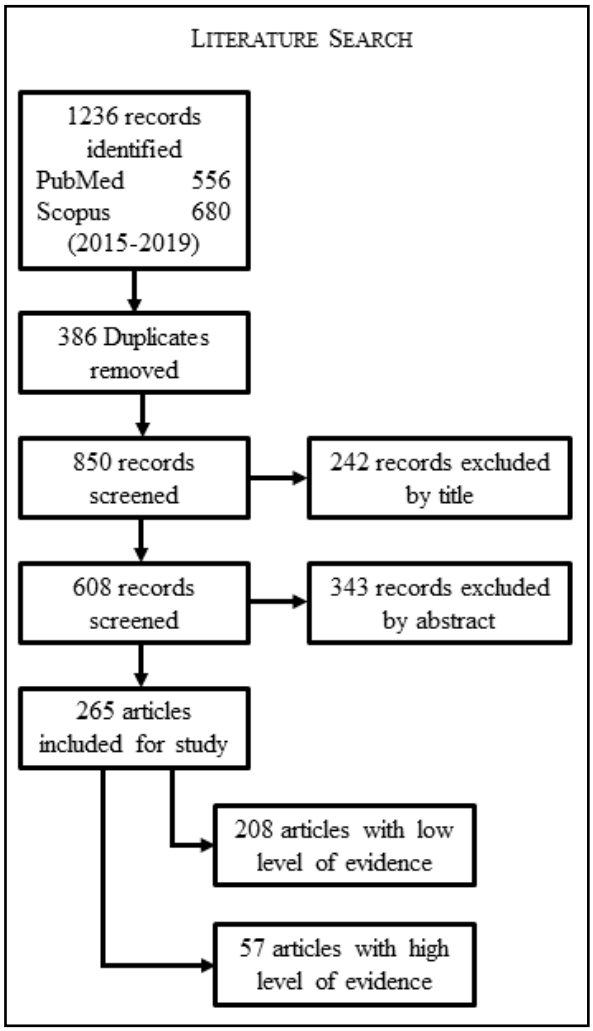

Figure 8 Literature search and screening flow chart showing the combined results of all 10 literature searches. Individual flow charts can be found in Appendix III. High level of evidence refers to studies that compared different treatment methods and randomly placed patients in different treatment groups.

V. Extent and Effectiveness of Found Procedures

A. *Citation retrieval*

The literature search resulted in a total of 1,236 citations of which 386 were duplicates. A further 242 titles could be excluded because they clearly did not meet the criteria. Based on the abstracts of the remaining articles a further 322 could be excluded resulting in a final data set of 286 studies.

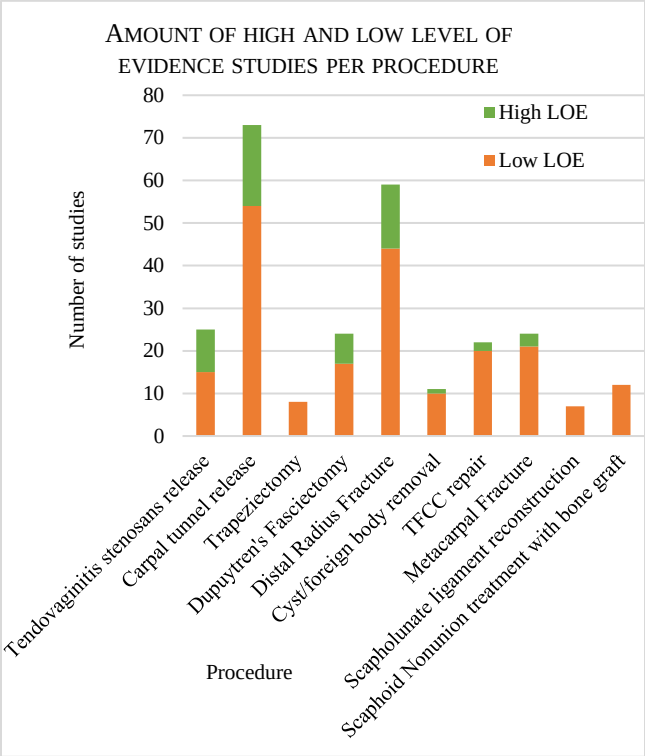

Figure 9 A bar graph showing the number of studies about each selected procedure found in the literature search. Each bar is divided into studies determined to have a high of low level of evidence (LOE). High LOE studies were randomized and controlled trials, or systematic reviews that analyzed such studies.

B. *Amount and level of evidence*

The amount of studies varied greatly per procedure ranging from 72 about carpal tunnel release to 10 about scapholunate ligament reconstruction. Dividing the number of studies by the amount of times each procedure had been performed (section III.B.) gives an indication of the amount of research relative to the frequency with which each procedure is performed. This also varied greatly with distal radius fractures being studied relatively much while tendovaginitis stenosans releases and trapeziectomies were underrepresented.

The majority of studies were uncontrolled case-series of a single treatment (n=155, 54%). In total 21% of studies were considered to have a high LOE but the proportion varied greatly per procedure. For trapeziectomy, scapholunate ligament reconstruction, and scaphoid non-unions there were no high LOE studies while for tendovaginitis stenosans 40% of studies had a high LOE.

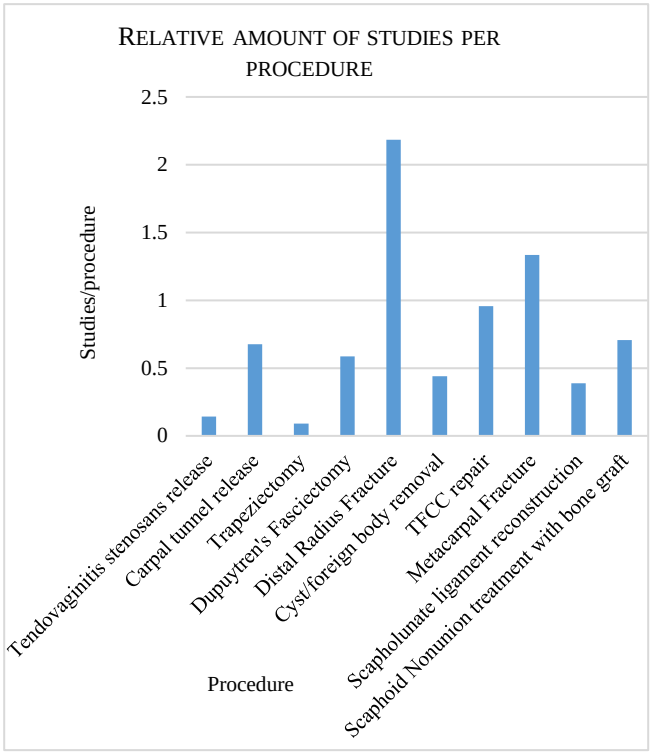

Figure 10 A bar graph showing the number of studies about each procedure relative to the amount of times it was performed.

C. *Used techniques and results*

Tendovaginitis stenosans release

The techniques used for minimally invasive treatment of stenosing tenosynovitis can be divided into two basic categories;

- Endoscopic
- Percutaneous

The first percutaneous technique was introduced in 1992 by Eastwood et al.[4] In this method a needle is used to first pierce the tunnel or pulley where after the surgeon moves it back and forth in order to dissect the tunnel or pulley. 5 studies described modifications to this procedure by replacing the needle with another tool such as a scalpel or a purpose designed blade.

Another modification found in the literature is the addition of ultrasonic guidance to help the surgeon visualize the relevant structures during the procedure. Most of these studies used the same needle technique but two studies described a new method in which a thread is passed through the tunnel or pulley and then back again creating a loop

around the tissue which is to be dissected. The thread is then pulled back and forth slowly dissecting the tissue.

Three studies were found using endoscopic techniques two of which were for the treatment of De Quervain's syndrome. A 2 cm incision is made on the side of the wrist at the base of the thumb, an angled endoscope is inserted and used to lift the skin creating a tent-like working space. Then

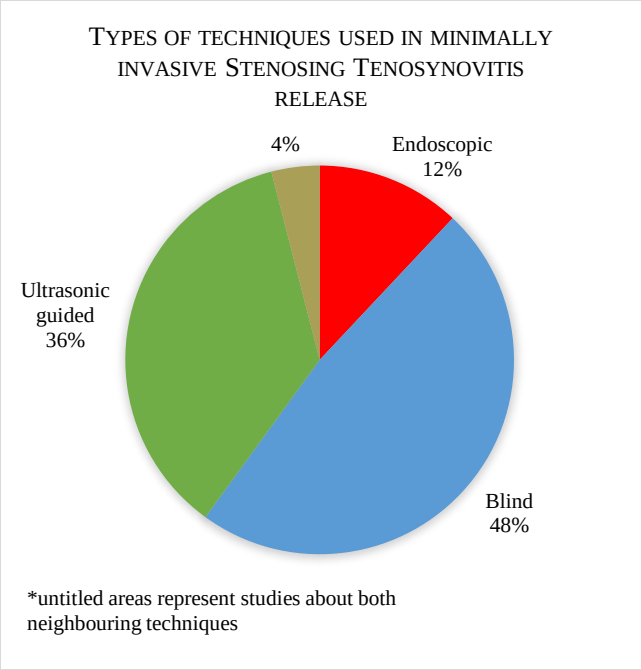

Figure 11 A pie chart showing the percentage of studies using different types of techniques for minimally invasive treatment of stenosing tenosynovitis.

either a scissor or hook knife is used to dissect the tunnel. No studies specifically described an endoscopic technique for trigger finger release but one systematic review referred to a comparative study between open and endoscopic trigger finger release.

High LOE studies comparing blind percutaneous with open release showed no difference in effectiveness. Wang et al.[5] found looped thread transection to achieve the same curative effects as open release but with less trauma and a faster recovery time. Nikolaou et al.[6] found that US-guided needle release resulted in fewer days absent from work and better cosmetic results compared to open release.

OVERVIEW OF HIGH LOE STUDIES OF STENOSING TENOSYNOVITIS

	Blind	US-guided	Endoscopic
Chobtangsilp[7]	=		
Fiorini [8]		?	?
Huisstede [9]	?		
Park [10]		=	
Ranjeet [11]	=		
Wang [5]		+	
Xie [12]	=		
Nikolaou [6]		+	

Figure 13 The effectiveness found in high level of evidence studies of stenosing tenosynovitis release compared to open release. + : better results, = : similar results, ? : insufficient evidence.

Carpal Tunnel Release

For the minimally invasive treatment of carpal tunnel syndrome the results can be divided into three main categories:

- Endoscopic
- Ultrasonic guided
- Minimal open.

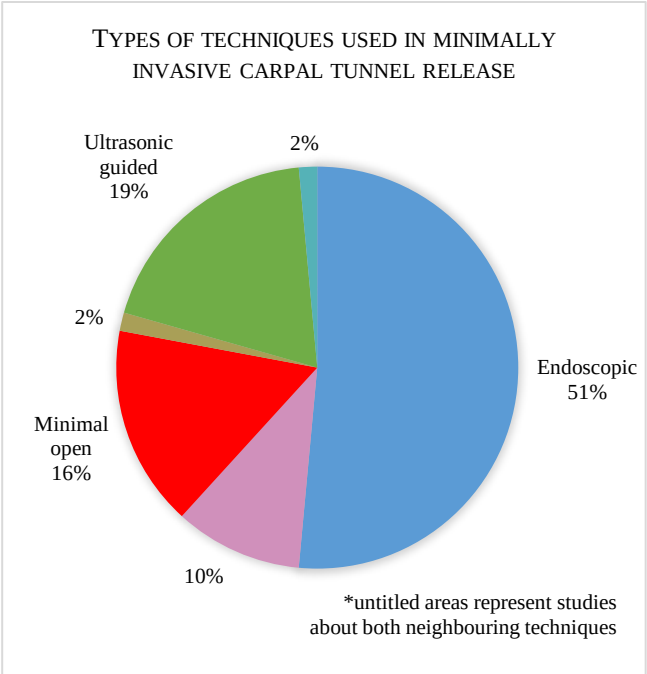

Figure 12 A pie chart showing the percentage of studies using different types of techniques for minimally invasive treatment of carpal tunnel syndrome.

Minimal open techniques refer to variations of open release that aim to minimize the size of the necessary incision. Two studies used novel instrumentation while the rest focused solely on the surgical approach.

15 studies used ultrasonic visualization to guide the surgeon allowing for a percutaneous approach while still minimizing the risk of incomplete resection or damage to the median nerve. Two types of techniques were used for dissection namely hooked blades or thread resection.

Five studies were cadaveric studies determining the safety of these US-guided techniques. The majority of the studies however pertained to endoscopic carpal tunnel release. Two of these studies proposed novel surgical techniques. The rest focused on comparison with open release, long term outcomes, and combinations with other procedures.

The evidence of the high LOE studies clearly shows that endoscopic release has better results compared to open release. Most studies conclude that while the long-term results are similar, short term results improve with endoscopic release. Sayegh et al.[13] however noted that in addition to better short term results there was also a higher risk of complications. While there is much less evidence for minimal open and US-guided techniques the found studies did also conclude better results than open release. All three

studies comparing endoscopic and minimal open techniques found them to be similarly effective.

OVERVIEW OF HIGH LOE STUDIES OF CT-RELEASE

	Endoscopic	US-guided	Mini Open
Orak [14]	+		
Rojo-Manaute [15]		+	
Vanni [16]			+
Hu [17]	+		
Huisstede [18]	+		+
Akhtar [19]	+		
Gurpinar [20]	+		
Sayegh [13]	+		
Gumustas [21]	=		
Michelotti [22]	=		
Peters [23]	=		
Gaspar [24]	+		
Alp [25]	=		=
Oh [26]	=		=
Zhang [27]	=		=

Figure 14 The comparative effectiveness found in high level of evidence studies of carpal tunnel release. Under the dotted line are studies comparing endoscopic and minimal open release. + : better results, = : similar results.

Trapeziectomy

Eight studies were found about minimally invasive alternatives for a trapeziectomy. Each study involved removing some tissue from the interface of the trapezium and first metacarpal using a shaver or burr. They varied however in the amount of tissue removed and whether or not interposition material was used.

Four of these described an endoscopic partial trapeziectomy with soft tissue interpostition. In this procedure an endoscopic burr is used to remove the part of the trapezium in contact with the first metacarpal. A tendon graft is then taken from palmar longus tendon and rolled into a ball. This ball is then inserted into the space between the trapezium and first metacarpal. In addition a radiofrequency probe is used to achieve thermal shrinkage of the surrounding ligaments to reduce laxity.

Another study compared arthroscopic abrasion to a trapeziectomy with LRTI. For arthroscopic abrasion a shaver is used to remove all loose bodies, bone spurs, and flapping cartilage, but leaving the trapezium intact. This procedure however resulted in higher revision rates and higher postoperative pain. Rog et al.[28] conclude that this may be due to the lack of use of interposition material. A similar study by Cobb et al.[29] however concluded that interposition material is not necessary. Neither study was considered to have a high LOE.

Dupuytren's Fasciectomy

The resulting studies for the treatment of Dupytren's disease all used a percutaneous needle technique. While referred to either percutaneous needle aponeurotomy (PA) or percutaneous needle fasciotomy they are both the same procedure. In this procedure a needle is used to weaken the contracted fascia which then sever due to tension when the palm and fingers are straightened by the surgeon. The surgeon continues to combine tension on the chords with needle perforations until all the chords are severed. The main variation in the found studies was whether or not lipofilling was used in addition to needle fasciotomy. For percutaneous needle aponeurotomy with lipofilling (PALF) a fat graft is injected into the surgical site after release of the chords. In addition one study implemented US-guidance for better visualization of the chords.

OVERVIEW OF HIGH LOE STUDIES OF DUPUYTREN'S CONTRACTURE

	PA	PALF
Huisstede [9]	?	
Selles [31]		-
Konneker [30]		+
Soreide [32]	?	

Figure 15 The effectiveness found in high level of evidence studies of Dupuytren's syndrome compared to open surgery. + : better results, - : worse results, ? : insufficient evidence.

Of the four high LOE studies found, two referred to the same patient group with Konneker et al.[30] describing the results up to 1 year after operation and Selles et al.[31] describing the results after 5 years. The initial results showed similar clinical results but with faster patient recovery and a lower incidence of complications. After 5 years however a higher recurrence rate was observed in comparison with open limited fasciectomy. The other two were both systematic reviews that conclude there is insufficient evidence to determine the superior procedure.

Distal radius fracture

The minimally invasive techniques for the treatment of distal radius fractures fall into four main categories:

- Intramedullary nailing
- Minimally invasive plate osteosynthesis (MIPO)
- External fixation
- Percutaneous pinning

Intramedullary nailing involves inserting a nail into the medullary cavity (inside) of the radius. This nail is then secured inside the bone using screws under fluoroscopic guidance. MIPO uses plates similar to in ORIF but advances are made in the shape of the plate and the surgical approach to minimize the size of the incision. For external fixation pins are percutaneously drilled into the bone which are then fixed to a rigid external fixator to stabilize the bone fragments. Percutaneous pinning, often using k-wires, is similar but relies on pinning the bone fragments to each other for stability as opposed to using an external fixator.

In addition three studies described completely different techniques. The IlluminOss system (IlluminOss® Medical, East Providence, RI, USA) uses a photodynamic liquid

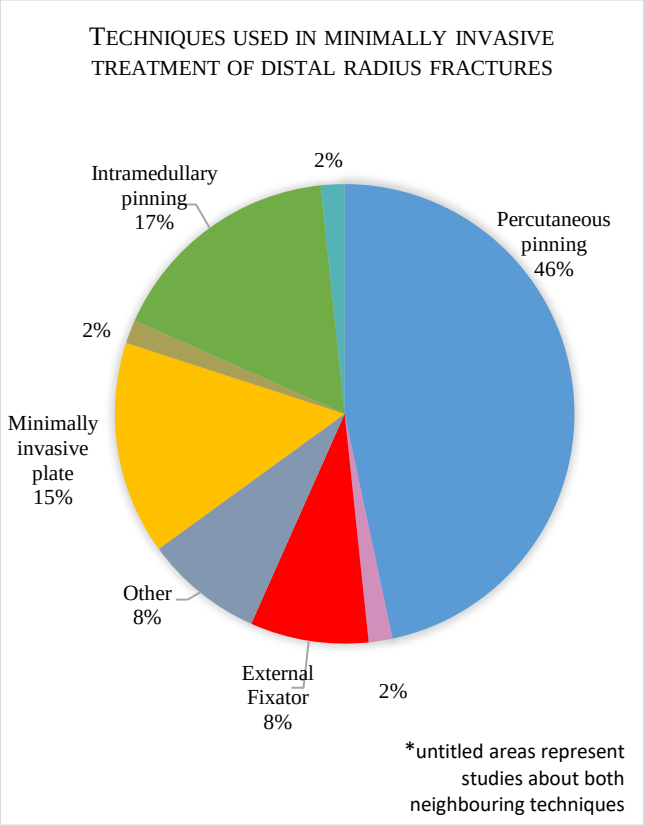

Figure 17 A pie chart showing the percentage of studies using different types of techniques for minimally invasive treatment of distal radius fractures.

which turns into a solid upon activation. A slender balloon is inserted into the medullary cavity which is then filled with this liquid. A light system is then used to harden the liquid resulting in hardened nail. Specifically for die-punch fractures (fractures of the intra-articular surface of the radius caused by compression) Fontaine et al.[33] describe an arthroscopic approach using bone cement. In their cadaver study they insert a balloon under the fractured surface to reduce it and fill the void with cement to stabilize the fracture. In a pilot study by Atiyya et al.[34] they used the ulna as an internal fixator for the radius by attaching the fragments of the radius to the ulna with long screws.

A large majority of the high LOE studies compared percutaneous pinning with ORIF volar plating. While most concluded that the two show equal clinical results Peng et al.[35] concluded that ORIF was the preferred method citing better supination and grip strength. In contrast Khan et al.[36] found percutaneous k-wire pinning to give superior clinical results. Only one study was found comparing ORIF and MIPO which found MIPO to have better patient satisfaction but also acknowledged a lack of high level evidence. Intramedullary pinning showed similar results to ORIF but had a higher complication rate according to Jordan et al.[37]

OVERVIEW OF HIGH LOE STUDIES OF DISTAL RADIUS FRACTURES

	Perc.	MIPO	Ext. fix.	Intra.	vs.
Peng, Fei [35]	-				
Lee, Dong Yeong [38]		+			
Mellstrand [39]	=				
Costa [40]	=				
Youlden [41]	=				
Chaudhry [42]	=				
Plate [43]				=	Volar plate
Costa [44]	=				
Zong [45]	?				
Chung [46]	?		?		
Jordan [37]				-	
Khan [36]	+				
Gradl [47]				=	Palmar plate
Venkatesh [48]	+				Casting

Figure 16 The comparative effectiveness found in high level of evidence studies of distal radius fractures. The right column indicates with which technique it is being compared.. + : better results, = : similar results, - : worse results, ? : insufficient evidence. Perc: percutaneous, MIPO: minimally invasive plate osteosynthesis, Ext. fix.: external fixator, Intra: intramedullary.

Cyst/foreign body removal

Of the 11 studies found 10 described the arthroscopic resection of ganglion cysts and one case report of arthroscopic resection of a giant cell tumor. For ganglions a shaver is used to puncture and resect the cyst. The giant cell tumor was resected piece by piece with forceps. Only one high LOE study was found; a systematic review by Head et al.[49] which concluded that arthroscopic resection is a promising procedure but that there is not enough comparative data to determine superiority.

TFCC repair

22 studies were found about arthroscopic repair of the TFCC. They all fall into two categories;

- Outside-in repair
- All-inside repair

Transosseus outside-in repair, where the suture is passed through a tunnel in the ulna as opposed to the capsule as described in section III.C., was the most common (8 studies). In all-inside repair the tying of the suture is also done arthroscopically.

Three studies described all-inside techniques. Sarkissan et al.[50] implemented a pre-tied suture device, full text was not available however so no detailed description of the technique can be given. In their case report Edgerton et al.[51] describe a knotless technique using a PushLock anchor (Arthrex, Naples, Florida) which directly attaches the sutures to the bone. Atzei et al.[52] use a slightly different method in which a suture anchor with four strand is first attached to the bone, the strands are then passed through the TFCC and tied arthroscopically using a knot pusher.

Six studies were cadaveric studies which mainly aimed to determine safe portals for the arthroscopic procedure and to compare different techniques. Johnson et al.[53] compared transosseous outside-in repair to capsular repair. They concluded that transosseous repair could restore DRUJ

stability. Ma et al.[54] compared open and arthroscopic repair and additionally evaluated a novel aiming device for creation of the bone tunnels in the procedure. They concluded arthroscopic repair to be biomechanically superior and the device was found to effective.

Two high LOE studies were found, both of which were systematic reviews investigating open vs. arthroscopic TFCC repair. Both Andersson et al.[55], and Robba et al.[56] concluded that there is insufficient evidence to determine superiority of either technique due to a lack of high level comparative studies.

Metacarpal fracture

As mentioned in section III.C. metacarpal fractures can be fixated transversely or intramedullarly. Varying methods of fixation were found for intramedullary pinning but transverse fixation was only done with k-wires. For transverse fixation only k-wires were used. For intramedullary fixation

- K-wires
- Flexible nails
- Rigid nails
- or Screws

were used. Within intramedullary pinning there were two categories namely antegrade or retrograde pinning which refer to the direction from which the pin is inserted. In antegrade fixation the pin is inserted from the wrist side to the fingers while retrograde fixation is the opposite. In addition one study proposed a novel sled design which has two prongs, one of which is fixed intramedullary while the other is fixed to the outside of the bone.

Three high LOE studies were found. Kim et al.[57] compared the effectiveness of antegrade and retrograde intramedullary pinning of the fifth metacarpal, concluding that long term results are the same but with antegrade pinning showing better short term results. Cepni et al.[58] compared antegrade pinning with casting, also of the fifth metacarpal. They concluded that antegrade pinning was a reliable procedure which minimized functional loss and recovery time. Lastly Melamed et al.[59] performed a meta-analysis of plate fixation vs. percutaneous pinning. They concluded that there is evidence to support the use of percutaneous pinning over ORIF but that more randomized studies were necessary to determine superiority of one technique.

Scapholunate ligament reconstruction

Of the seven resulting studies about minimally invasive scapholunate ligament reconstruction five specifically described a technique, one cadaveric study investigated the force on the ligament required to maintain reduction, and one compared postoperative pinning versus splint immobilization after arthroscopic capsulodesis.

Two of the studies describing a technique used a palmaris longus tendon graft. As opposed to the method described in section III.C. the palmaris longus tendon was passed through the scaphoid but was then also passed back through a hole in the lunate, and subsequently fixed to the scaphoid where it began, effectively creating a loop. In two other studies that used an extensor carpi radialis graft the lunate and scaphoid were not reconnected but instead the scaphoid was reduced and sutured to an extensor tendon of the wrist in order to fix it in the correct position. Another study described a technique using a bone-ligament-bone graft between the scaphoid and lunate. This means that a ligament was grafted from another carpal bone together with a bit of bone on each end of the ligament. The bony ends are then fixed in lunate and scaphoid, joining them with the ligament.

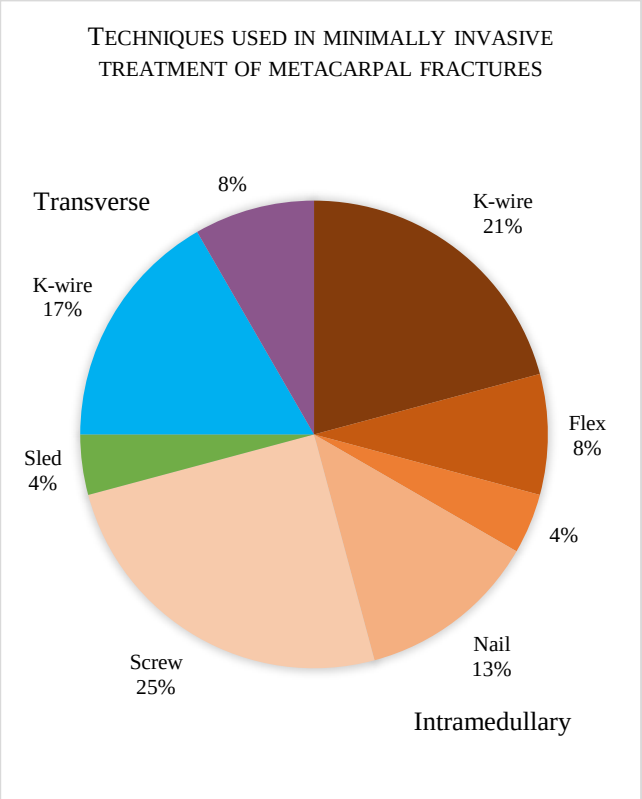

Figure 18 A pie chart showing the percentage of studies using different types of techniques for minimally invasive treatment of metacarpal fractures. Orange shades are intramedullary and blue in transverse.

Scaphoid nonunion fixation with bone graft

Twelve studies were found with minimally invasive alternatives for treatment of scaphoid nonunions with bone grafts. Two used a percutaneous technique, nine used arthroscopy and one study described a minimal open procedure. In both percutaneous techniques a hole was drilled into the scaphoid crossing through the fracture site. A biopsy trocar was then used to obtain a cylindrical bone graft which was then inserted and impacted into the hole. Subsequently a headless screw was placed in the same hole to fixate the fracture.

All studies using arthroscopy used a similar technique. After locating the fracture site, a shaver and burr were used to debride the nonunion site until healthy-looking bone was exposed on both sides. Subsequently bone grafted from either the distal radius or the iliac crest was inserted into the resulting gap piece by piece. After sufficient grafted bone

had been placed the fragments were fixated percutaneously with either a screw or k-wires.

Although no high LOE studies were found, there were two retrospective comparative studies. One of these by Kang et al.[60] investigated if it was necessary to simultaneously debride damaged ligaments when performing arthroscopic management of scaphoid nonunion, but concluded that there was no difference in union rates or clinical outcomes. Oh et al.[61] retrospectively compared open and arthroscopic bone grafting and fixation of scaphoid nonunions and found no difference in clinical outcomes.

VI. Discussion

A. *Trends per pathology*

For the treatment of stenosing tenosynovitis percutaneous release appears to be the most promising approach, accounting for 88% of the studies. Of these a large majority used blind or US-guided percutaneous needle release, however no studies compared these two procedures. Further research must be done to determine if the addition of ultrasonic guidance is necessary to reduce the risk of complications, or improve the effectiveness of the procedure.

Carpal tunnel release is the most extensively researched procedure in this study. High LOE studies comparing minimally invasive techniques with regular open surgery indicate improved results for all three types of techniques. Most improvements are in short term recovery and cosmetic appearance. There is much less evidence however comparing the various minimally invasive techniques with each other. These techniques must be compared to determine the future standard technique for the treatment of carpal tunnel syndrome. Despite accounting for around 20% of the studies, only one high LOE study was found about US-guided techniques, this could be because these techniques have been developed more recently and are still at an earlier stage of development.

Despite being the third most common procedure, trapeziectomies accounted for only 8 studies. This may be due in part to the fact the even among open procedures there is no consensus about the best treatment for CMC arthritis, with the trapeziectomy being one of the more common options[2].

Perutaneous needle aponeurotomy is the only minimally invasive surgical technique for the release of Dupuytren's contractures found in the literature in the last 5 years. Once again there is a clear lack of high level evidence to support or refute the use of this technique. In addition, the fact that only one minimally invasive technique has been suggested indicates that there is either no necessity for better techniques, or that it is a difficult technical challenge such that no other solutions have been found. The former is not the case however since current techniques still result in high levels of recurrence.

Distal radius fractures had the highest amount of studies per performed procedure. Together with the fact that a variety of different techniques were used this indicate that distal radius fixation is a popular subject of research. Percutaneous pinning is the most common technique accounting for 10 of the 15 high LOE studies found. It has however shown little or no difference in comparison with volar ORIF. The limited evidence for MIPO did show an improvement with respect to volar plating, perhaps combining the benefits of minimal invasion found in percutaneous pinning, with the superior fixation of ORIF.

For the removal of ganglion cysts the literature indicates arthroscopic resection to be a promising technique. More evidence is needed however to determine if the same effectiveness can be achieved as in open resection, especially with respect to recurrence rates, which are the most common complication.

Different arthroscopic techniques were found for the repair of the TFCC. Despite surgeons using variations in approach and fixation method it is not clear why one is superior to the other. Surgeon preference seems to be the leading motivation in these varying techniques. More large scale and comparative studies must be done to determine the pros and cons of each technique to aid in the selection and development of superior techniques. In addition the high LOE studies could not even determine that arthroscopic methods are superior to traditional open repair, further highlighting the need for high quality studies to guide decision making for the treatment of TFCC lesions.

The treatment of metacarpal fractures is largely done using minimally invasive techniques already. Which minimally invasive technique is superior is however not clear, also depending greatly on the type and location of the fracture. Considering the large amount of options, especially within intramedullary techniques, comparative studies should be performed to gain more insight into the advantages and disadvantages of each method.

The smallest amount of studies was found about scapholunate ligament reconstruction. This may be due to the fact that it is quite a complex procedure involving tunneling through small carpal bones, finding and grafting a tendon, and attaching it in a way that can endure large forces. Open surgery allows better visualization and workspace to achieve these tasks. Simpler procedures such as the flexor carpi radialis graft or the bone-ligament-bone graft may be better suited for arthroscopy, but comparative studies are necessary to compare their effectiveness.

The main difference between using percutaneous or arthroscopic techniques for the treatment of scaphoid nonunion is whether or not the non-union site can be debrided. The percutaneous techniques described in the literature do not allow for debridement of the surface but instead insert the bone graft through one channel in the middle of the scaphoid. With arthroscopy the nonunion site can be prepared much more extensively to increase the chance of union. Because there are no comparative studies it has not been proven that this improves clinical outcomes. In addition these techniques should also be compared to open procedures to determine which method is superior.

B. *General trends*

The wide scope of this study not only gives insight into the state of the research about each procedure but also more generally into the current state of minimally invasive surgery in hand and wrist surgery. Of the top 10 procedures performed at the two hospitals from which data was acquired only TFCC repairs and metacarpal fracture fixation are currently performed using minimally invasive techniques, despite minimally invasive options being available for each procedure. Perhaps this is because in many cases there is not enough evidence yet to support the adoption of a new technique, thus resulting in the choice of procedure to be largely dependent on surgeon preference. As is clear from the previous section large randomized controlled studies are needed throughout the field of minimally invasive hand and wrist surgery. Not only to aid surgeons in selecting the best treatment, but also to guide research by highlighting the advantages and disadvantages of the techniques. It is also apparent that the amount of research being done higher for simpler procedures such as releases and is much lower for the more complex procedures like trapeziectomies and ligament reconstruction. As technology continues to improve, and surgeons become more experienced using these techniques, the possibilities for these more complex procedures are likely to increase.

C. *Limitations of this research*

The main limitation of this study is that the results were limited to the last 5 years. A longer time frame would allow for an analysis of temporal trends in the research, giving a better insight into the development and adoption into practice of the techniques. Also, insight into previously researched methods that are now common practice, or have been abandoned can help give direction for future research. Another limitation is the decision to focus exclusively on studies involving surgery, and to exclude studies about factors other than clinical results such as costs. While this does focus the study on surgical techniques, it also excludes information which can play an important role in deciding which techniques are more promising.

Apart from the method of the literature search, the method used to determine which studies to include also has some shortcomings. By using the data of only two surgeons it is likely to be influenced by the personal preferences of the surgeons as well as local trends in the Netherlands. The data is therefore not a reliable indication of the worldwide usage of the different procedures.

VII. Conclusions

Overall this study provides a broad overview of the research being done on minimally invasive surgical techniques in hand and wrist surgery. The top ten most common surgical procedures were determined. For each procedure the recent literature about minimally invasive techniques was summarized and categorized according to the type of procedure, giving a succinct overview of fields being researched. Minimally invasive alternatives were found for each procedure but the amount and variety of techniques varied greatly. The common conclusion across all ten procedures was a great need for large randomized controlled studies to determine which techniques are superior and which shortcomings must still be addressed.

VIII. Acknowledgments

I would like to thank prof. Breedveld for his guidance in approaching and writing this report. I would like to thank Dr. Kraan for sharing his expertise in hand and wrist surgery and encouraging me throughout the process. Lastly I would like to thank Dr. Mathijssen for her input about the methodology of this report and her practical help in collecting data.

BIBLIOGRAPHY

[1] R. L. Drake PhD, FAAA, A. W. Vogl PhD, FAAA, and A. W. M. Mitchell MBBS, FRCS, FRCR, "Upper Limb," R. L. Drake PhD, FAAA, A. W. Vogl PhD, FAAA, and A. W. M. Mitchell MBBS, FRCS, FRCR, Eds. 2018, pp. 341–412.

[2] S. W. Wolfe MD, R. N. Hotchkiss MD, W. C. Pederson MD, FACS, S. H. Kozin MD, and M. S. Cohen MD, *Green's Operative Hand Surgery*. 2017.

[3] Y.-C. Yoon and J.-R. Baek, "Current Concepts of Fractures and Dislocation of the Hand," *J. Korean Fract. Soc.*, vol. 29, no. 2, p. 143, 2016.

[4] D. M. Eastwood, K. J. Gupta, and D. P. Johnson, "Percutaneous release of the trigger finger: An office procedure," *J. Hand Surg. Am.*, vol. 17, no. 1, pp. 114–117, 1992.

[5] C. L. Wang, S. F. Huang, Z. Q. Wang, Q. L. Ge, and X. G. Dong, "Preliminary outcomes of percutaneously looped thread transection in the surgical treatment of stenosing tenosynovitis," *Zhonghua Yi Xue Za Zhi*, vol. 97, no. 37, pp. 2923–2927, Oct. 2017.

[6] V. S. Nikolaou, M.-A. Malahias, M.-K. Kaseta, I. Sourlas, and G. C. Babis, "Comparative clinical study of ultrasound-guided A1 pulley release vs open surgical intervention in the treatment of trigger finger," *World J. Orthop.*, vol. 8, no. 2, pp. 163–169, 2017.

[7] P. Chobtangsilp, V. Vijitpornkul, and D. Thanbuasawan, "Comparison of trigger finger treatment with open surgery and percutaneous release by Blade Probe with or without corticosteroid injection: A randomized clinical trial," *J. Med. Assoc. Thail.*, vol. 101, no. 3, pp. S203–S210, 2018.

[8] H. J. H. J. H. J. Fiorini, M. J. M. J. M. J. Tamaoki, M. Lenza, J. B. J. B. J. B. Gomes dos Santos, F. Faloppa, and J. carlos J. carlos. J. carlos Belloti, "Surgery for trigger finger," *Cochrane Database Syst. Rev.*, vol. 2018, no. 2, p. CD009860, Feb. 2018.

[9] B. M. B. M. B. M. Huisstede, S. Gladdines, M. S. M. S. M. S. M. S. Randsdorp, and B. W. B. W. B. W. B. W. Koes, "Effectiveness of Conservative, Surgical, and Postsurgical Interventions for Trigger Finger, Dupuytren Disease, and De Quervain Disease: A Systematic Review.," vol. 99, no. 8, pp. 1635-1649.e21, Aug. 2018.

[10] K.-H. Park, W.-J. Shin, S.-J. Kim, and J.-P. Kim, "Does Bowstringing Affect Hand Function in Patients Treated with A1 Pulley Release for Trigger Fingers?: Comparison between Percutaneous Versus Open Technique," *Ann. Plast. Surg.*, vol. 81, no. 5, pp. 537–543, 2018.

[11] N. Ranjeet *et al.*, "Trigger finger: A prospective randomised control trial comparing percutaneous release versus open release," *J. Clin. Diagnostic Res.*, vol. 12, no. 7, pp. RC05–RC08, 2018.

[12] P. Xie *et al.*, "Stenosing tenosynovitis: Evaluation of percutaneous release with a specially designed needle vs. open surgery," *Orthopade*, vol. 48, no. 3, pp. 202–206, Mar. 2019.

[13] E. T. E. T. Sayegh and R. J. R. J. R. J. Strauch, "Open versus Endoscopic Carpal Tunnel Release: A Meta-analysis of Randomized Controlled Trials," *Clin. Orthop. Relat. Res.*, vol. 473, no. 3, pp. 1120–1132, 2015.

[14] M. Orak, S. Gumustas, T. Onay, S. Uludag, G. Bulut, and U. Boru, "Comparison of postoperative pain after open and endoscopic carpal tunnel release: A randomized controlled study," *Indian J. Orthop.*, vol. 50, no. 1, pp. 65–69, Jan. 2016.

[15] J. M. Rojo-Manaute *et al.*, "Ultra-minimally invasive ultrasound-guided carpal tunnel release: A randomized clinical trial," *J. Ultrasound Med.*, vol. 35, no. 6, pp. 1149–1157, Jun. 2016.

[16] D. Vanni, F. S. Sirabella, R. Galzio, V. Salini, and V. Magliani, "The double tunnels technique: An alternative minimally invasive approach for carpal tunnel syndrome," *J. Neurosurg.*, vol. 123, no. 5, pp. 1230–1237, Nov. 2015.

[17] K. Hu, T. Zhang, and W. Xu, "Intraindividual comparison between open and endoscopic release in bilateral carpal tunnel syndrome: A meta-analysis of randomized controlled trials," *Brain Behav.*, vol. 6, no. 3, pp. 1–9, Mar. 2016.

[18] B. M. Huisstede, J. van den Brink, M. S. Randsdorp, S. J. Geelen, and B. W. Koes, "Effectiveness of Surgical and Postsurgical Interventions for Carpal Tunnel Syndrome—A Systematic Review," *Arch. Phys. Med. Rehabil.*, vol. 99, no. 8, pp. 1660-1680.e21, 2018.

[19] S. Akhtar, M. J. M. J. Bradley, F. D. F. D. Burke, N. H. N. H. N. H. Dubin, and E. F. F. Shaw Wilgis, "Study to assess outcome after open and closed carpal tunnel decompression," *Ann. Plast. Surg.*, vol. 75, no. 5, pp. 548–551, 2015.

[20] T. Gurpinar, B. Polat, A. E. A. E. Polat, E. Carkci, A. S. A. S. Kalyenci, and Y. Ozturkmen, "Comparison of open and endoscopic carpal tunnel surgery regarding clinical outcomes, complication and return to daily life: A prospective comparative study," *Pakistan J. Med. Sci.*, vol. 35, no. 6, pp. 1532–1537, Nov. 2019.

[21] S. A. Gumustas *et al.*, "Similar effectiveness of the open versus endoscopic technique for carpal tunnel syndrome: a prospective randomized trial.," *Eur. J. Orthop. Surg. Traumatol.*, vol. 25, no. 8, pp. 1253–1260, Dec. 2015.

[22] B. Michelotti, D. Romanowsky, and R. M. Hauck, "Prospective, randomized evaluation of endoscopic versus open carpal tunnel release in bilateral carpal tunnel syndrome: an interim analysis," *Ann. Plast. Surg.*, vol. 73, pp. S157–S160, Dec. 2014.

[23] B. R. B. R. Peters *et al.*, "Morphologic Analysis of the Carpal Tunnel and Median Nerve Following Open and Endoscopic Carpal Tunnel Release," *Hand*, p. 155894471986171, Jul. 2019.

[24] M. P. Gaspar, B. A. Sessions, B. S. Dudoussat, and P. M. Kane, “Single-Incision Carpal Tunnel Release and Distal Radius Open Reduction and Internal Fixation: A Cadaveric Study,” *J. Wrist Surg.*, vol. 05, no. 03, pp. 241–246, Mar. 2016.

[25] N. B. N. B. N. B. Alp, G. Akdağ, and A. C. A. C. A. C. Macunluoğlu, “Median nerve and carpal tunnel volume changes after two different surgical methods: A comparative magnetic resonance imaging study of mini-open and endoscopic carpal tunnel release,” *Eklem Hastalik. Cerrahisi*, vol. 30, no. 3, pp. 212–216, Dec. 2019.

[26] W. T. W.-T. W. T. W.-T. Oh, H. J. H.-J. Kang, Y. M. Y.-M. Y. M. Chun, I. H. I.-H. I. H. Koh, Y.-J. Y. J. Y.-J. Y. J. Y.-J. Lee, and Y. R. Y.-R. Y. R. Choi, “Retrospective Comparative Outcomes Analysis of Arthroscopic Versus Open Bone Graft and Fixation for Unstable Scaphoid Nonunions,” *Arthrosc. - J. Arthrosc. Relat. Surg.*, vol. 34, no. 10, pp. 2810–2818, Oct. 2018.

[27] X. Zhang, X. Huang, X. Wang, S. Wen, J. Sun, and X. Shao, “A Randomized Comparison of Double Small, Standard, and Endoscopic Approaches for Carpal Tunnel Release,” *Plast. Reconstr. Surg.*, vol. 138, no. 3, pp. 641–647, Sep. 2016.

[28] D. Rog, T. Ozyurekoglu, and K. K. Karuppiah, “Arthroscopic Abrasion Arthroplasty Is Not Superior to Ligament Reconstruction and Tendon Interposition for Thumb Carpometacarpal Arthritis,” *Hand*, 2018.

[29] T. K. T. K. T. K. Cobb, A. L. A. L. Walden, and Y. Cao, “Long-Term Outcome of Arthroscopic Resection Arthroplasty With or Without Interposition for Thumb Basal Joint Arthritis.,” *J. Hand Surg. Am.*, vol. 40, no. 9, pp. 1844–1851, Sep. 2015.

[30] S. Könneker *et al.*, “Percutaneous Aponeurotomy and Lipofilling (PALF) versus Limited Fasciectomy in Patients with Primary Dupuytren’s Contracture: A Prospective, Randomized, Controlled Trial,” *Plast. Reconstr. Surg.*, Jun. .

[31] R. W. R. W. R. W. Selles, C. Zhou, H. J. H. J. H. J. Kan, R. M. R. M. R. M. Wouters, C. A. C. A. C. A. van Nieuwenhoven, and S. E. R. S. E. R. Hovius, “Percutaneous Aponeurotomy and Lipofilling versus Limited Fasciectomy for Dupuytren’s Contracture: 5-Year Results from a Randomized Clinical Trial,” *Plast. Reconstr. Surg.*, vol. 142, no. 6, pp. 1523–1531, Dec. 2018.

[32] E. Soreide *et al.*, “Treatment of Dupuytren’s contracture: A systematic review,” *Bone Jt. J.*, vol. 100B, no. 9, pp. 1138–1145, Sep. 2018.

[33] V. Fontaine, M. Grunberg, J. Soret, K. El-Youssef, L.-E. E. Gayet, and R. Taberne, “Role for cementoplasty in intra-articular distal radius fractures: Cadaver study and application to arthroscopy,” *Orthop. Traumatol. Surg. Res.*, vol. 104, no. 1, pp. 105–108, Feb. 2018.

[34] A. N. Atiyya, A. S. Eid, and T. El-Husseini, “Distal radius fractures: using the ulna as an internal fixator: pilot study,” *Eur. Orthop. Traumatol.*, vol. 6, no. 1, 2015.

[35] F. Peng, Y. X. Y.-X. Liu, and Z. Y. Z.-Y. Wan, “Percutaneous pinning versus volar locking plate internal fixation for unstable distal radius fractures: a meta-analysis,” *J. Hand Surg. Eur. Vol.*, vol. 43, no. 2, pp. 158–167, Feb. 2018.

[36] J. I. Khan, F. N. Hussain, T. Mehmood, and O. Adil, “A comparative study of functional outcome of treatment of intra articular fractures of distal radius fixed with percutaneous Kirschner’s wires vs T-plate,” *Pakistan J. Med. Sci.*, vol. 33, no. 3, pp. 709–713, 2017.

[37] R. W. W. Jordan and A. Saithna, “Defining the role of intramedullary nailing for fractures of the distal radius: a systematic review.,” *Bone Jt. J.*, vol. 97-B, no. 10, pp. 1370–1376, Oct. 2015.

[38] D. Y. D.-Y. Lee, Y. J. Y.-J. Park, and J.-S. J. S. Park, “A meta-analysis of studies of volar locking plate fixation of distal radius fractures: Conventional versus minimally invasive plate osteosynthesis,” *CiOS Clin. Orthop. Surg.*, vol. 11, no. 2, pp. 208–219, Jun. 2019.

[39] C. Mellstrand Navarro, L. Ahrengart, H. Törnqvist, and S. Ponzer, “Volar Locking Plate or External Fixation with Optional Addition of K-Wires for Dorsally Displaced Distal Radius Fractures: A Randomized Controlled Study,” *J. Orthop. Trauma*, vol. 30, no. 4, pp. 217–224, 2016.

[40] M. L. M. L. Costa *et al.*, “UK DRAFFT: A randomised controlled triaof percutaneous fixation with kirschner wires versus volar locking-plate fixation in the treatment of adult patients with a dorsally displaced fracture of the distal radius,” *Health Technol. Assess. (Rockv).*, vol. 19, no. 17, Feb. 2015.

[41] D. J. D. J. Youlden, K. Sundaraj, and C. Smithers, “Volar locking plating versus percutaneous Kirschner wires for distal radius fractures in an adult population: a meta-analysis,” *ANZ J. Surg.*, vol. 89, no. 7, pp. 821–826, 2019.

[42] H. Chaudhry, Y. V. Kleinlugtenbelt, R. Mundi, B. Ristevski, J. C. Goslings, and M. Bhandari, “Are Volar Locking Plates Superior to Percutaneous K-wires for Distal Radius Fractures? A Meta-analysis,” *Clin. Orthop. Relat. Res.*, vol. 473, no. 9, pp. 3017–3027, 2015.

[43] J. F. J. F. Plate *et al.*, “Randomized comparison of volar locking plates and intramedullary nails for unstable distal radius fractures,” *J. Hand Surg. Am.*, vol. 40, no. 6, pp. 1095–1101, Jun. 2015.

[44] M. L. Costa, J. Achten, A. Rangan, S. E. Lamb, and N. R. Parsons, “Percutaneous fixation with Kirschner wires versus volar locking-plate fixation in adults with dorsally displaced fracture of distal radius: five-year follow-up of a randomized controlled trial.,” *Bone Jt. J.*, vol. 101-B, no. 8, pp. 978–983, Aug. 2019.

[45] S.-L. Zong, S.-L. Kan, L.-X. Su, and B. Wang, "Meta-analysis for dorsally displaced distal radius fracture fixation: Volar locking plate versus percutaneous Kirschner wires," *J. Orthop. Surg. Res.*, vol. 10, no. 1, 2015.

[46] K. C. K. C. Chung, S. Malay, M. J. M. J. Shauver, and H. M. M. Kim, "Assessment of Distal Radius Fracture Complications Among Adults 60 Years or Older: A Secondary Analysis of the WRIST Randomized Clinical Trial," *JAMA Netw. open*, vol. 2, no. 1, p. e187053, Jan. 2019.

[47] G. Gradl, S. Falk, T. Mittlmeier, M. Wendt, N. Mielsch, and G. Gradl, "Fixation of intra-articular fractures of the distal radius using intramedullary nailing: a randomized trial versus palmar locking plates," *Injury*, vol. 47, pp. S25–S30, 2016.

[48] R. B. Venkatesh, G. K. Maranna, and R. K. B. Narayanappa, "A comparative study between closed reduction and cast application versus percutaneous K-wire fixation for extraarticular fracture distal end of radius," *J. Clin. Diagnostic Res.*, vol. 10, no. 2, pp. RC05–RC09, Feb. 2016.

[49] L. Head, J. R. Gencarelli, M. Allen, and K. U. Boyd, "Wrist ganglion treatment: Systematic review and meta-analysis," *J. Hand Surg. Am.*, vol. 40, no. 3, pp. 546-553.e8, Mar. 2015.

[50] E. J. Sarkissian, M. B. Burn, and J. Yao, "Long-Term Outcomes of All-Arthroscopic Pre-Tied Suture Device Triangular Fibrocartilage Complex Repair.," *J. Wrist Surg.*, vol. 8, no. 5, pp. 403–407, Oct. 2019.

[51] M. T. Edgerton and R. C. Kollmorgen, "A Novel All-Inside Arthroscopic Technique for Radial-Sided Triangular Fibrocartilage Complex Tears: A Case Report and Review of Literature," vol. 12, no. 5, pp. NP166–NP169, Sep. 2017.

[52] A. Atzei, R. Luchetti, and F. Braidotti, "Arthroscopic Foveal Repair of the Triangular Fibrocartilage Complex," *J. Wrist Surg.*, vol. 04, no. 01, pp. 022–030, Feb. 2015.

[53] J. C. J. C. Johnson, F. M. F. M. Pfeiffer, J. E. J. E. Jouret, and D. M. D. M. Brogan, "Biomechanical Analysis of Capsular Repair Versus Arthrex TFCC Ulnar Tunnel Repair for Triangular Fibrocartilage Complex Tears," *Hand (N. Y).*, vol. 14, no. 4, pp. 547–553, Jul. 2019.

[54] C. H. Ma, T. S. Lin, C. H. Wu, D. Y. Li, S. C. Yang, and Y. K. Tu, "Biomechanical Comparison of Open and Arthroscopic Transosseous Repair of Triangular Fibrocartilage Complex Foveal Tears: A Cadaveric Study," *Arthrosc. - J. Arthrosc. Relat. Surg.*, vol. 33, no. 2, pp. 297–304, Feb. 2017.

[55] J. K. Andersson, M. Åhlén, and D. Andernord, "Open versus arthroscopic repair of the triangular fibrocartilage complex: a systematic review," *J. Exp. Orthop.*, vol. 5, no. 1, Dec. 2018.

[56] V. Robba, A. Fowler, A. Karantana, D. Grindlay, and T. Lindau, "Open Versus Arthroscopic Repair of 1B Ulnar-Sided Triangular Fibrocartilage Complex Tears: A Systematic Review," *Hand*, p. 1558944718815244, Jan. 2019.

[57] J. K. Kim and D. J. Kim, "Antegrade Intramedullary Pinning Versus Retrograde Intramedullary Pinning for Displaced Fifth Metacarpal Neck Fractures," *Clin. Orthop. Relat. Res.*, vol. 473, no. 5, pp. 1747–1754, May 2015.

[58] S. K. Cepni, S. Aykut, T. Bekmezci, and A. Kilic, "A minimally invasive fixation technique for selected patients with fifth metacarpal neck fracture," *Injury*, vol. 47, no. 6, Jun. 2016.

[59] E. Melamed, L. Joo, E. Lin, D. Perretta, and J. T. Capo, "Plate Fixation versus Percutaneous Pinning for Unstable Metacarpal Fractures: A Meta-analysis," *J. hand Surg. Asian-Pacific Vol.*, vol. 22, no. 1, pp. 29–34, 2017.

[60] H. J. Kang, Y. M. Chun, I. H. Koh, J. H. Park, and Y. R. Choi, "Is Arthroscopic Bone Graft and Fixation for Scaphoid Nonunions Effective?," *Clin. Orthop. Relat. Res.*, vol. 474, no. 1, pp. 204–212, Jan. 2016.

[61] W.-T. Oh, H.-J. Kang, Y.-M. Chun, I.-H. Koh, Y.-J. Lee, and Y.-R. Choi, "Retrospective Comparative Outcomes Analysis of Arthroscopic Versus Open Bone Graft and Fixation for Unstable Scaphoid Nonunions," *Arthrosc. - J. Arthrosc. Relat. Surg.*, vol. 34, no. 10, pp. 2810–2818, 2018.

Figures

[A] Orthobullets, retrieved feb. 2020 from https://upload.orthobullets.com/topic/6005/images/TTC%20Illustration%20-%20volar%20wrist%20ligaments_moved.jpg

[B] HealthLink BC, retrieved feb. 2020 from https://www.healthlinkbc.ca/health-topics/zm6309

Appendix I Amounts of procedures at Haga and Reinier de Graaf

DIS code	Description	Amount Haga	Amount Reinier de Graaf	Comment	Total	Top 10
038856	Operatieve behandeling tendovaginitis stenosans.	45	130	Combined 038856 and 038857	175	
038340	Operatieve behandeling carpaaltunnel syndroom, open procedure (zie 038341 voor endoscop	15	93		108	
038300	Extirpatie van handwortelbeentjes.	17	72		89	
038382	Operatieve behandeling contractuur van dupuytren door middel van excisie van de fascia palr	7	34	Combined 038382 and 038305	41	
038234	Operatieve behandeling van fractuur distale radius.	12	15		27	
038912	Huid afwijking excisie (groot)/Lipoom (groot)/Corpus alienum verwijdering	13	12		25	
038887	Plastiek Triangulare Fibrocartilage Complex.	2	21		23	
038345	Operatieve behandeling fractuur van een os metacarpale met K-draad en/of schroef- en/of pl	9	9		18	
038367	Operatieve behandeling luxatie perilunate		18		18	
038305	Operatieve behandeling pseudarthrose hand en/of pols, met bottransplantaat	7	10		17	
038329	Operatieve behandeling van fractuur van een grondlid van een vinger met K-draad en/of schr	1	11		12	
038369	Intercarpale artrodese.	7	4		11	
038201	Osteotomie van radius-of ulnaschacht (zie 038203 voor osteotomie met distractie) (excl. oper	6			6	
038351	Arthrodese van een interphalangeaal gewricht.	3	1		4	
030461	Neurolysen m.b.v. operatiemicroscoop of loupevergroting	1	3		4	
038859	Secundair herstel extensor.	1	3		4	
030470	Transpositie nervus ulnaris.	1	3		4	
030463	Decompressie zenuw, per zenuw, exclusief neurolysen (zie 030460 en 030461)	3			3	
038306	Prothese implantatie interphalangeaal gewricht.	3			3	
190323	Vingerprothese.	3			3	
038339	Operatieve behandeling van een of meerdere fracturen van handwortelbeentjes met K-draad	2	1		3	
038354	Arthrodese van het polsgewricht.	1	2		3	
038802	Excochleatie en/of sequestrotomie van kleine beenderen.	1	2		3	
190321	Polsprothese.	2			2	
038316	Prothese implantatie polsgewricht.	2			2	
038375	Synoviectomie van de strekkers van de handrug met synoviectomie van een of twee metacarp	2			2	
038362	Artrolyse polsgewricht.	1	1		2	
038372	Operatieve behandeling scaphoidfractuur met K-draad en/of schroef- en/of plaatfixatie, open	1	1		2	
190320	Prothese Radiuskopje.	1			1	
038301	Proximale rij-carpectomie.	1			1	

	Excluded	Amount Haga	Amount Reinier de Graaf	Reasoning
039417	Artroscopie van de pols in combinatie met een heelkundige ingreep aan dezelfde pols	36	33	General term used in different procedures
038872	Transpositie van een pees, verzetten van de insertie.	32	14	General term used in different procedures
038867	Endoscopisch verlengen, verkorten of uitsnijden van pezen, fascien of spieren (zie 03	27		General term used in different procedures
038865	Tenolyse extensor pols.	20	5	General term used in different procedures
038824	Verwijdering plaat en schroeven uit een bot.	13		General term used in different procedures
190305	Totale heup.	8		Not hand or wrist
038567	Vervanging van de femurkop en het acetabulum.	7		Not hand or wrist
038822	Verwijdering van cerclages of K-draad uit een bot.	3		General term used in different procedures
038807	Verkrijgen van autotransplantaat van grote beenderen.	3		General term used in different procedures
038233	Operatieve behandeling van een geisoleerde fractuur van de radius- of ulnaschacht.	2		Not hand or wrist
038203	Osteotomie van radius-of ulnaschacht met distractie (excl. operatieve verlenging van	2		Not hand or wrist
038804	Verkrijgen van autotransplantaat van middelgrote beenderen.	2		General term used in different procedures
038868	Verlengen, verkorten of uitsnijden van pezen, fascien of spieren, open procedure (zie	2		General term used in different procedures
038540	Artrotomie van heupgewricht.	1		Not hand or wrist
038830	Beenplastiek van andere beenderen dan lange pijpbeenderen van arm of been.	1		Not hand or wrist
038251	Bloedige repositie van een verouderde elleboogluxatie.	1		Not hand or wrist
038591	Exarticulatie van het heupgewricht.	1		Not hand or wrist
038210	Multilevel correctie-osteotomie van radius en/of ulna.	1		Not hand or wrist
038630	Operatieve behandeling bi- of trimalleolaire fractuur.	1		Not hand or wrist
038533	Operatieve behandeling fractuur van het collum van het femur.	1		Not hand or wrist
038535	Operatieve behandeling van per- en intertrochantaire fractuur van het femur.	1		Not hand or wrist
038534	Operatieve behandeling, ongeacht de techniek, fractuur van de schacht van het femu	1		Not hand or wrist
039035	Transpositie van bot of kraakbeen.	1		General term used in different procedures
038267	Verwijderen prothese elleboog.	1		Not hand or wrist
038569	Verwijderen van een geïmplanteerde total hip + reïmplantatie nieuwe total hip.	1		Not hand or wrist
038812	Verwijderen van een of meerdere exostosen van middelgrote beenderen zoals hand-	1		Not hand or wrist
038231	Operatieve behandeling van een fractuur van het caput radii, bloedige repositie.	1		Not hand or wrist
038378	Kapselplastiek bij luxatie van een vingergewricht(DIP,PIP)		24	General term used in different procedures

APPENDIX II – SEARCH TERMS

Stenosing tenosynovitis release	PubMed	((minimal* AND invasive OR minimal incision OR percutaneous OR scop* OR endoscop* OR arthroscop* OR ((US OR ultrasonic OR sonographic) AND guidance)) AND (trigger finger[title] OR stenosing tenosynovitis[title] OR quervain*)) AND hasabstract[text] AND (("2015/01/01"[PDat] : "2019/12/31"[PDat]))
	Scopus	TITLE ((trigger AND finger) OR (stenosing AND tenosynovitis) OR quervain*) AND TITLE-ABS-KEY (" *minimal* invasive" OR "*scop*" OR "percutaneous " OR ((" ultrasonic " OR "US" OR "sonographic") AND "guidance" OR " minimal incision ") AND (LIMIT TO (PUBYEAR , 2019) OR LIMIT-TO (PUBYEAR , 2018) OR LIMIT-TO (PUBYEAR , 2017) OR LIMIT-TO (PUBYEAR , 2016) OR LIMIT-TO (PUBYEAR , 2015))
Carpal tunnel release	PubMed	((minimal* AND invasive OR minimal incision OR percutaneous OR scop* OR endoscop* OR arthroscop* OR ((US OR ultrasonic OR sonographic) AND guidance)) AND (carpal tunnel[title] OR CTS[title])) AND hasabstract[text] AND (("2015/01/01"[PDat] : "2019/12/31"[PDat]))
	Scopus	TITLE (carpal AND tunnel OR cts) AND TITLE-ABS-KEY (" *minimal* invasive " OR "*scop*" OR " percutaneous " OR ((" ultrasonic " OR "US" OR "sonographic") AND "guidance") OR " minimal incision ") AND (LIMIT-TO (PUBYEAR , 2019) OR LIMIT-TO (PUBYEAR , 2018) OR LIMIT-TO (PUBYEAR , 2017) OR LIMIT-TO (PUBYEAR , 2016) OR LIMIT-TO (PUBYEAR , 2015))
CMC Arthritis	PubMed	(minimal* AND invasive OR minimal incision OR percutaneous OR scop* OR endoscop* OR arthroscop* OR ((US OR ultrasonic OR sonographic) AND guidance)) AND (((osteoarthritis[title] OR arthritis[title]) AND (CMC[title] OR carpometacarpal[title] OR carpal-metacarpal[title] OR (bas*[title] AND thumb[title]))) OR trapeziectomy[title]) AND hasabstract[text] AND (("2015/01/01"[PDat] : "2019/12/31"[PDat]))
	Scopus	TITLE (("*arthritis" AND ("CMC" OR "carpometacarpal" OR "carpal-metacarpal" OR (bas* AND thumb))) OR trapeziectomy) AND TITLE-ABS-KEY (" *minimal* invasive " OR "*scop*" OR " percutaneous " OR ((" ultrasonic " OR "US" OR "sonographic") AND "guidance") OR " minimal incision ") AND (LIMIT-TO (PUBYEAR , 2019) OR LIMIT-TO (PUBYEAR , 2018) OR LIMIT-TO (PUBYEAR , 2017) OR LIMIT-TO (PUBYEAR , 2016) OR LIMIT-TO (PUBYEAR , 2015))
Dupuytren's contracture	PubMed	(minimal* AND invasive OR minimal incision OR percutaneous OR scop* OR endoscop* OR arthroscop* OR ((US OR ultrasonic OR sonographic) AND guidance)) AND (dupuytren*[title]) AND hasabstract[text] AND (("2015/01/01"[PDat] : "2019/12/31"[PDat]))
	Scopus	TITLE (dupuytren*) AND TITLE-ABS-KEY (" *minimal* invasive " OR "*scop*" OR " percutaneous " OR ((" ultrasonic " OR "US" OR "sonographic") AND "guidance") OR " minimal incision ") AND (LIMIT-TO (PUBYEAR , 2019) OR LIMIT-TO (PUBYEAR , 2018) OR LIMIT-TO (PUBYEAR , 2017) OR LIMIT-TO (PUBYEAR , 2016) OR LIMIT-TO (PUBYEAR , 2015))
Distal radius fractures	PubMed	(minimal* AND invasive OR minimal incision OR percutaneous OR scop* OR endoscop* OR arthroscop* OR ((US OR ultrasonic OR sonographic) AND guidance)) AND distal[title] AND radius[title] AND fracture*[title] AND hasabstract[text] AND (("2015/01/01"[PDat] : "2019/12/31"[PDat]))
	Scopus	TITLE (distal AND radius AND fracture*) AND TITLE-ABS-KEY (" *minimal* invasive " OR "*scop*" OR " percutaneous " OR ((" ultrasonic " OR "US" OR "sonographic") AND "guidance") OR " minimal incision ") AND (LIMIT-TO (PUBYEAR , 2019) OR LIMIT-TO (PUBYEAR , 2018) OR LIMIT-

		TO (PUBYEAR , 2017) OR LIMIT-TO (PUBYEAR , 2016) OR LIMIT-TO (PUBYEAR , 2015))
Cyst removal	PubMed	(minimal* AND invasive OR minimal incision OR percutaneous OR scop* OR endoscop* OR arthroscop* OR ((US OR ultrasonic OR sonographic) AND guidance)) AND ((gangli*[title] OR cyst*[title] OR tumor*[title]) AND (wrist[title] OR hand[title] OR finger[title] OR carpal[title] OR retinacular[title] OR dip[title] OR interphalangeal[title])) AND hasabstract[text] AND (("2015/01/01"[PDat] : "2019/12/31"[PDat]))
	Scopus	TITLE ((gangli* OR cyst* OR tumor*) AND (hand OR wrist OR finger OR carpal OR retinacular OR dip OR interphalangeal)) AND TITLE-ABS-KEY (" *minimal* invasive " OR "*scop*" OR " percutaneous " OR ((" ultrasonic " OR "US" OR "sonographic") AND "guidance") OR " minimal incision ") AND (LIMIT-TO (PUBYEAR , 2019) OR LIMIT-TO (PUBYEAR , 2018) OR LIMIT-TO (PUBYEAR , 2017) OR LIMIT-TO (PUBYEAR , 2016) OR LIMIT-TO (PUBYEAR , 2015))
TFCC repair	PubMed	(minimal* AND invasive OR minimal incision OR percutaneous OR scop* OR endoscop* OR arthroscop* OR ((US OR ultrasonic OR sonographic) AND guidance)) AND (TFCC[title] OR triangular fibrocartilage complex[title] AND (repair*[title] OR tear*[title] OR lesion*[title])) AND hasabstract[text] AND (("2015/01/01"[PDat] : "2019/12/31"[PDat]))
	Scopus	TITLE ((tfcc OR (triangular AND fibrocartilage AND complex)) AND (repair* OR tear* OR lesion*)) AND TITLE-ABS-KEY (" *minimal* invasive " OR "*scop*" OR " percutaneous " OR ((" ultrasonic " OR "US" OR "sonographic") AND "guidance") OR " minimal incision ") AND (LIMIT-TO (PUBYEAR , 2019) OR LIMIT-TO (PUBYEAR , 2018) OR LIMIT-TO (PUBYEAR , 2017) OR LIMIT-TO (PUBYEAR , 2016) OR LIMIT-TO (PUBYEAR , 2015))
Metacarpal fractures	PubMed	(minimal* AND invasive OR minimal incision OR percutaneous OR scop* OR endoscop* OR arthroscop* OR ((US OR ultrasonic OR sonographic) AND guidance)) AND (metacarp*[title] AND fracture*[title]) AND hasabstract[text] AND (("2015/01/01"[PDat] : "2019/12/31"[PDat]))
	Scopus	TITLE (metacarp* AND fracture*) AND TITLE-ABS-KEY (" *minimal* invasive " OR "*scop*" OR " percutaneous " OR ((" ultrasonic " OR "US" OR "sonographic") AND "guidance") OR " minimal incision ") AND (LIMIT-TO (PUBYEAR , 2019) OR LIMIT-TO (PUBYEAR , 2018) OR LIMIT-TO (PUBYEAR , 2017) OR LIMIT-TO (PUBYEAR , 2016) OR LIMIT-TO (PUBYEAR , 2015))
Scapholunate ligament reconstruction	PubMed	(minimal* AND invasive OR minimal incision OR percutaneous OR scop* OR endoscop* OR arthroscop* OR ((US OR ultrasonic OR sonographic) AND guidance)) AND (((osteoarthritis[title] OR arthritis[title]) AND (CMC[title] OR carpometacarpal[title] OR carpal-metacarpal[title] OR (bas*[title] AND thumb[title]))) OR trapeziectomy[title]) AND hasabstract[text] AND (("2015/01/01"[PDat] : "2019/12/31"[PDat]))
	Scopus	TITLE ((*lunate) AND (reconstruction OR *capsulo* OR dissociation OR *ligamento*)) AND TITLE-ABS-KEY (" *minimal* invasive " OR "*scop*" OR " percutaneous " OR ((" ultrasonic " OR "US" OR "sonographic") AND "guidance") OR " minimal incision ") AND (LIMIT-TO (PUBYEAR , 2019) OR LIMIT-TO (PUBYEAR , 2018) OR LIMIT-TO (PUBYEAR , 2017) OR LIMIT-TO (PUBYEAR , 2016) OR LIMIT-TO (PUBYEAR , 2015)
Scaphoid nonunion	PubMed	(minimal* AND invasive OR minimal incision OR percutaneous OR scop* OR endoscop* OR arthroscop* OR ((US OR ultrasonic OR sonographic) AND guidance)) AND (scaphoid[title] AND (nonunion*[title] OR "non union" AND *[title] OR non-union*[title] OR graft*[title] OR pseudarthrosis[title])) AND hasabstract[text] AND (("2015/01/01"[PDat] : "2019/12/31"[PDat]))

	Scopus	TITLE (scaphoid AND (nonunion OR non-union OR "non union" OR graft)) AND TITLE-ABS-KEY (" *minimal* invasive " OR "*scop*" OR " percutaneous " OR ((" ultrasonic " OR "US" OR "sonographic") AND "guidance") OR " minimal incision ") AND (LIMIT-TO (PUBYEAR , 2019) OR LIMIT-TO (PUBYEAR , 2018) OR LIMIT-TO (PUBYEAR , 2017) OR LIMIT-TO (PUBYEAR , 2016) OR LIMIT-TO (PUBYEAR , 2015))

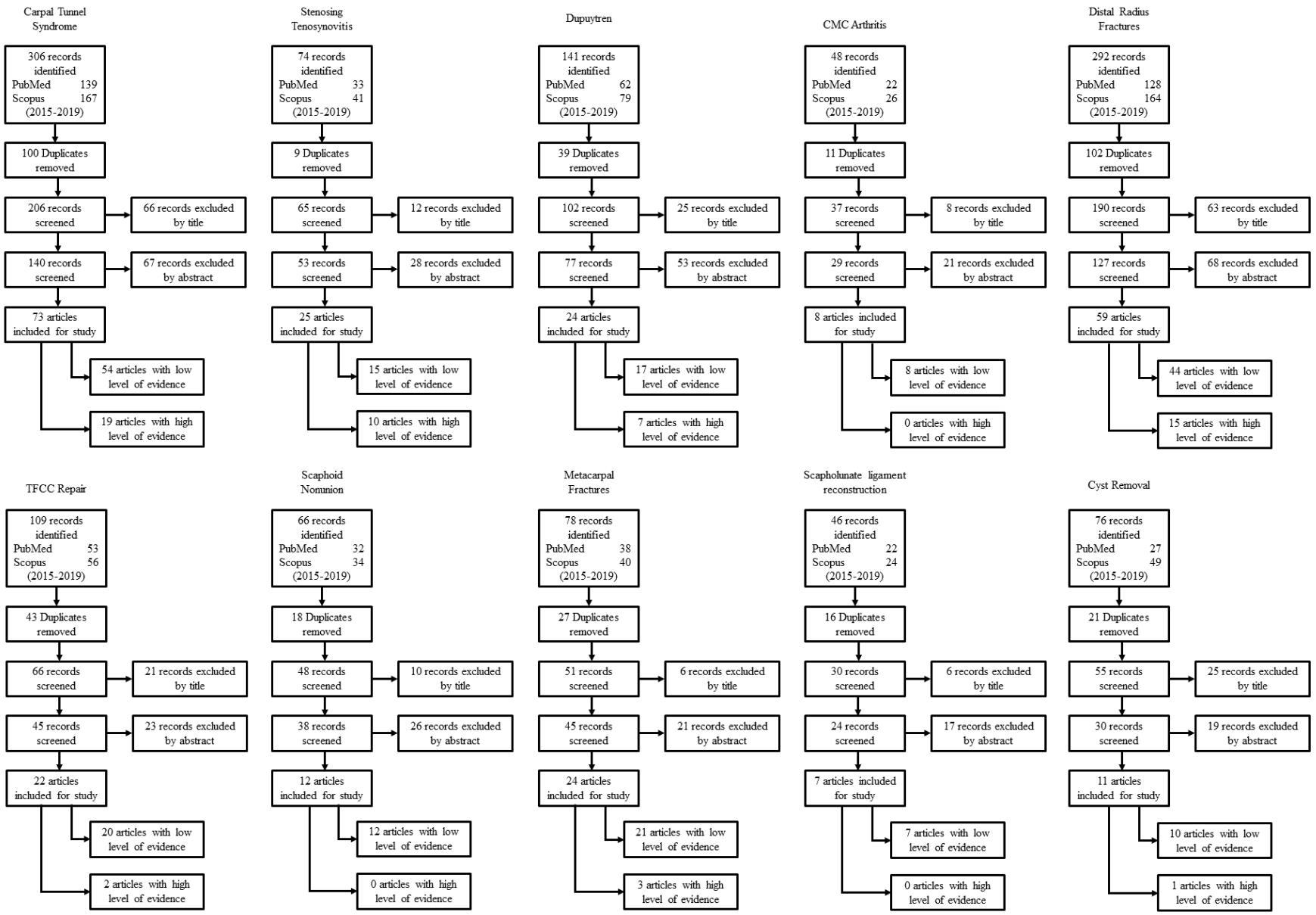

APPENDIX III – SEARCH FLOW DIAGRAMS OF ALL SEARCHES